AD NUMBER

AD887904

LIMITATION CHANGES

TO:

Approved for public release; distribution is unlimited.

FROM:

Distribution authorized to U.S. Gov't. agencies only; Test and Evaluation; SEP 1971. Other requests shall be referred to Armament Development and Test Center, Attn: DLGC Eglin AFB, FL 32512.

AUTHORITY

AFATL TAB 74-10, 10 May 1974

AEDC-TR-71-188
AFATL-TR-71-116

Cy 2

INVESTIGATION OF THE SEPARATION CHARACTERISTICS OF VARIOUS STORES FROM THE A-7D AIRCRAFT AT MACH NUMBERS FROM 0.34 TO 0.95

David Hill, Jr.

ARO, Inc.

September 1971

PROPULSION WIND TUNNEL FACILITY
ARNOLD ENGINEERING DEVELOPMENT CENTER
AIR FORCE SYSTEMS COMMAND
ARNOLD AIR FORCE STATION, TENNESSEE

NOTICES

When U. S. Government drawings specifications, or other data are used for any purpose other than a definitely related Government procurement operation, the Government thereby incurs no responsibility nor any obligation whatsoever, and the fact that the Government may have formulated, furnished, or in any way supplied the said drawings, specifications, or other data, is not to be regarded by implication or otherwise, or in any manner licensing the holder or any other person or corporation, or conveying any rights or permission to manufacture, use, or sell any patented invention that may in any way be related thereto.

Qualified users may obtain copies of this report from the Defense Documentation Center.

References to named commercial products in this report are not to be considered in any sense as an endorsement of the product by the United States Air Force or the Government.

INVESTIGATION OF THE SEPARATION CHARACTERISTICS OF VARIOUS STORES FROM THE A-7D AIRCRAFT AT MACH NUMBERS FROM 0.34 TO 0.95

David Hill, Jr.
ARO, Inc.

FOREWORD

The work reported herein was sponsored by the Air Force Armament Laboratory (DLGC/Lt Steve Braud), Air Force Armament Development and Test Center (ADTC), Air Force Systems Command (AFSC), under Program Element 27121F, System 337A.

The test results presented were obtained by ARO, Inc. (a subsidiary of Sverdrup & Parcel and Associates, Inc.), contract operator of the Arnold Engineering Development Center (AEDC), AFSC, Arnold Air Force Station, Tennessee, under Contract F40600-72-C-0003. The test was conducted April 19 and 20 and from May 28 through June 7, 1971, under ARO Project No. PC0147. The manuscript was submitted for publication on August 3, 1971.

This technical report has been reviewed and is approved.

George F. Garey
Lt Colonel, USAF
AF Representative, PWT
Directorate of Test

Joseph R. Henry
Colonel, USAF
Director of Test

ABSTRACT

Tests were conducted in the Aerodynamic Wind Tunnel (4T) using 0.05-scale models to investigate the separation characteristics of the unfinned and finned BLU-1C/B, M-117GP, MK-82GP, and MK-82SE when released from various wing pylon locations on the A-7D aircraft. Captive trajectory data were obtained at Mach numbers from 0.34 to 0.95 at simulated pressure altitudes from 5000 to 7000 ft. The parent aircraft angle of attack was varied from 1.8 to 12.3, depending on Mach number, climb angle, and simulated altitude. At selected test conditions, parent climb angles of 0, -35, -50, and -70 deg were simulated. In some cases, the separation trajectories of the BLU-1C/B were initiated at the end of the ejector piston stroke using flight-test data to determine the initial store positions and velocities. In general, the separation trajectories agreed well with flight-test data for the trajectory interval of the test. For the trajectory intervals of the test, most of the stores separated from the parent aircraft without store-to-parent contact.

CONTENTS

APPENDIXES

I. ILLUSTRATIONS

Figure

Figure | Page

Figure | Page

II. TABLES

Page

II. TABLES (Continued)

NOMENCLATURE

BL	Aircraft buttock line from plane of symmetry, in., model scale
b	Store reference diameter, ft
C_A	Store axial-force coefficient, axial force/$q_\infty S_m$
C_ℓ	Store rolling-moment coefficient, rolling moment/$q_\infty S_m b_m$
C_m	Store pitching-moment coefficient, referenced to the store cg, pitching moment/$qS_m \bar{c}_m$
C_{m_q}	Store pitch-damping derivative, $dC_m/d(q\bar{c}/2V_\infty)$
C_N	Store normal-force coefficient, normal force/$q_\infty S_m$
C_n	Store yawing-moment coefficient, referenced to the store cg, yawing moment/$q_\infty S_m b_m$
C_{n_r}	Store yaw-damping derivative, $dC_n/d(rb/2V_\infty)$
C_Y	Store side-force coefficient, side force/$q_\infty S_m$
$\bar{c}$	Store reference length, ft
FS	Aircraft fuselage station, in., model scale
F_Z	MER/TER ejector force, lb
F_{Z_1}	Pylon forward ejector force, lb
F_{Z_2}	Pylon aft ejector force, lb
H	Pressure altitude, ft
I	Total linear impulse, lb-sec

I_{xx} Full-scale moment of inertia about the store X_B axis, slug-ft^2

I_{yy} Full-scale moment of inertia about the store Y_B axis, slug-ft^2

I_{zz} Full-scale moment of inertia about the store Z_B axis, slug-ft^2

I_a Total angular impulse, ft-lb-sec

M_∞ Free-stream Mach number

$\overline{m}$ Full-scale store mass, slugs

p Store angular velocity about the X_B axis, radians/sec

p_∞ Free-stream static pressure, psfa

q Store angular velocity about the Y_B axis, radians/sec

q_∞ Free-stream dynamic pressure of wind tunnel, psf

r Store angular velocity about the Z_B axis, radians/sec

S Store reference area ($\pi b^2/4$), ft^2

t Real trajectory time from initiation of trajectory, sec

u Velocity of the full-scale store in the positive X_B direction relative to the origin of the flight-axis system, ft/sec

V_∞ Free-stream velocity, ft/sec

v Velocity of the full-scale store in the positive Y_B direction relative to the origin of the flight-axis system, ft/sec

WL Aircraft waterline from reference horizontal plane, in., model scale

w Velocity of the full-scale store in the positive Z_B direction relative to the origin of the flight-axis system, ft/sec

X Separation distance of the store cg parallel to the flight axis system X_F direction, ft, full scale measured from the prelaunch position

X_{cg} Full-scale cg location, ft, from nose of store

X_L Ejector piston location relative to the store cg, positive forward of store cg, ft full scale

X_{L_1} Forward ejector piston location relative to the store cg, positive forward of store cg, ft, full scale

X_{L_2} Aft ejector piston location relative to the store cg, positive forward of store cg, ft, full scale

Y Separation distance of the store cg parrallel to the flight-axis system Y_F direction, ft, full scale measured from the prelaunch position

Z Separation distance of the store cg parallel to the flight-axis system Z_F direction, ft, full scale measured from the prelaunch position

ZE Ejector stroke length, ft, full scale

α Parent-aircraft model angle of attack relative to the free-stream velocity vector, deg

θ Angle between the store longitudinal axis and its projection in the X_F-Y_F plane, positive when store nose is raised as seen by pilot, deg

$\Delta\theta$ Change in θ from its value when the store is in the carriage position, deg

$\overline{\theta}$ Simulated parent-aircraft climb angle; angle between the flight direction and the earth horizontal, deg, positive for increasing altitude

ϕ Angle between the projection of the store lateral axis in the Y_F-Z_F plane and the Y_F axis, positive for clockwise rotation when looking upstream, deg

ψ Angle between the projection of the store longitudinal axis in the X_F-Y_F plane and the X_F axis, positive then the store nose is to the right as seen by the pilot, deg

$\Delta\psi$ Change in ψ from its value when the store is in the carriage position, deg

SUBSCRIPTS

i Conditions at the end of the ejector stroke

m Model scale

FLIGHT-AXIS SYSTEM COORDINATES

Directions

X_F Parallel to the free-stream wind vector, positive direction is forward as seen by the pilot

Y_F Perpendicular to the X_F and Z_F directions, positive direction is to the right as seen by the pilot

Z_F In the aircraft plane of symmetry, perpendicular to the free-stream wind vector, positive direction is downward

The flight-axis system origin is coincident with the aircraft cg and remains fixed with respect to the parent aircraft during store separation. The X_F, Y_F, and Z_F coordinate axes do not rotate with respect to the initial flight direction and attitude.

STORE BODY-AXIS SYSTEM COORDINATES

Directions

X_B Parallel to the store longitudinal axis, positive direction is upstream in the launch position

Y_B Perpendicular to the store longitudinal axis, and parallel to the flight-axis system X_F-Y_F plane when the store is at zero roll angle, positive direction is to the right looking upstream when the store is at zero yaw and roll angles

Z_B Perpendicular to both the X_B and Y_B axes, positive direction is downward as viewed by the pilot when the store is at zero pitch and roll angles.

The store body-axis system origin is coincident with the store cg and moves with the store during separation from the parent airplane. The X_B, Y_B, and Z_B coordinate axes rotate with the store in pitch, yaw, and roll so that mass moments of inertia about the three axes are not time varying quantities.

SECTION I
INTRODUCTION

A captive trajectory test was conducted in the Aerodynamic Wind Tunnel (4T) to determine the separation characteristics of the unfinned and finned BLU-1C/B, M-117, MK-82GP, and MK-82SE bombs. Separation trajectories were initiated from both the pylon carriage positions and at the end of the ejector stroke for the unfinned BLU-1C/B. The remaining stores were separated from their respective carriage positions with simulated ejector forces acting on the stores.

To determine the separation trajectories, 0.05-scale models of the A-7D aircraft and the various stores were employed. The flight conditions simulated were Mach numbers from 0.34 to 0.95 and pressure altitudes from 5000 to 7000 ft. At selected test conditions, parent aircraft climb angles of 0, -35, -50, and -70 deg were simulated. The separation trajectories were initiated from various wing pylon locations on the parent aircraft. The ejector forces used were time or displacement variant functions provided by the Air Force Armament Development and Test Center (ADTC).

In addition to the separation trajectories, aerodynamic loads were measured on the unfinned and finned BLU-1C/B store models in their carriage position on the A-7D aircraft at Mach numbers from 0.70 to 1.05. At each Mach number, the parent aircraft angle of attack was varied from 0 to 16 deg.

SECTION II
APPARATUS

2.1 TEST FACILITY

The Aerodynamic Wind Tunnel (4T) is a closed-loop, continuous flow, variable-density tunnel in which the Mach number can be varied from 0.2 to 1.3. At all Mach numbers, the stagnation pressure can be varied from 200 to 3400 psfa. The test section is 4 ft square and 12.5 ft long with perforated, variable porosity (0.5- to 10-percent open) walls. It is completely enclosed in a plenum chamber from which the air can be evacuated, allowing part of the tunnel airflow to be removed through the perforated walls of the test section.

For store separation testing, two separate and independent support systems are used to support the models. The parent aircraft model is inverted in the test section and supported by an offset sting attached to the main pitch sector. The store model is supported by the captive trajectory support (CTS) which extends down from the tunnel top wall and provides store movement (six degreees of freedom) independent of the parent-aircraft model. An isometric drawing of a typical store separation installation is shown in Fig. 1, Appendix I.

Also shown in Fig. 1 is a block diagram of the computer control loop used during captive trajectory testing. The analog system and the digital computer work as an integrated unit and, utilizing required input information, control the store movement during a

trajectory. Store positioning is accomplished by use of six individual d-c electric motors. Maximum translational travel of the CTS is ±15 in. from the tunnel centerline in the lateral and vertical directions and 36 in. in the axial direction. Maximum angular displacements are ±45 deg in pitch and yaw and ±360 deg in roll. A more complete description of the test facility can be found in the Test Facilities Handbook.[1] A schematic showing the test section details and the location of the models in the tunnel is shown in Fig. 2.

2.2 TEST ARTICLES

The test articles were 0.05-scale models of the A-7D parent aircraft and the various stores. A sketch showing the basic dimensions of the A-7D parent model is shown in Fig. 3. Details and dimensions of the pylons, Multiple Ejection Rack (MER), and Triple Ejection Rack (TER) are shown in Figs. 4, 5, and 6, and the store models are shown in Figs. 7 through 12.

The A-7D parent model was geometrically similar to the full-scale airplane except for some modifications incident to the wind tunnel installation and CTS operation. Horizontal tail surfaces were removed because of interference with the CTS support. The parent model was inverted in the tunnel and attached by a 23-deg offset sting to the main sting support system (Fig. 2). Figure 13 shows a typical tunnel installation photograph of the parent aircraft and store model.

The A-7D aircraft has three pylon stations on each wing. The mounting surfaces of all three pylons are inclined at a 3.0-deg nose-down angle with respect to the aircraft waterline.

The store models were mounted on an internal balance which was an integral part of a 30-deg offset sting. The sting was in turn connected to the CTS support (Figs. 2 and 13).

2.3 INSTRUMENTATION

Five- and six-component, internal strain-gage balances were used to obtain the force and moment data on the store models. Translational and angular positions of the store models were obtained from the CTS analog outputs. The parent-aircraft angle of attack was set using an absolute angle-of-attack indicator located in the nose of the parent model. The CTS was electrically connected to automatically stop and give a visual indication if the store model or sting contacted the parent-aircraft surface. Spring-loaded plungers were located in the pylons, MER, and TER in order to provide a position indication when the store model was in the launch position. The plunger circuit was independent of the parent-aircraft grounding circuit.

---

[1] Test Facilities Handbook (Ninth Edition). "Propulsion Wind Tunnel Facility, Vol. 4." Arnold Engineering Development Center, July 1971.

SECTION III
TEST DESCRIPTION

3.1 TEST CONDITIONS

For the carriage loads investigation, pitch polar data were obtained at Mach numbers from 0.70 to 1.05. The tunnel stagnation pressure was varied to produce a free-stream dynamic pressure from 500 to 1000 psf. Tunnel stagnation temperature varied between 90 and 120°F. The tunnel conditions were held constant while each configuration was tested through a range of angle of attack.

Separation trajectory data were obtained at Mach numbers from 0.34 to 0.95. Tunnel dynamic pressure ranged from 250 psf at $M_\infty = 0.34$ to 500 psf at $M_\infty = 0.95$, and tunnel stagnation temperature was maintained near 110°F.

Tunnel conditions were held constant at the desired Mach number and stagnation pressure while data for each trajectory were obtained. The trajectories were terminated when the store or sting contacted the parent-aircraft model or when a CTS limit was reached.

3.2 DATA ACQUISITION

To obtain carriage loads data, test conditions were established in the tunnel, and the parent model was positioned at the desired initial angle of attack. The store model was then automatically moved by the CTS to its carriage position at the touch point. At this point, the force and moment data were recorded. The store model was then automatically moved clear of the parent model, and the next data point was initiated by a manually controlled angle-of-attack movement of the parent model.

The force and moment coefficients were calculated using the dimensions (Appendix II, Table I) of the actual weapons as supplied by ADTC. The maximum store model diameter was used in calculating the reference area, and the longitudinal length of the store model was used as the reference length in calculating the pitching-moment coefficients.

To obtain a trajectory, test conditions were established in the tunnel and the parent model was positioned at the desired angle of attack. The store model was then oriented to a position corresponding to the store carriage location (or position at the end of the ejector stroke). After the store was set at the desired initial position, operational control of the CTS was switched to the digital computer which controlled the store movement during the trajectory through commands to the CTS analog system (see block diagram, Fig. 1). Data from the wind tunnel, consisting of measured model forces and moments, wind tunnel operating conditions, and CTS rig positions, were input to the digital computer for use in the full-scale trajectory calculations.

The digital computer was programmed to solve the six-degree-of-freedom equations to calculate the angular and linear displacements of the store relative to the parent aircraft pylon. In general, the program involves using the last two successive measured values of

each static aerodynamic coefficient to predict the magnitude of the coefficients over the next time interval of the trajectory. These predicted values are used to calculate the new position and attitude of the store at the end of the time interval. The CTS is then commanded to move the store model to this new position and the aerodynamic loads are measured. If these new measurements agree with the predicted values, the process is continued over another time interval of the same magnitude. If the measured and predicted values do not agree within the desired precision, the calculation is redone over a time interval one-half the previous value. This process is repeated until a complete trajectory has been obtained.

In applying the wind tunnel data to the calculations of the full-scale store trajectories, the measured forces and moments are reduced to coefficient form and then applied with proper full-scale store dimensions and flight dynamic pressure. Dynamic pressure was calculated using a flight velocity equal to the free-stream velocity component plus the components of store velocity relative to the aircraft, and a density corresponding to the simulated altitude.

The initial portion of each trajectory from the carriage position incorporated simulated ejector forces in addition to the measured aerodynamic forces acting on the store. The ejector force functions for the stores are presented in Figs. 15 and 16. The ejector force was considered to act perpendicularly to the rack or pylon mounting surface. The locations of the applied ejector forces and other full-scale store parameters used in the trajectory calculations are listed in Table I, Appendix II.

For trajectories started at the end of the ejector stroke, store parameters and orientations from flight-test data were used as initial conditions. The flight test data are listed in Table II, Appendix II. The different sets of data in the table represent store parameters, flight conditions, and aircraft wing-loading configurations determined for specific flight tests.

3.3 CORRECTIONS

Balance, sting, and support deflections caused by the aerodynamic loads on the store models were accounted for in the data reduction program to calculate the true store-model angles. Corrections were also made for model weight tares to calculate the net aerodynamic forces on the store model.

3.4 PRECISION OF DATA

Uncertainties in the data on the store models were calculated taking into consideration probable inaccuracies in the balance measurements and tunnel conditions. The uncertainties in the coefficients are based on a 95-percent confidence level, and are presented in Table III.

The trajectory data are subject to error from several sources including tunnel conditions, balance measurements, extrapolation tolerances allowed in the predicted coefficients, computer inputs, and CTS positioning control. Maximum error in the CTS

position control was ±0.05 in. for the translational settings and ±0.15 deg for angular displacement settings in pitch and yaw. Extrapolation tolerances were ±0.10 for each of the aerodynamic coefficients. The maximum uncertainties in the full-scale position data caused by the balance precision limitations are given in Table IV. The estimated uncertainty in setting Mach number was no greater than ±0.003, and the uncertainty in parent-model angle of attack was estimated to be ±0.1 deg.

SECTION IV
RESULTS AND DISCUSSION

4.1 GENERAL

The data presented herein consist of aerodynamic coefficient variations with parent angle of attack for the BLU-1C/B in its carriage position (Figs. 17 through 19), effects of ejector-force variation on the separation trajectories of the BLU-1C/B (Fig. 20), effects of BLU-1C/B store-parameter variation on the separation trajectories (Figs. 21 through 26), the effects of wing-loading configuration and Mach number on the separation trajectories of the BLU-1C/B, M-117, MK-82GP, and MK-82SE bombs (Figs. 27 through 40).

In the trajectory data, the full-scale linear and angular displacements of the store relative to the carriage positions on the rack or pylon are presented as functions of full-scale trajectory time.

Table V describes the wing loading configurations used in the data presentation. The L or R notation for each configuration number denotes left or fight wing, respectively. In general, for the trajectory intervals of this test, most of the stores separated from the parent aircraft without store-to-parent contact. For data with trajectory flight times less than 0.10 sec, store-to-parent aircraft contact occurred.

4.2 AERODYNAMIC COEFFICIENTS OF THE BLU-1C/B

Figures 17 through 19 show the effect of parent aircraft angle of attack, aircraft wing-loading configuration, and Mach number on the aerodynamic coefficients of the finned and unfinned BLU-1C/B in their carriage positions on the A-7D aircraft. The aerodynamic coefficients are affected more by the flow field for the side carriage positions (configurations 2 and 4) on the MER than for the bottom (configurations 1 and 3) carriage position on the MER.

4.3 EJECTOR FORCE EFFECTS - BLU-1C/B TRAJECTORIES

Figure 20 shows several separation trajectories of the BLU-1C/B from one carriage position resulting from initiation with various ejection force functions. The ejection force function T3 was obtained from ADTC and was derived from static calibrations. The resulting separation trajectory is significantly different from flight-test trajectory data. Because of the disagreement, an attempt was made to evaluate the effects of the assumed ejector force function on the separation trajectory. Ejector force functions T2 and D1

were derived from ejector force function T3 (same total linear and angular impulse as T3). The ejector force function T2 is an average force equivalent to T3. Ejector force function DI is the force variation with displacement of the ejector foot. It was derived from ejector force function T3 and displacement varitions obtained from the flight-test data. Figure 20 shows the trajectory resulting from both ejector functions T2 and D1. The separation trajectories are approximately the same as the trajectory initiated with ejector force function T3.

Figure 20 also shows two trajectories without simulated ejector forces which were initiated using unpublished flight-test trajectory data supplied by ADTC. The time, linear and angular velocities, and store orientations (Table II, Set 1) were determined at a position in the trajectory when the BLU-1C/B was no longer subjected to ejector force. These store parameters and orientations were used to initiate the trajectories in the wind tunnel. For the separation time interval shown, the resultant trajectories agreed well with the flight-test trajectory data. These two trajectories were obtained during two different wind tunnel entries and show good repeatability.

As a result of this agreement, the ejector force function T1 was calculated from the flight-test data. The calculation is shown in Appendix III. The separation trajectory resulting from use of ejector force T1 is also shown in Fig. 20. This separation trajectory is in good agreement with the two trajectories initiated from positions obtained from flight test data.

In summary, these data indicate the influence of ejector force on the subsequent motion of the BLU-1C/B store. It appears that the shape of the force/time or force/displacement function used has little effect as long as the total linear and angular impulses are the same. However, ejector force functions obtained from static ground calibrations did not correspond to forces inferred from store motions determined from flight-test data. When the initial motions are matched, the wind-tunnel-generated trajectories agree well with the flight data, indicating that the aerodynamic flow field is properly simulated.

4.4 STORE PARAMETER AND TEST CONDITION EFFECTS - BLU-1C/B TRAJECTORIES

Figures 21 through 25 show the effects of varying the store cg location, damping derivatives, aircraft climb angle, Mach number, and aircraft angle of attack, respectively, on the separation trajectories of the unfinned BLU-1C/B. To initiate the simulated trajectories, time, linear and angular velocities, and store orientation, parameters were derived (Table V, sets 2 and 3) from flight test data at the time of the trajectory when the BLU-1C/B was no longer subjected to ejector forces.

In general, there was no significant effect of varying the store parameters and test conditions. The largest deviation from the flight test data occurred for a change in the aircraft angle of attack.

Figure 26 shows separation trajectories for the unfinned BLU-1C/B initiated from two sets of store parameters, orientations, and velocities (Table V, sets 3 and 4) which were derived from flight test trajectory data. These data represent repeat trajectories for the same nominal flight conditions. The measured trajectories show good agreement with the flight test trajectory data.

4.5 TRAJECTORIES FOR VARIOUS STORE AND WING-LOADING CONFIGURATIONS

Figures 27 through 40 show the trajectories for stores released directly from carriage position. The time variant ejector forces and store parameters shown in Figs. 15 and 16, and Table I, respectively, were used in determining the trajectories.

Figures 27 and 28 show the effects of aircraft wing-loading configuration, and Figures 29 and 30 show the effects of Mach number and climb angle on the separation trajectories of the unfinned BLU-1C/B. Only the angular displacements were affected appreciably.

The effects of varying the wing-loading configuration on the separation trajectories of finned BLU-1C/B are shown in Figs. 31 and 32. The angular displacements, especially pitch, were affected appreciably by varying the wing loading configuration.

Figures 33 and 34 show the effects of wing-loading configuration and Fig. 35 shows the effect of Mach number on the separation of the M-117 from the center pylon. The angular displacements during the trajectories were affected appreciably by the presence of the unfinned BLU-1C/B or the SUU-42/A on the inboard or outboard pylon.

Figures 36 and 37 show the effects of wing-loading configuration and Fig. 38 shows the effect of Mach number on the separation of the MK-82GP from the center pylon. The angular displacements of the MK-82GP were appreciably affected by the presence of the finned BLU-1C/B on the inboard and outboard pylon. For the trajectory time interval shown, the effect of Mach number on the separation trajectories of the MK-82GP is insignificant.

Figure 39 shows the effect of the presence of the finned BLU-1C/B on the inboard and outboard pylon on the separation of the MK-82SE from various stations on the MER, center pylon. The angular displacements were significantly affected, whereas the linear displacements showed little or no effect.

SECTION V
CONCLUSIONS

Based on the results of this investigation to determine the separation characteristics of various bombs from the A-7D aircraft, the following conclusions were reached:

1. The aerodynamic coefficients of the finned and unfinned BLU-1C/B in the carriage position on the MER were affected more by the flow field on the MER side station than on the bottom station.

2. For the same total linear and angular impulse, the shape of the force/time or force/displacement ejector force function had little effect on the separation trajectories of the unfinned BLU-1C/B.

3. The ejector force functions of the unfinned BLU-1C/B obtained from static ground calibrations did not correspond to forces inferred from store motions determined from flight-test data.

4. When the initial store motions are matched, the wind-tunnel-generated trajectories of the unfinned BLU-1C/B agreed well with the flight data, indicating that the aerodynamic flow field is properly simulated.

5. There was no significant effect of store cg location, damping derivative variation, climb angle variation, angle-of-attack variation, and Mach number variation on the separation trajectories of the unfinned BLU-1C/B initiated at the end of the ejector piston stroke using flight-test trajectory data as initial conditions.

6. Good repeatability of separation trajectories was obtained for the unfinned BLU-1C/B from two separate wind tunnel tests.

7. In general, only the angular displacements measured in the trajectories of the finned BLU-1C/B, unfinned BLU-1C/B, M-117, MK-82GP, and MK-82SE were significantly affected by variations in aircraft wing-loading configurations and Mach number.

8. For the trajectory time intervals of this test, most of the stores separated from the parent aircraft without store-to-aircraft contact.

APPENDIXES

I. ILLUSTRATIONS
II. TABLES
III. EJECTOR FORCE CALCULATION

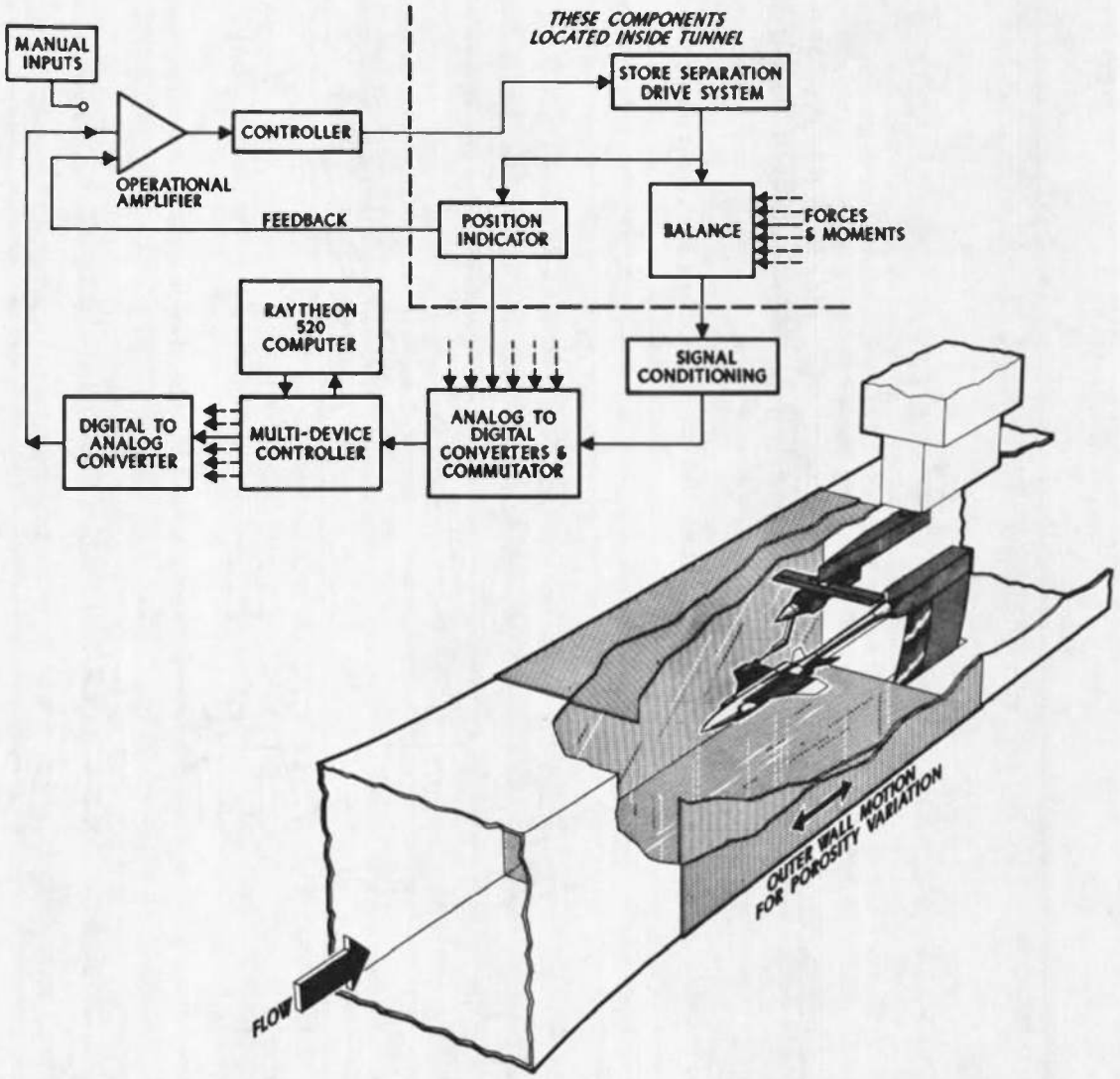

Fig. 1 Isometric Drawing of a Typical Store Separation Installation and a Block Diagram of the Computer Control Loop

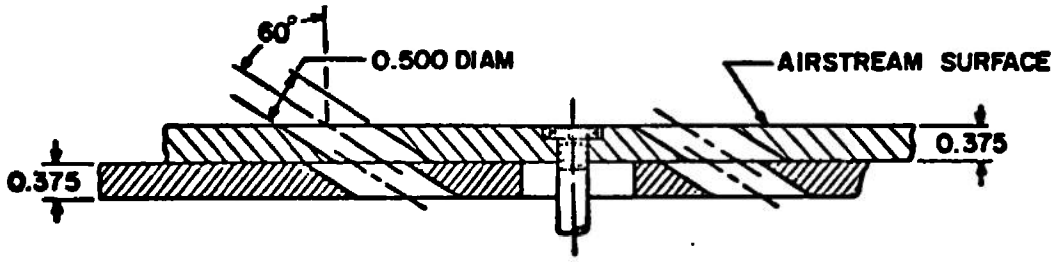

TYPICAL PERFORATED WALL CROSS SECTION

ALL DIMENSIONS AND TUNNEL STATIONS IN INCHES

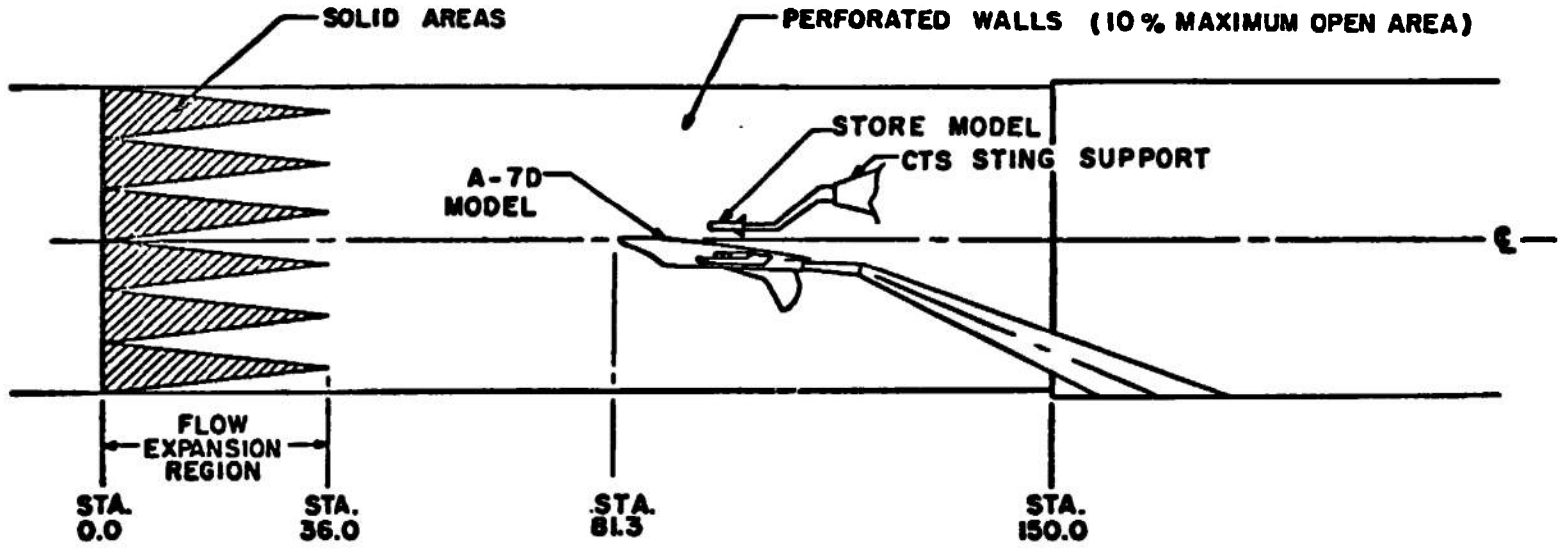

Fig. 2 Schematic of the Tunnel Test Section Showing Model Location

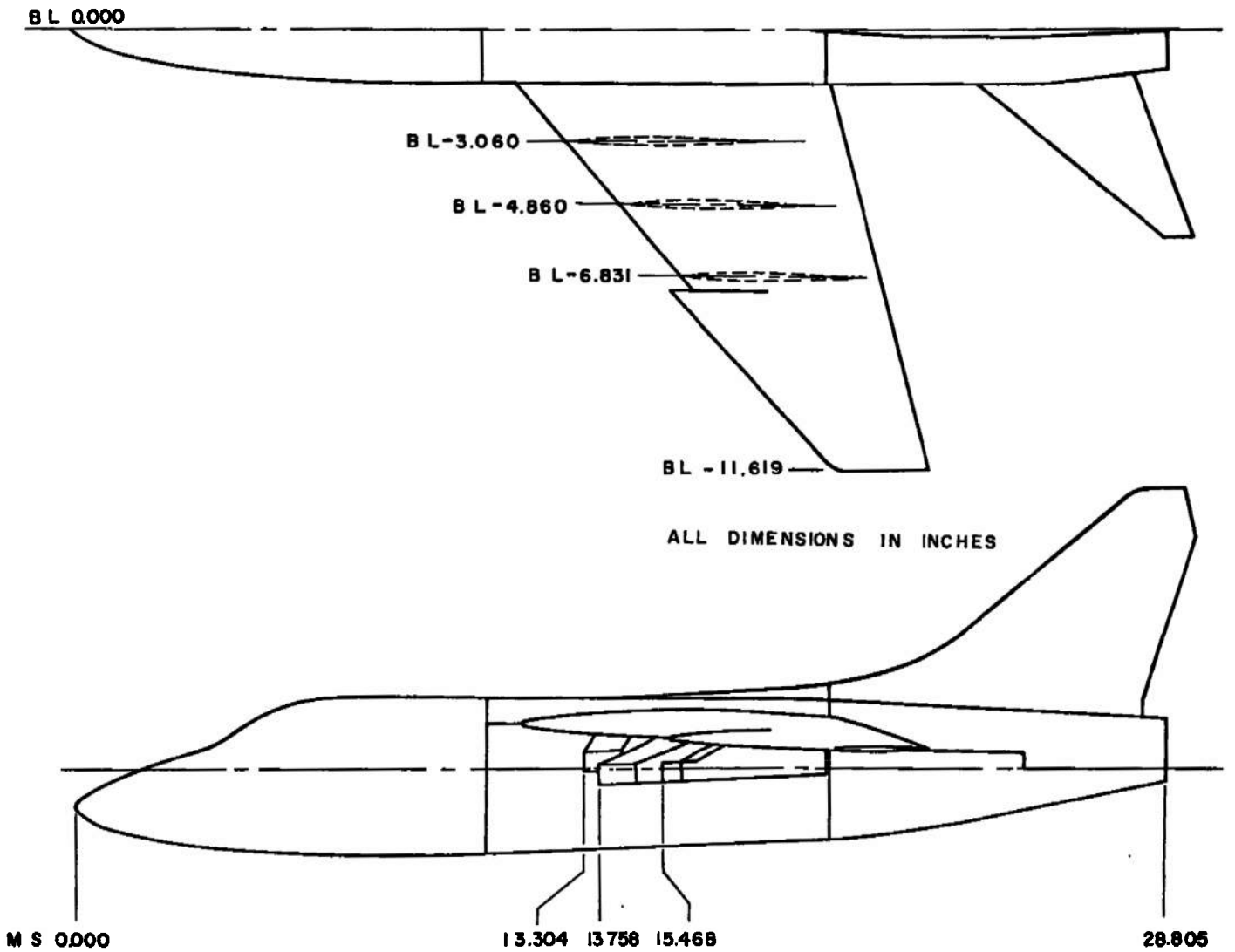

Fig. 3 Sketch of the A-7D Parent-Aircraft Model

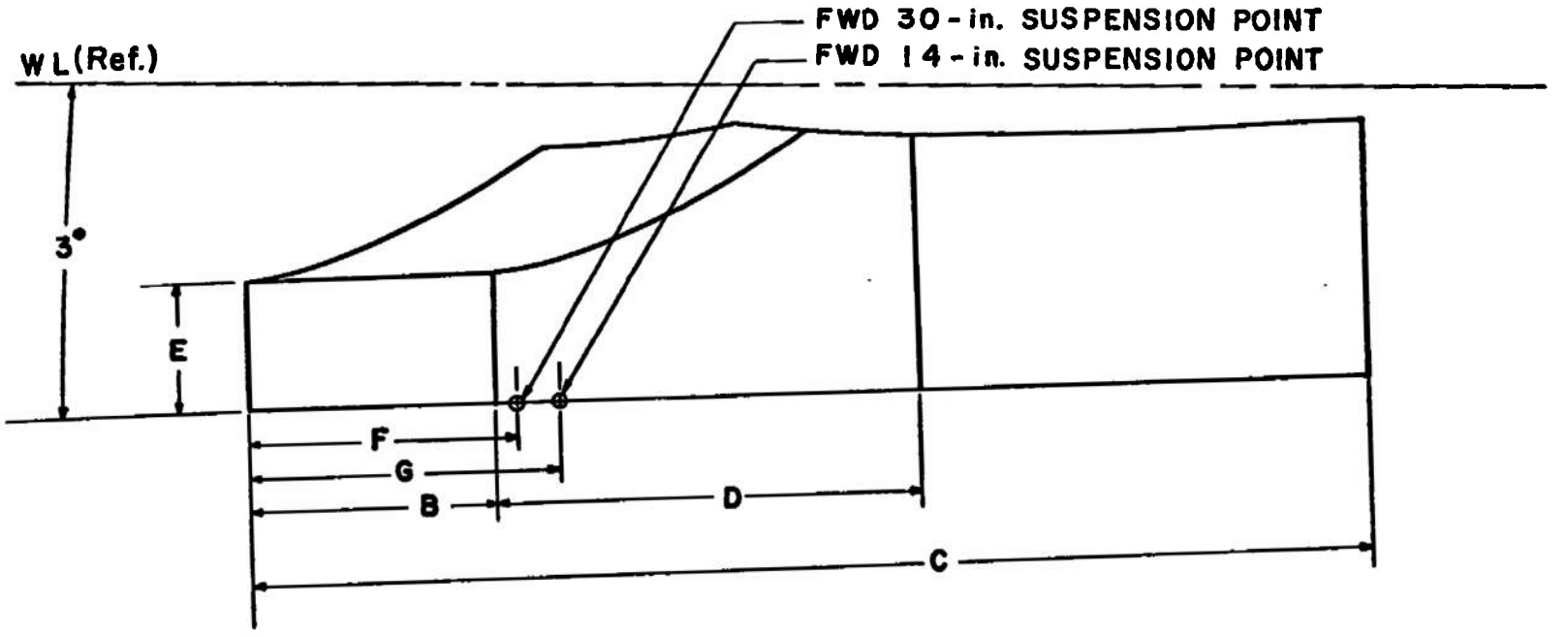

	INBOARD	CENTER	OUTBOARD
B	1.030	1.030	0.515
C	4.580	4.850	4.437
D	1.630	1.905	2.008
E	0.575	0.575	0.513
F	0.950	0.950	0.750
G	1.350	1.350	1.150

ALL DIMENSIONS IN INCHES

Fig. 4 Details and Dimensions of the A-7D Model Pylons

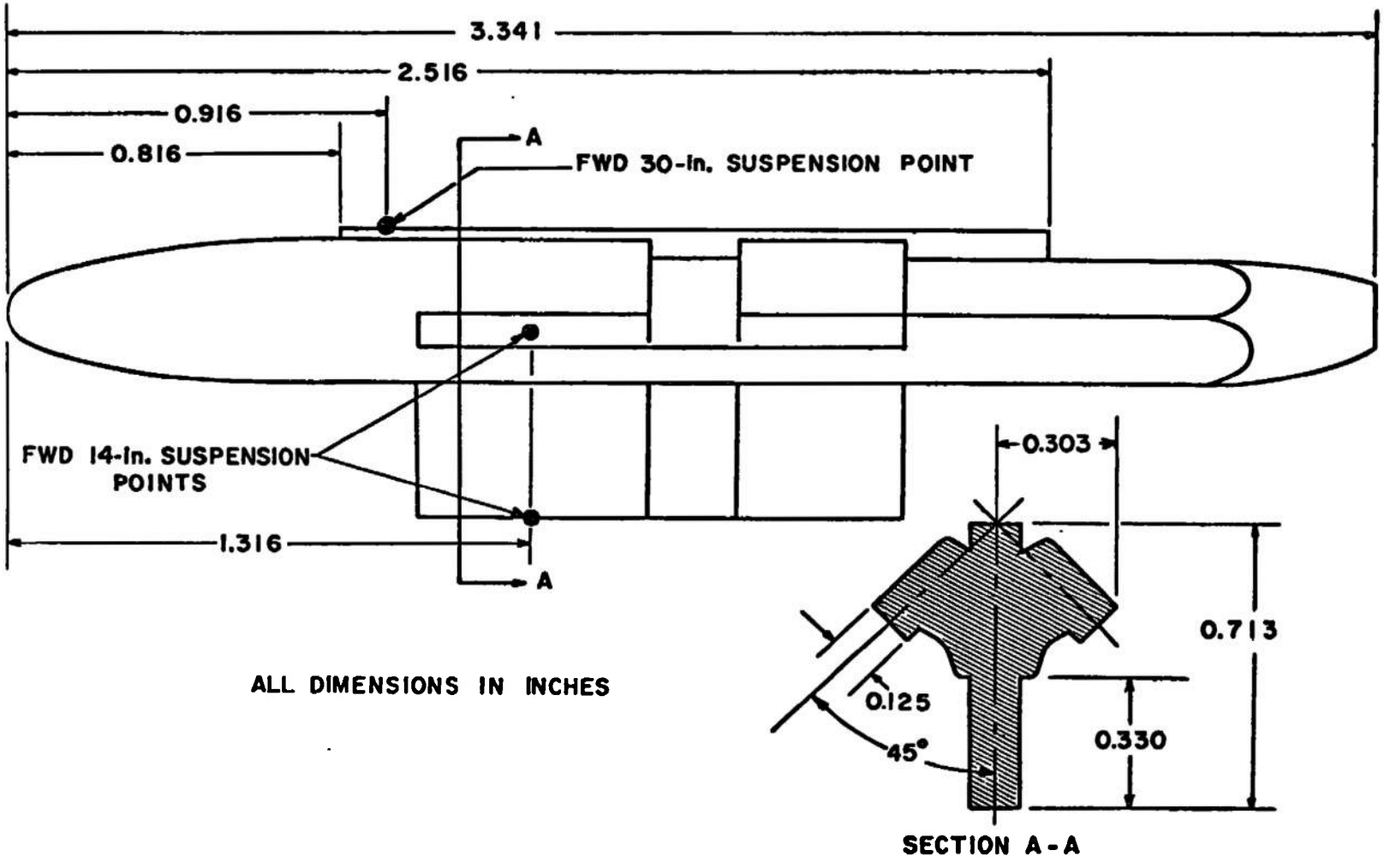

Fig. 5 Details and Dimensions of the TER Model

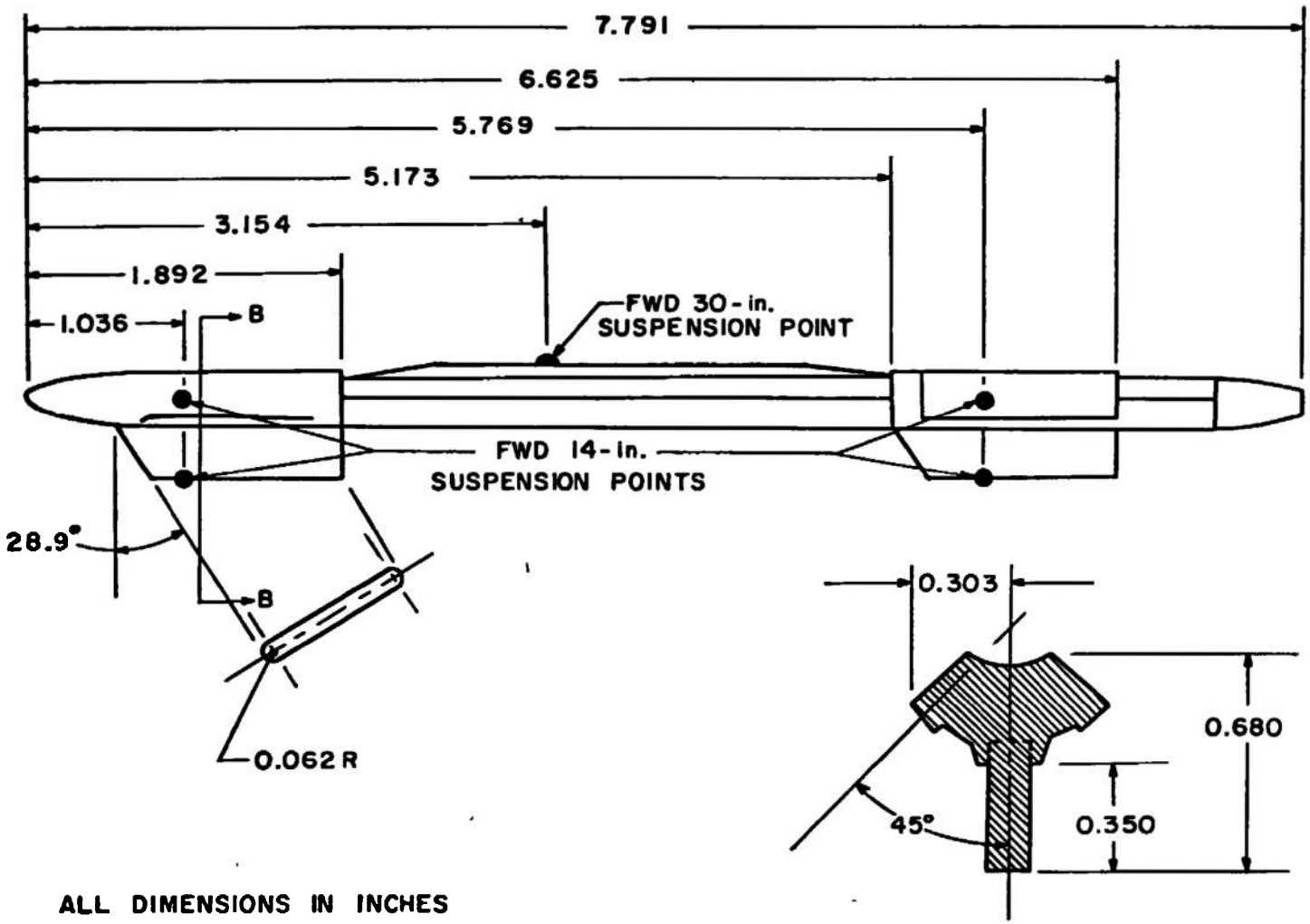

Fig. 6 Details and Dimensions of the MER Model

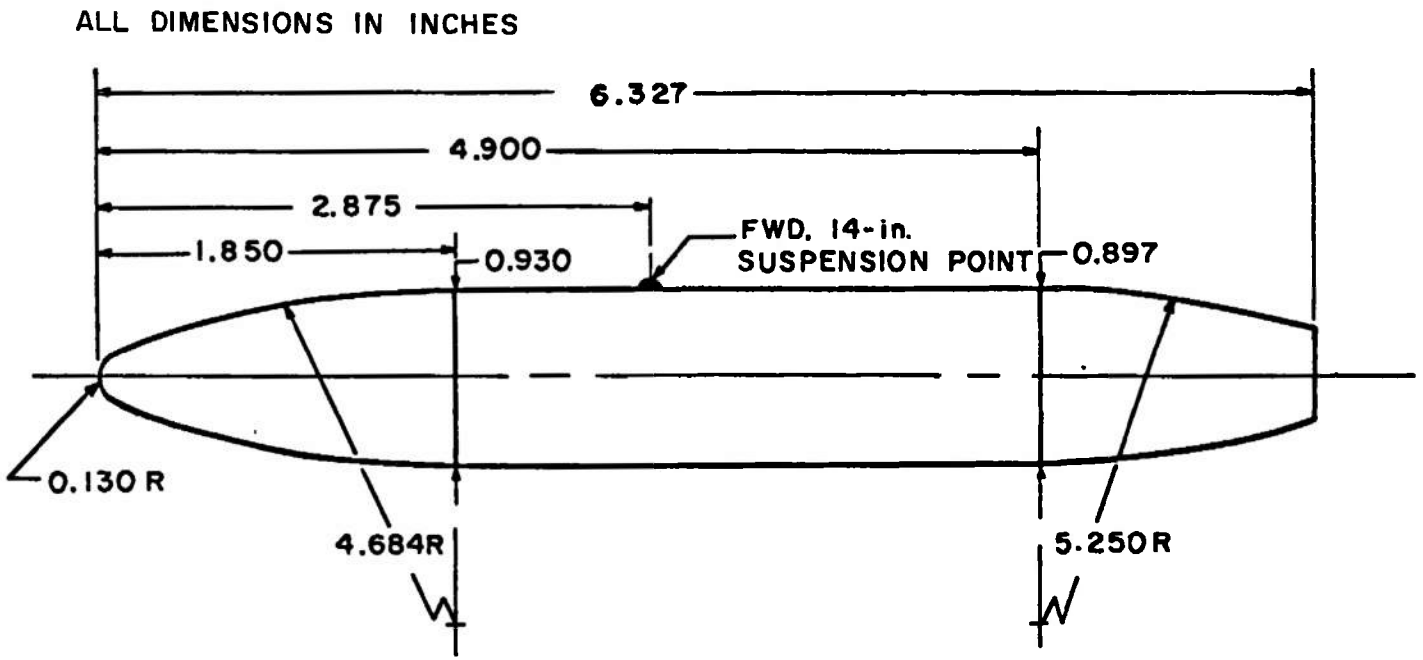

Fig. 7 Details and Dimensions of the BLU-1C/B Unfinned Model

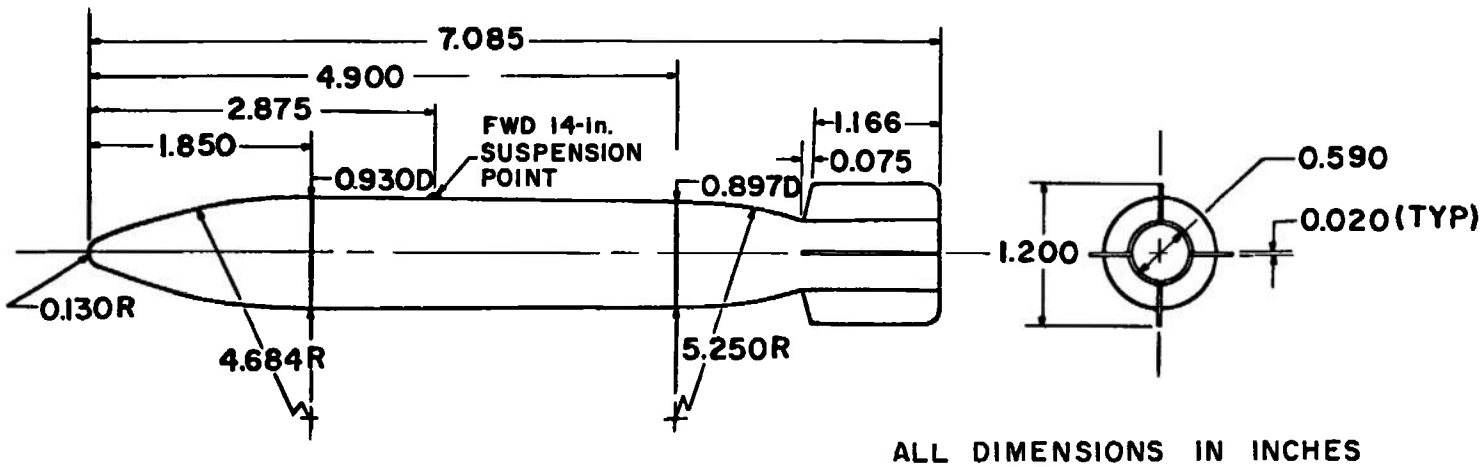

Fig. 8 Details and Dimensions of the BLU-1C/B Finned Model

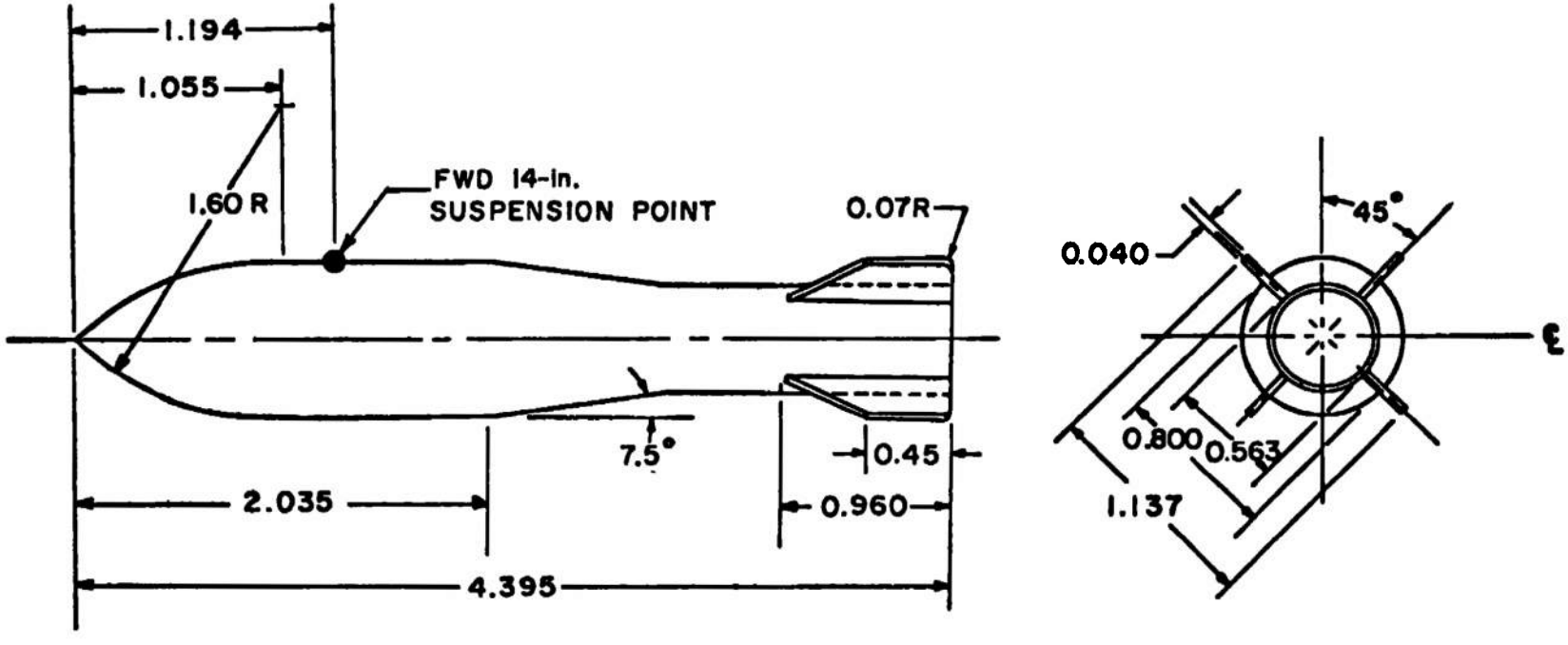

ALL DIMENSIONS IN INCHES

Fig. 9 Details and Dimensions of the M-117 Model

STA.	DIAM
0.000	0.150
0.210	0.150
0.212	0.231
0.312	0.282
0.412	0.322
0.512	0.361
0.612	0.391
0.712	0.421
0.812	0.445
0.912	0.465
1.012	0.483
1.112	0.497
1.212	0.510
1.312	0.520
1.412	0.525
1.512	0.530
1.612	0.532
1.712	0.533
1.812	0.535
1.912	0.537
2.312	0.537
2.412	0.535
2.512	0.525
2.612	0.520
2.712	0.510
2.812	0.497
2.912	0.483
3.012	0.465
3.173	0.438

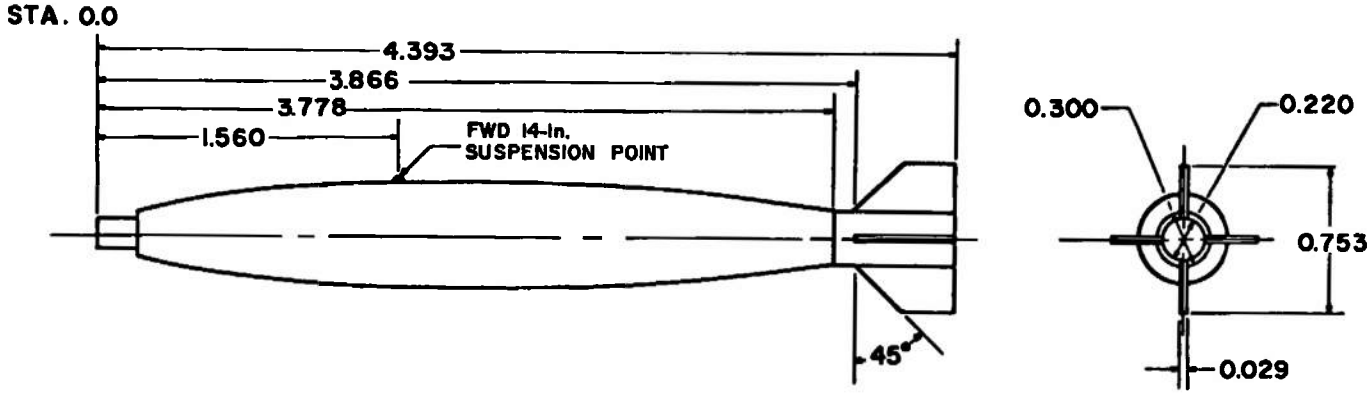

Fig. 10 Details and Dimensions of the MK-82GP Model

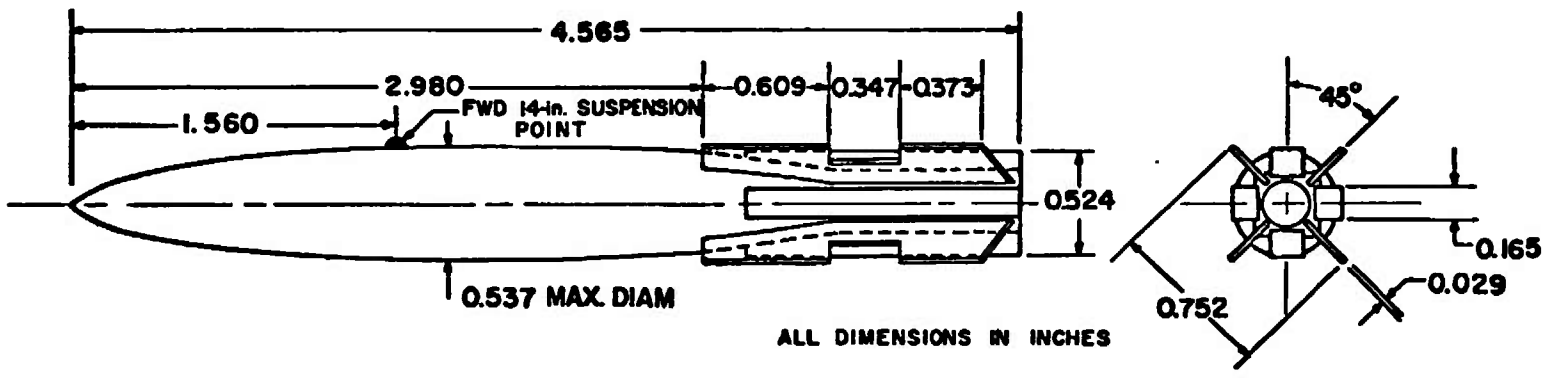

Fig. 11 Details and Dimensions of the MK-82SE Model

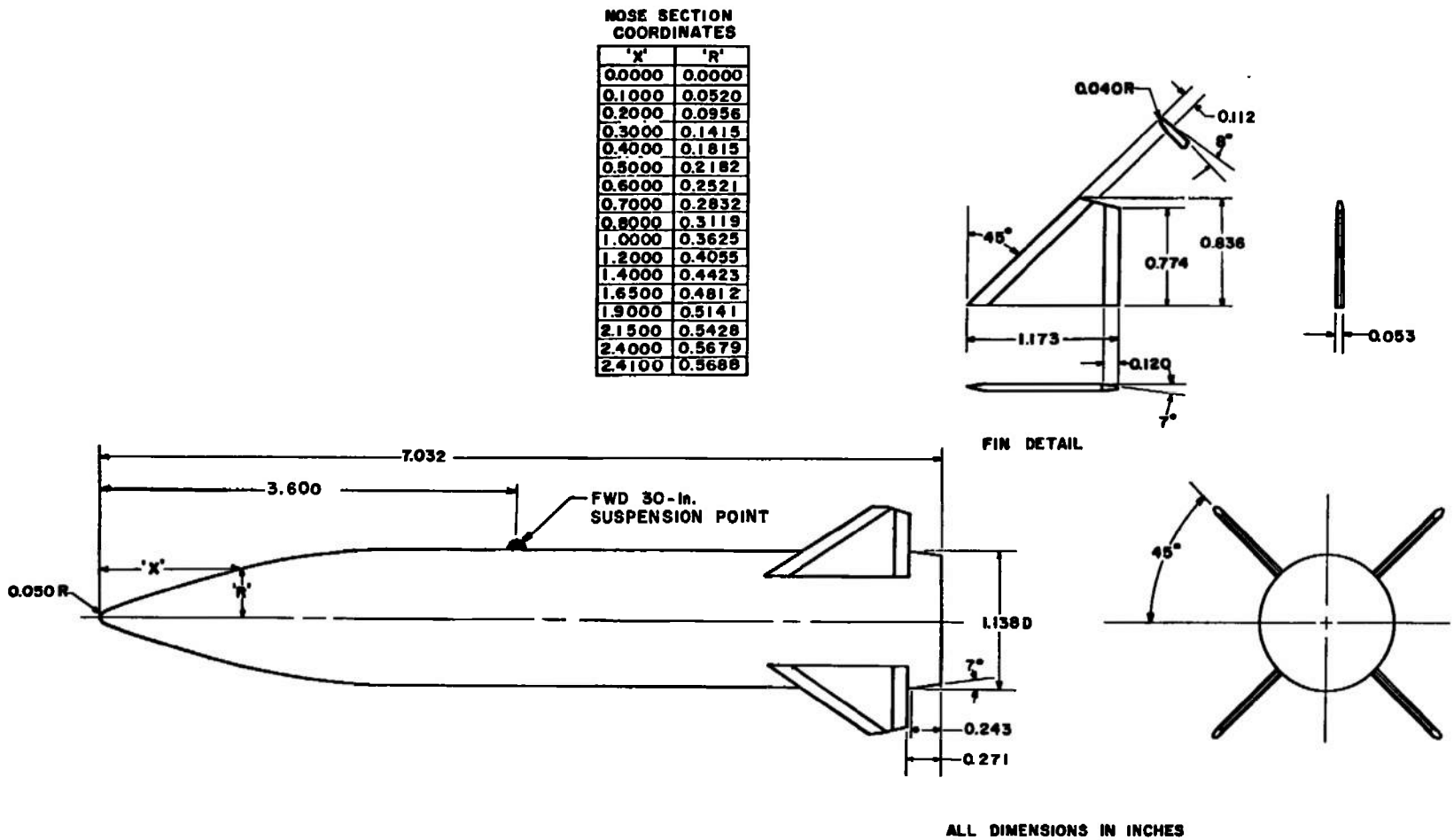

Fig. 12 Details and Dimensions of the SUU-42/A Model

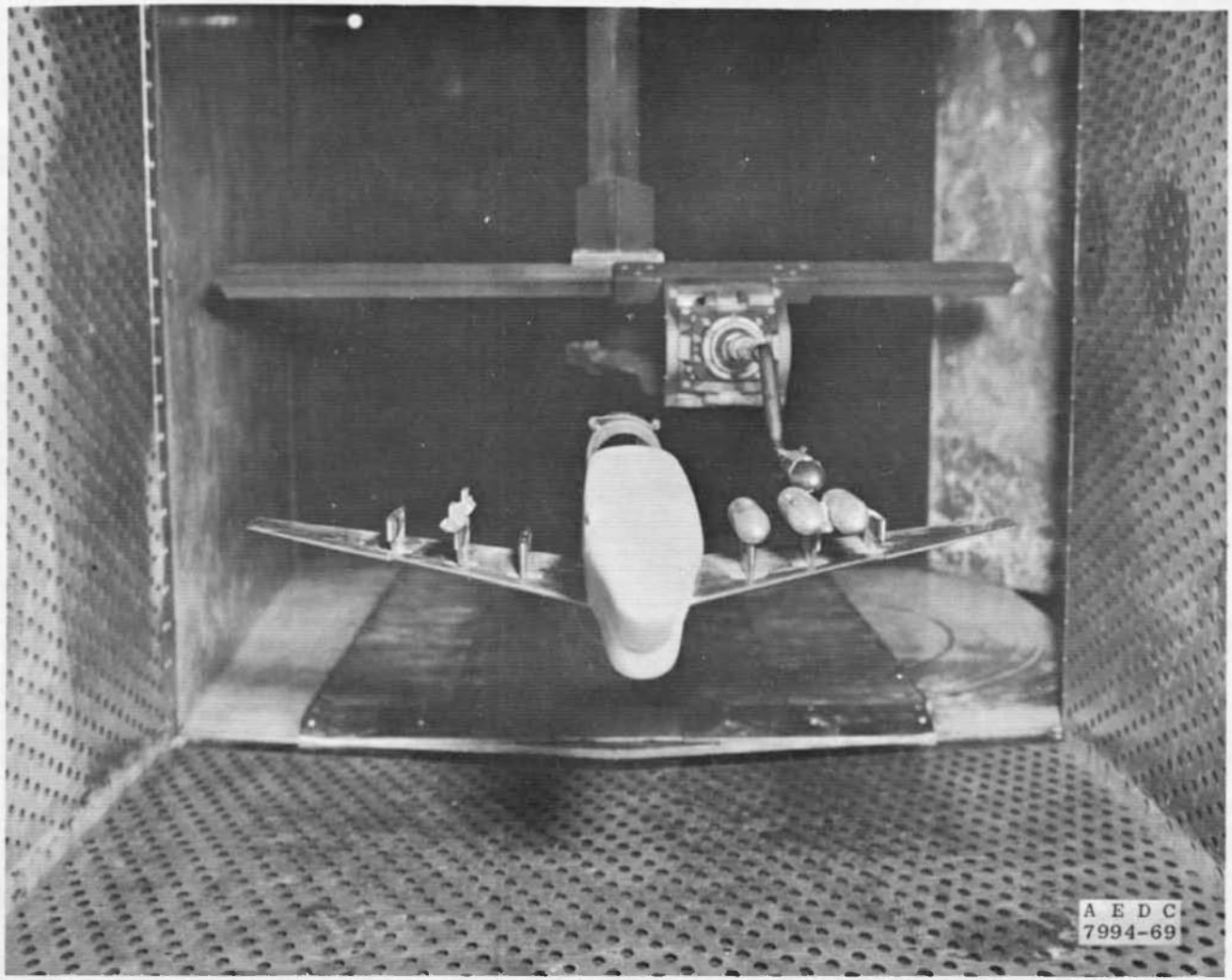

Fig. 13 Tunnel Installation Photograph Showing Parent Aircraft, Store, and CTS

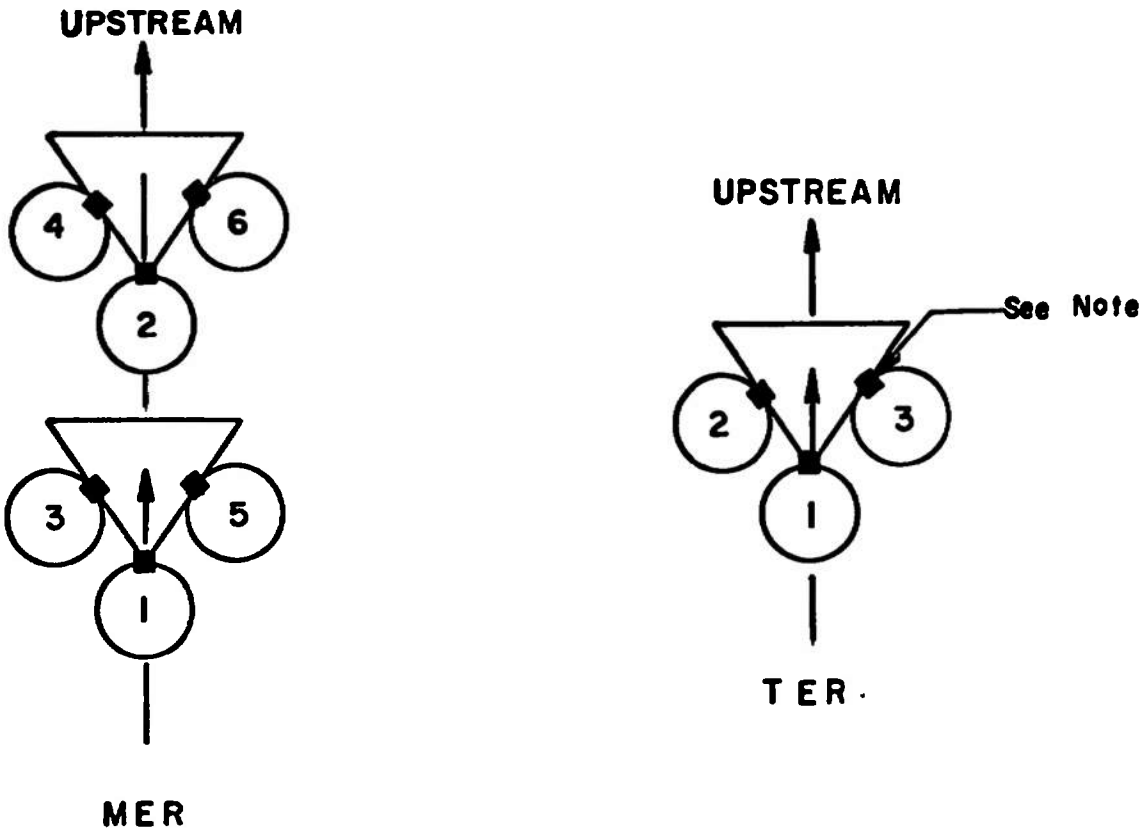

NOTE: The square indicates the orientation of the suspension lugs

TYPE RACK	STATION	ROLL ORIENTATION, deg
MER	1	0
	2	0
	3	45
	4	45
	5	-45
	6	-45
TER	1	0
	2	45
	3	-45

Fig. 14 Schematic of the TER and MER Store Stations and Orientations

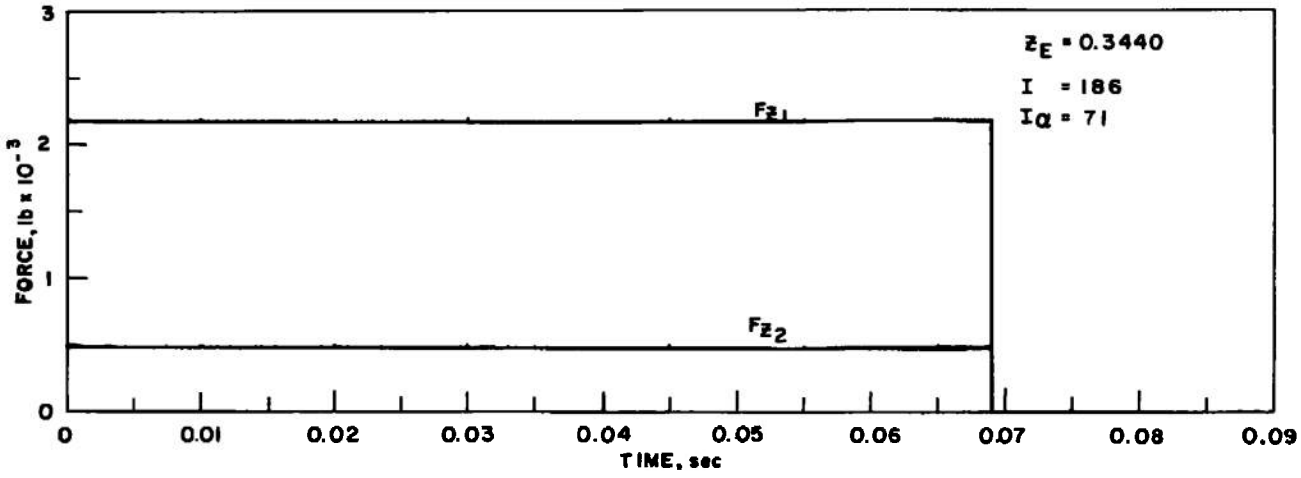

a. Time Function, T1

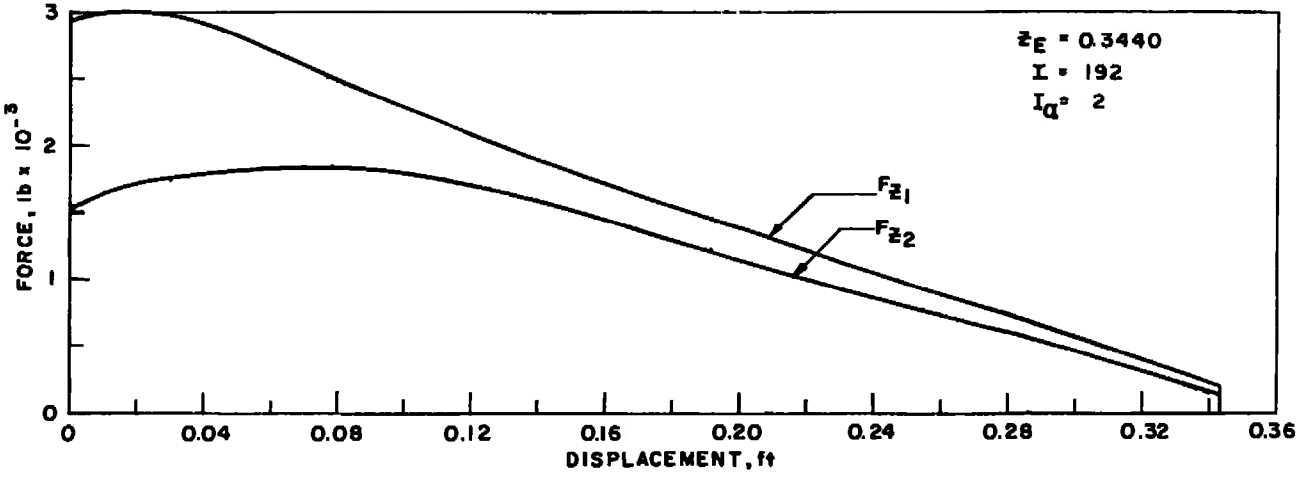

b. Displacement Function, D1

Fig. 15 Pylon Ejector Force Functions for BLU-1C/B Store

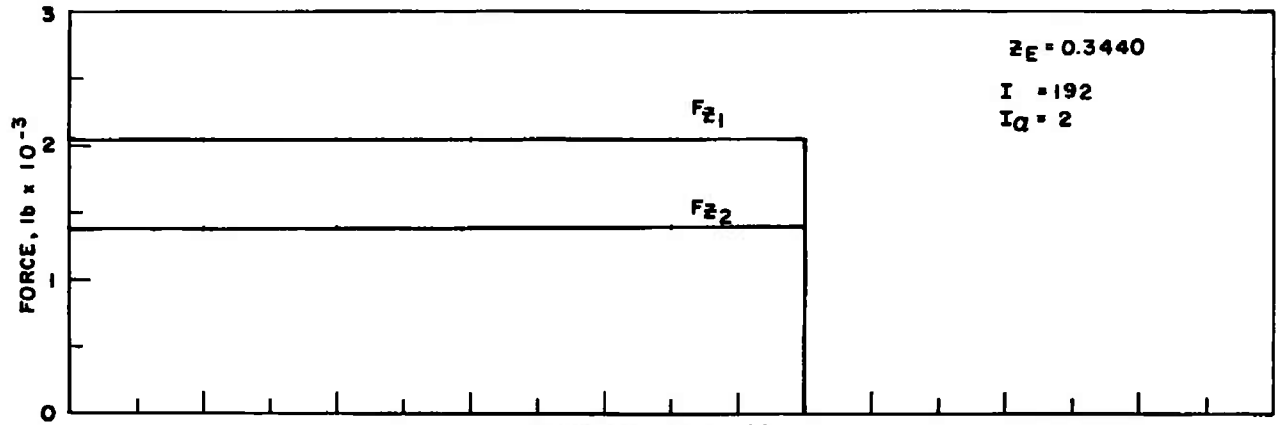

c. Time Function, T2

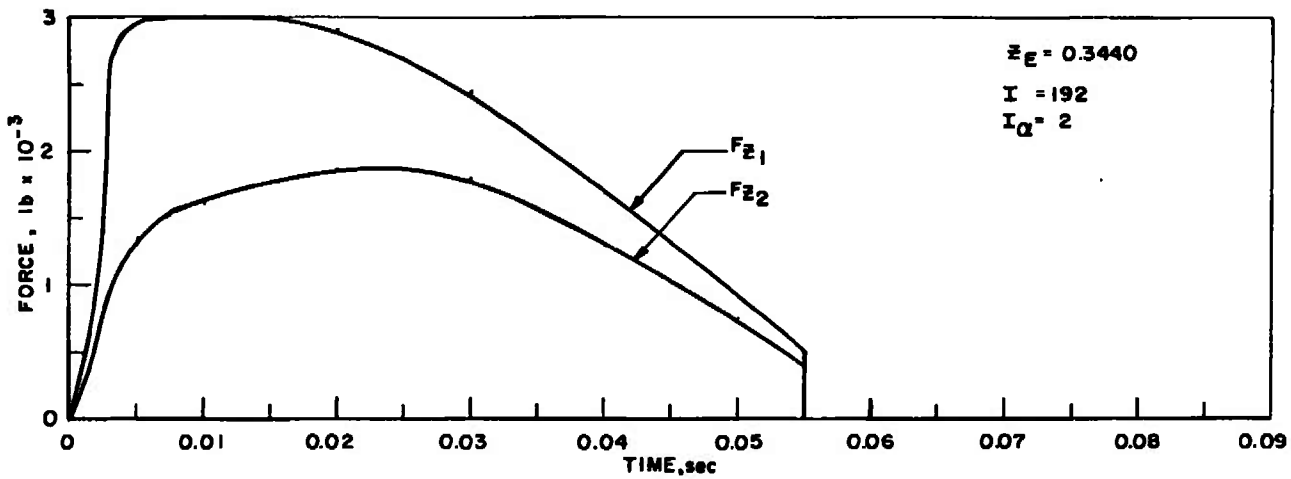

d. Time Function, T3

Fig. 15 Continued

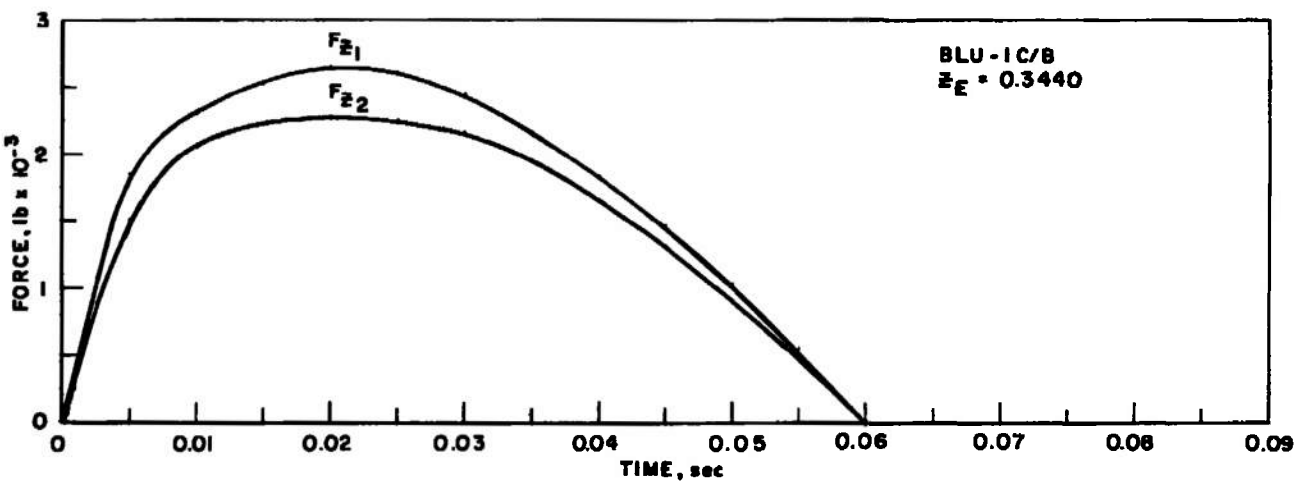

e. Time Function, T4
Fig. 15 Concluded

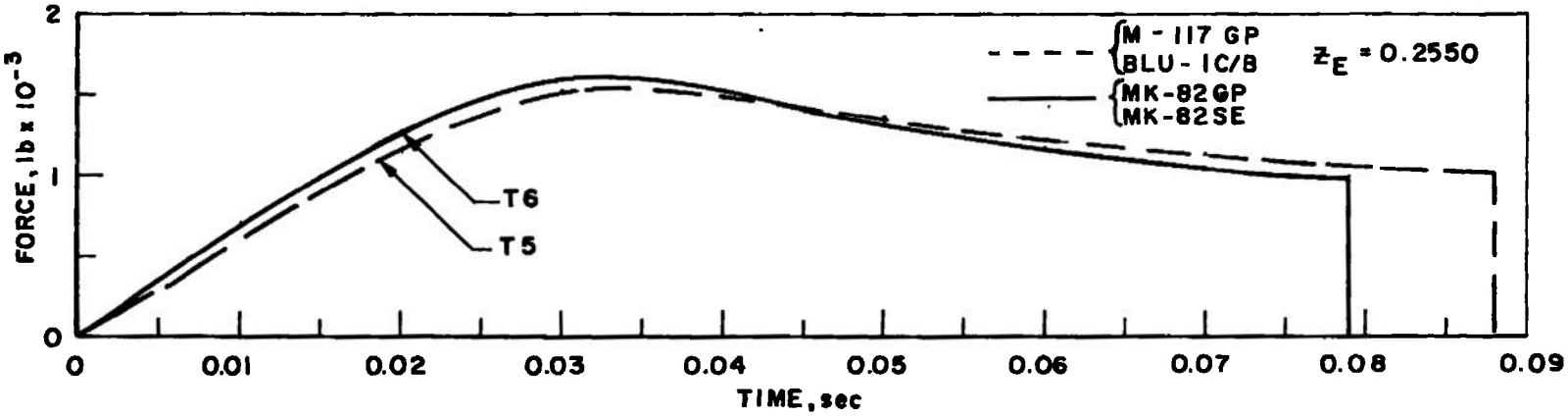

Fig. 16 MER/TER Ejection Force Functions, T5 and T6

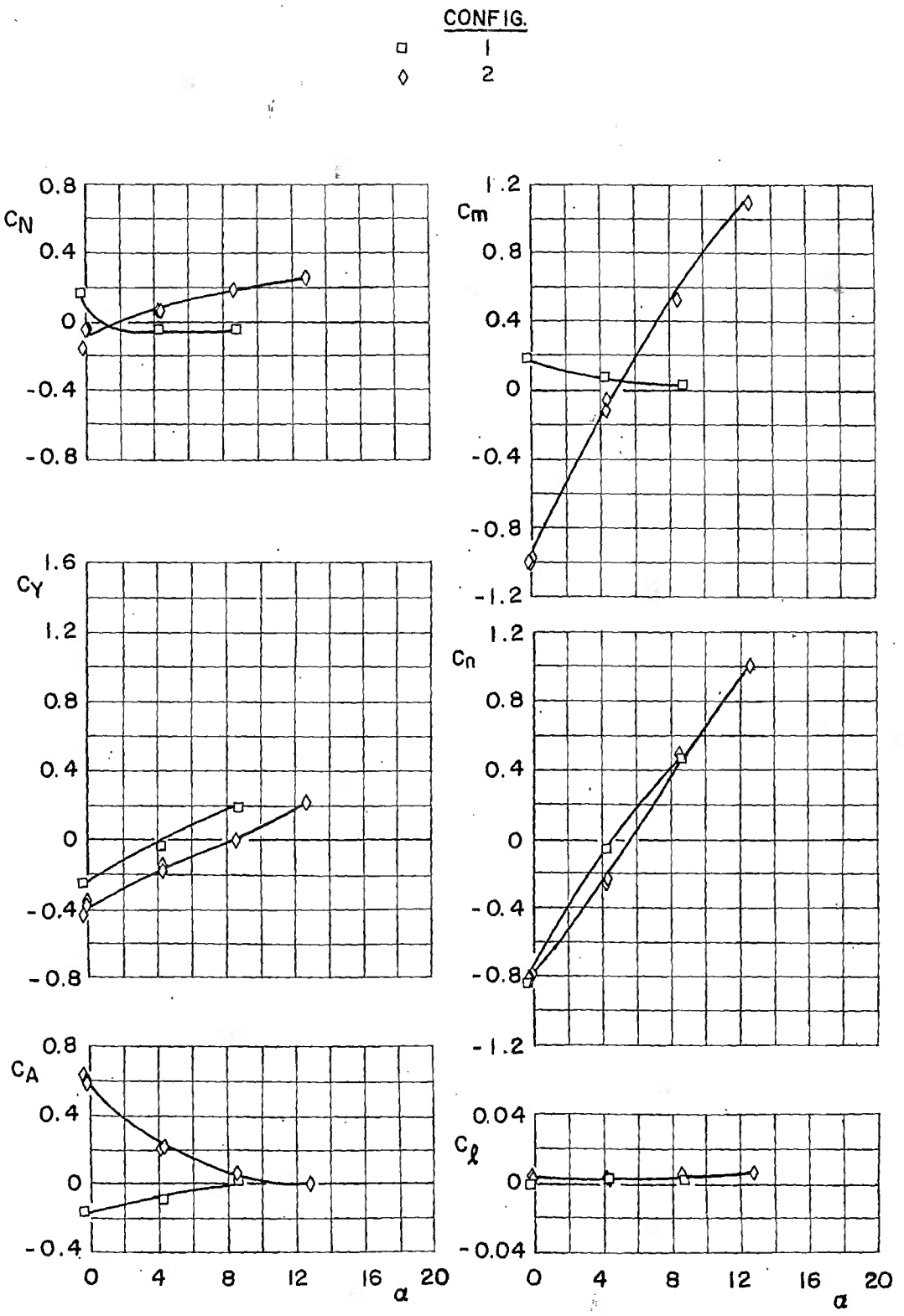

Fig. 17 Aerodynamic Coefficients of the Unfinned BLU-1C/B with Parent Angle of Attack at Mach Number 0.90

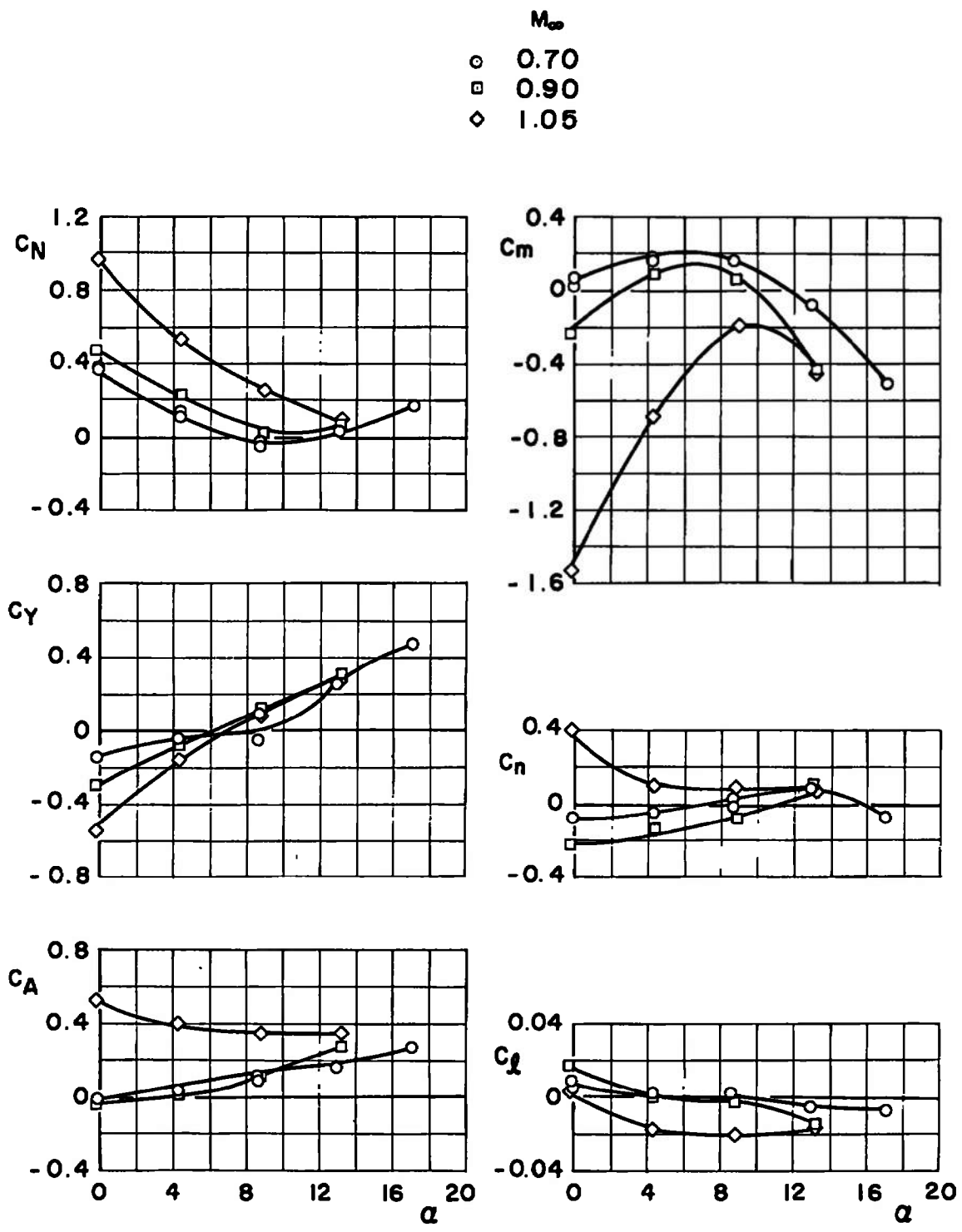

Fig. 18 Aerodynamic Coefficients of the Finned BLU-1C/B with Parent Angle of Attack; Configuration 3

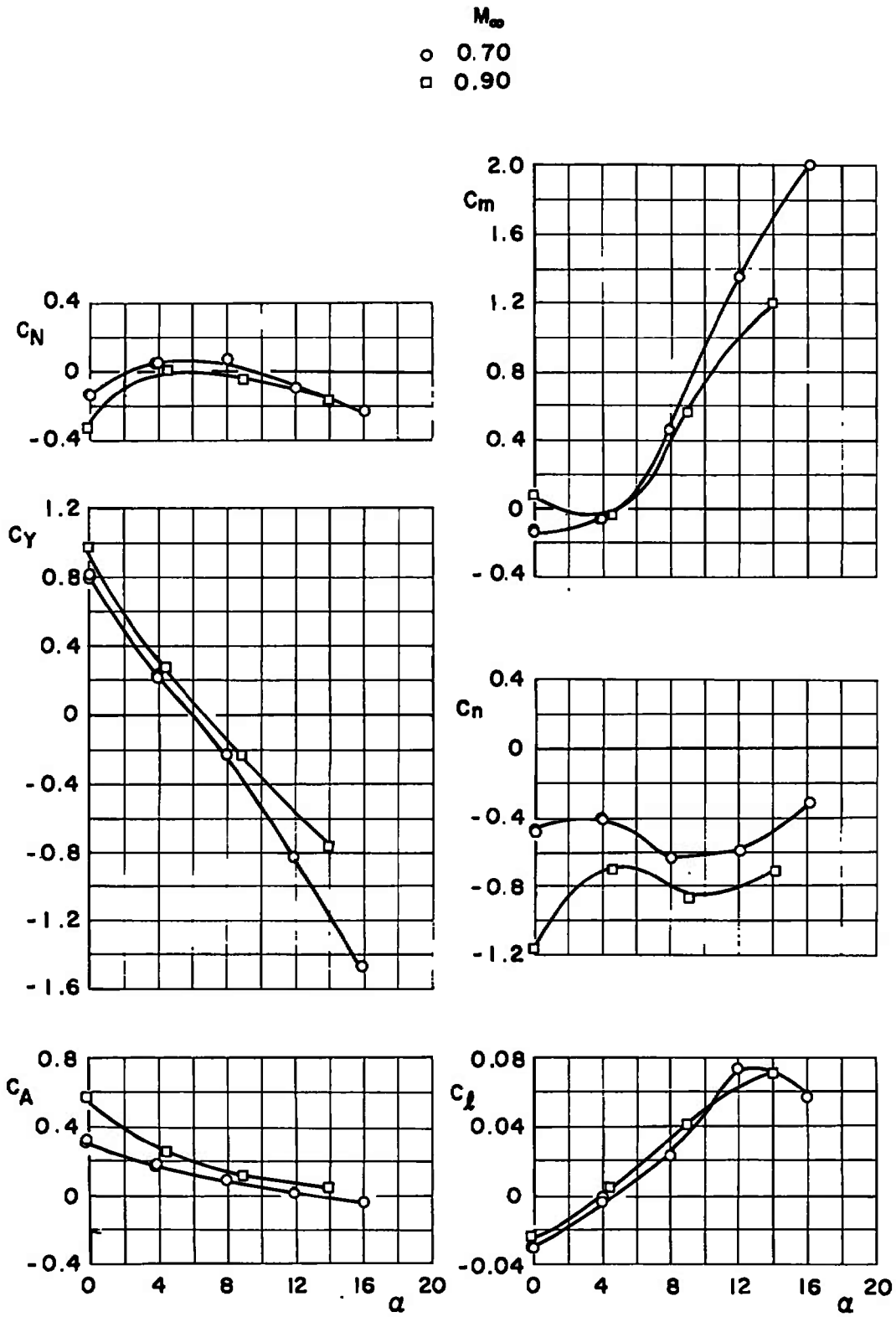

Fig. 19 Aerodynamic Coefficients of the Finned BLU-1C/B with Parent Angle of Attack; Configuration 4

SYMBOL	M_∞	α	H	$\bar{\theta}$	EJECTOR FORCE	INITIAL TRAJ. PARAMETERS TABLE	SET
□	0.68	3.2	6040	-30	–	II	I
◁	0.68	3.2	6040	-30	–	II	I
▽	0.68	3.2	6040	-30	T1	II	I
○	0.68	3.2	6040	-30	D1	II	I
△	0.68	3.2	6040	-30	T2	II	I
◇	0.68	3.2	6040	-30	T3	II	I

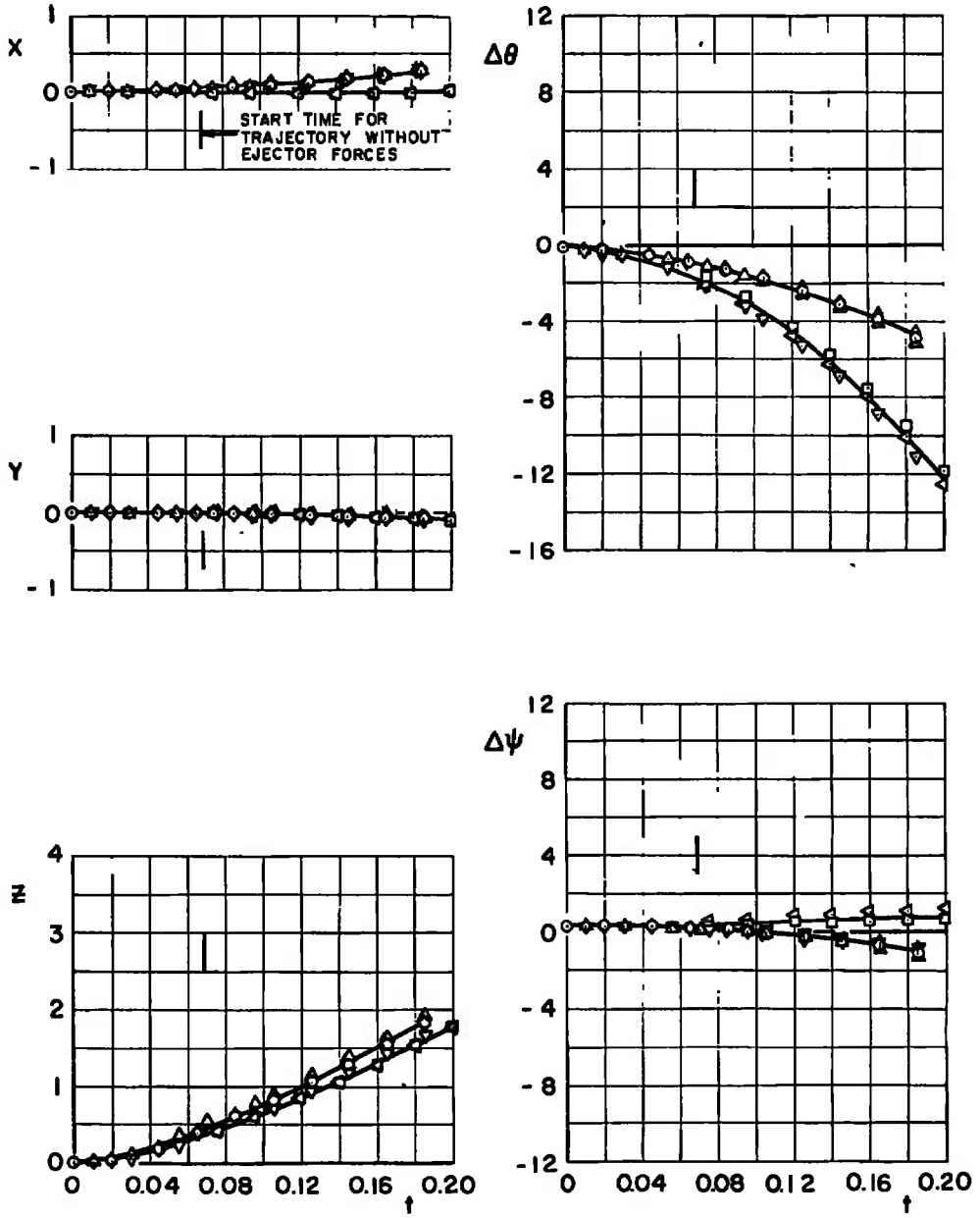

Fig. 20 Effect of Ejector Force Variation on the Separation Trajectories of the Unfinned BLU-1C/B; Configuration 5

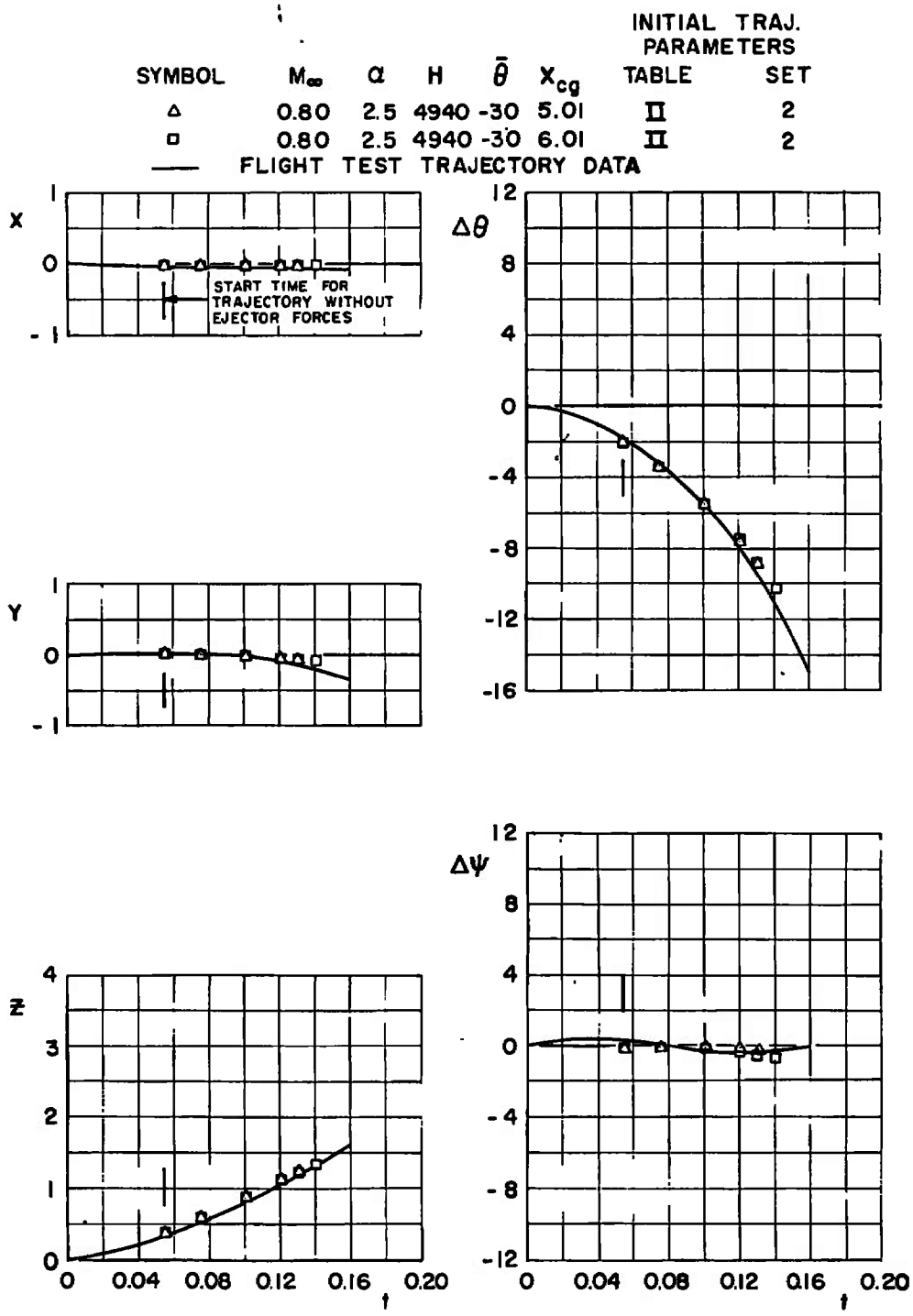

Fig. 21 Effect of Center-of-Gravity Location on the Unfinned BLU-1C/B Trajectories; Configuration 5

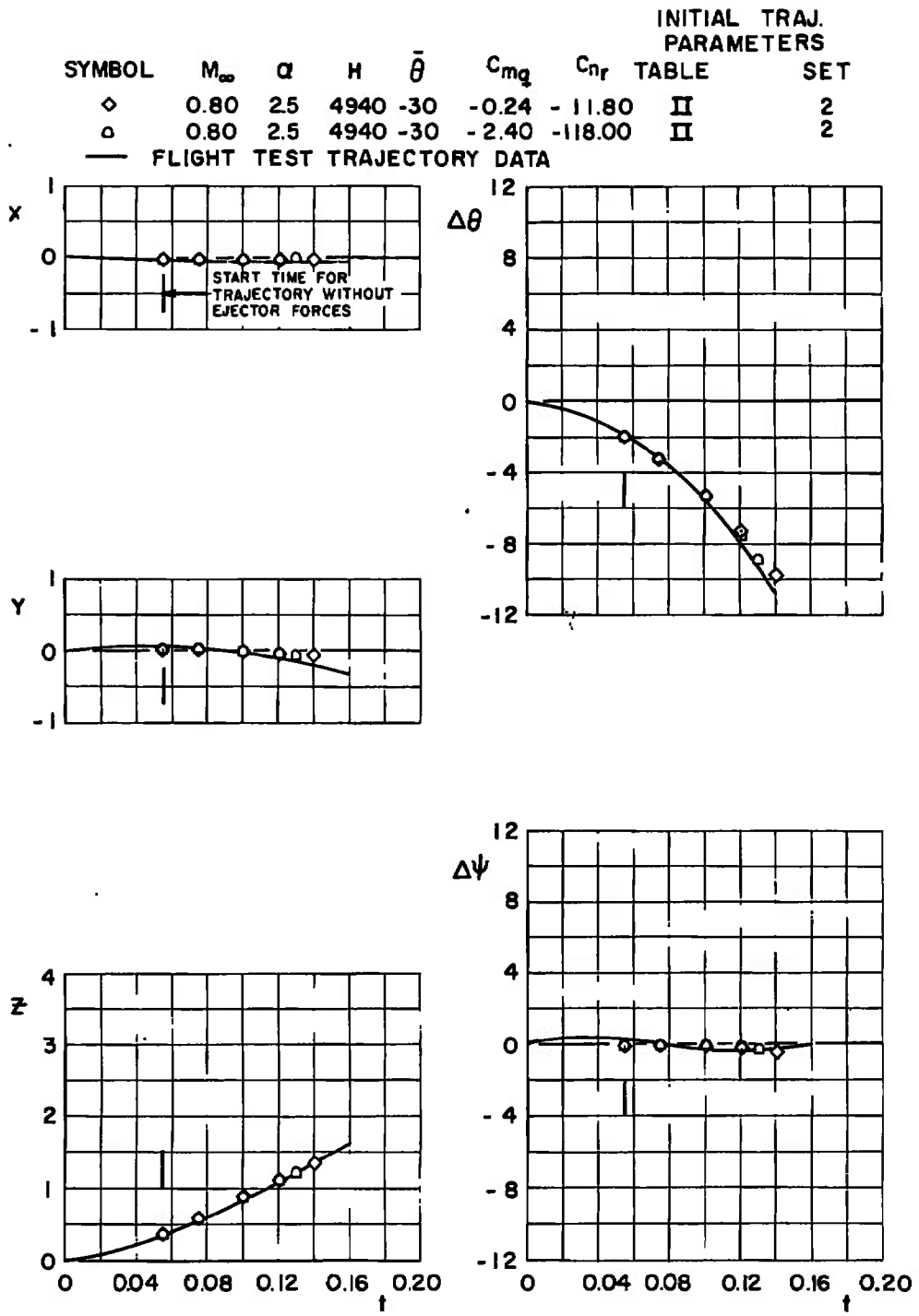

Fig. 22 Effect of Damping Derivative Variation on the Unfinned BLU-1C/B Trajectories; Configuration 5

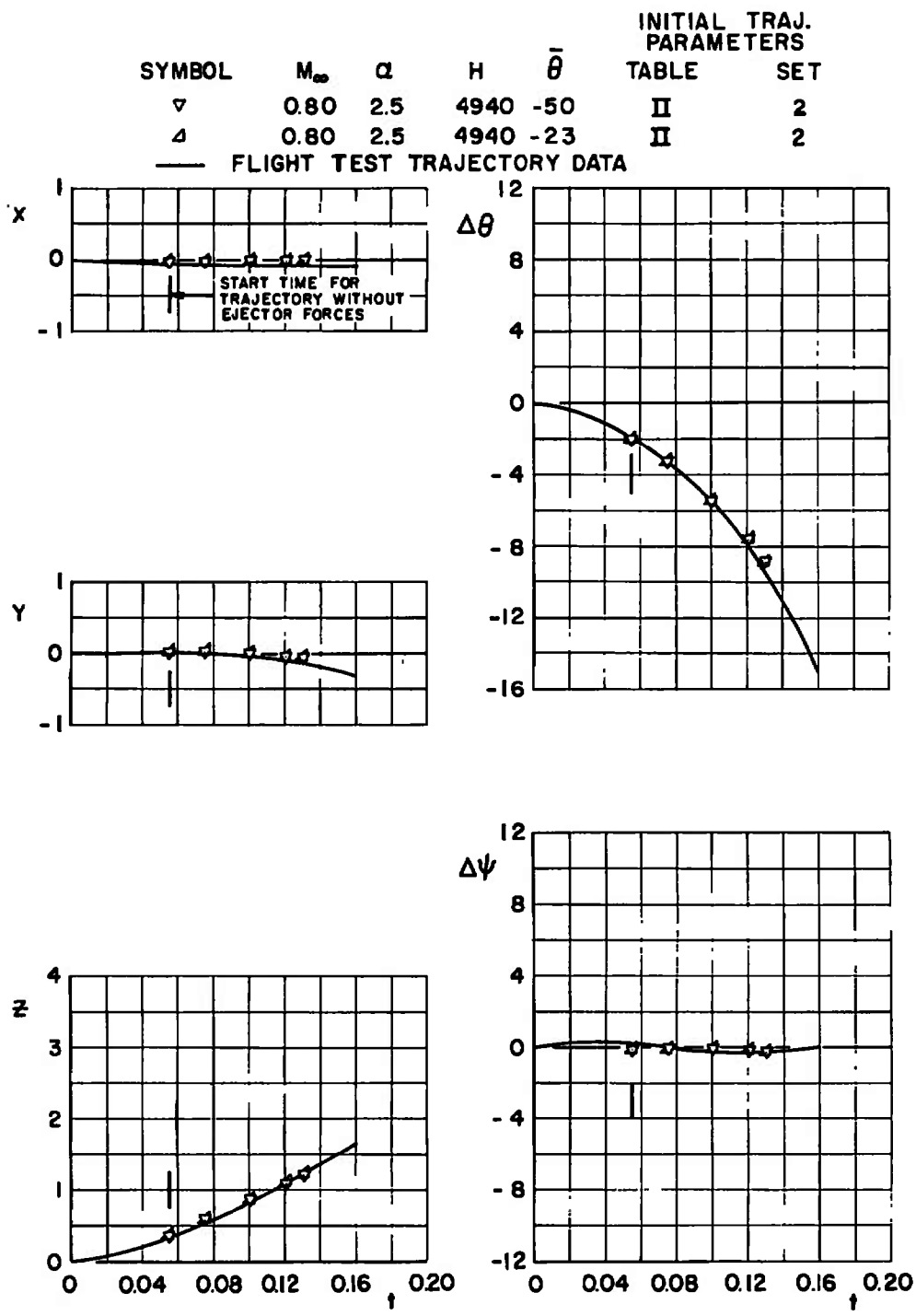

Fig. 23 Effect of Climb Angle Variation on the Unfinned BLU-1C/B Trajectories; Configuration 5

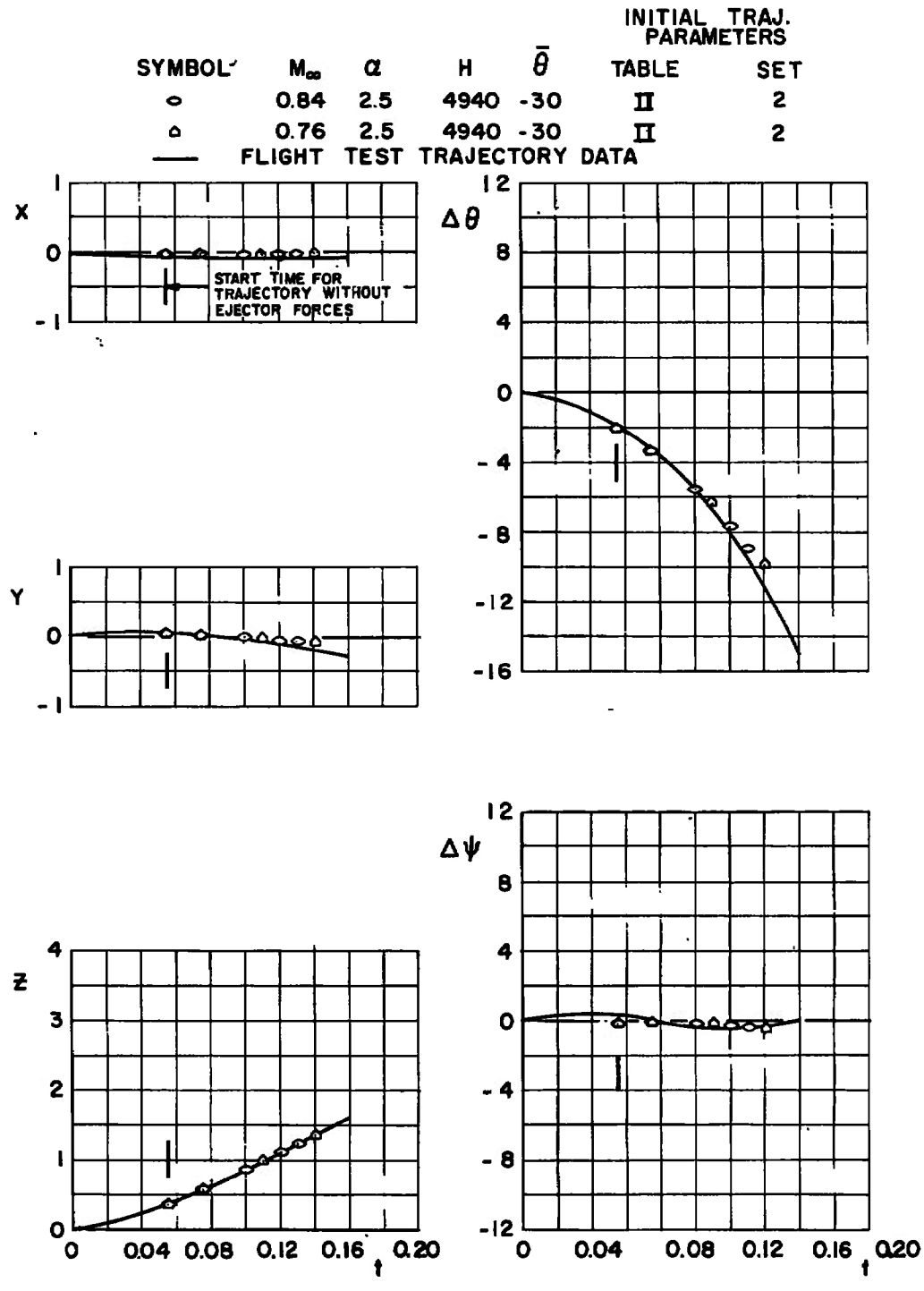

Fig. 24 Effect of Mach Number Variation on the Unfinned BLU-1C/B Trajectories; Configuration 5

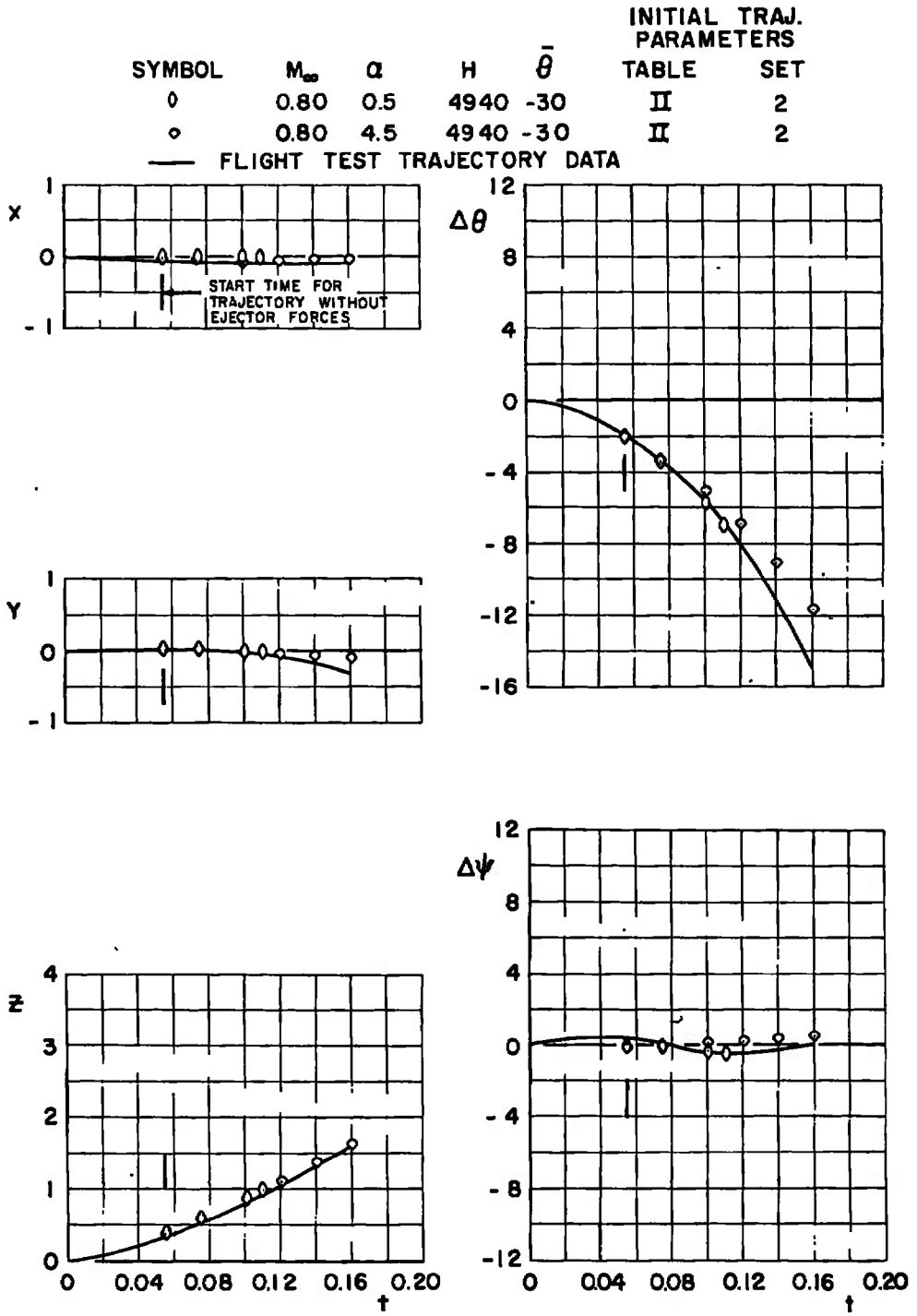

Fig. 25 Effect of Angle-of-Attack Variation on the Unfinned BLU-1C/B Trajectories; Configuration 5

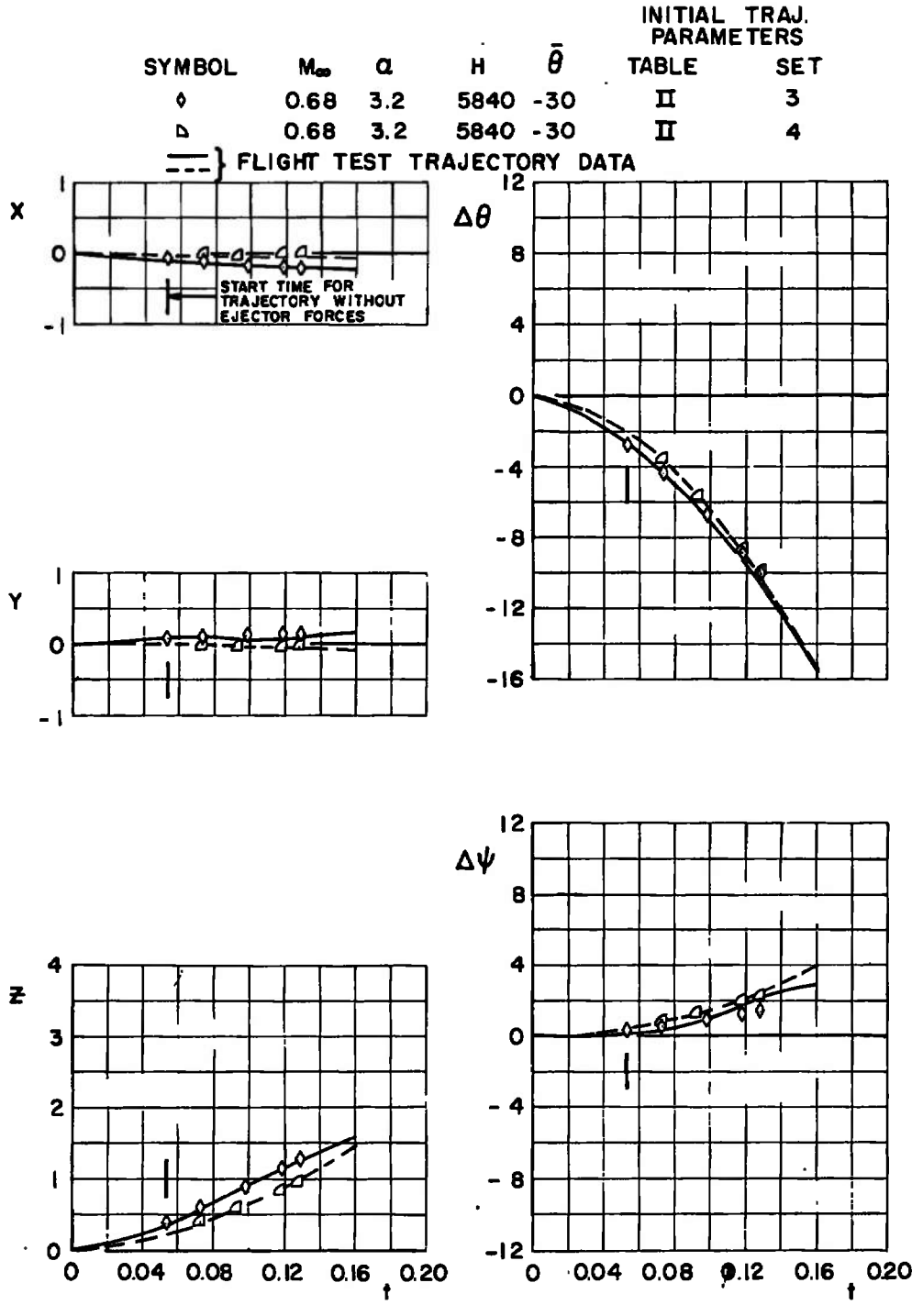

Fig. 26 Separation Trajectories of the Unfinned BLU-1C/B; Configuration 6

SYMBOL	CONF.	M_∞	α	H	$\bar{\theta}$	EJECTION FORCE
□	8	0.42	8.5	5000	0	T4
○	9	0.42	8.5	5000	0	T4
△	10	0.42	8.5	5000	0	T4

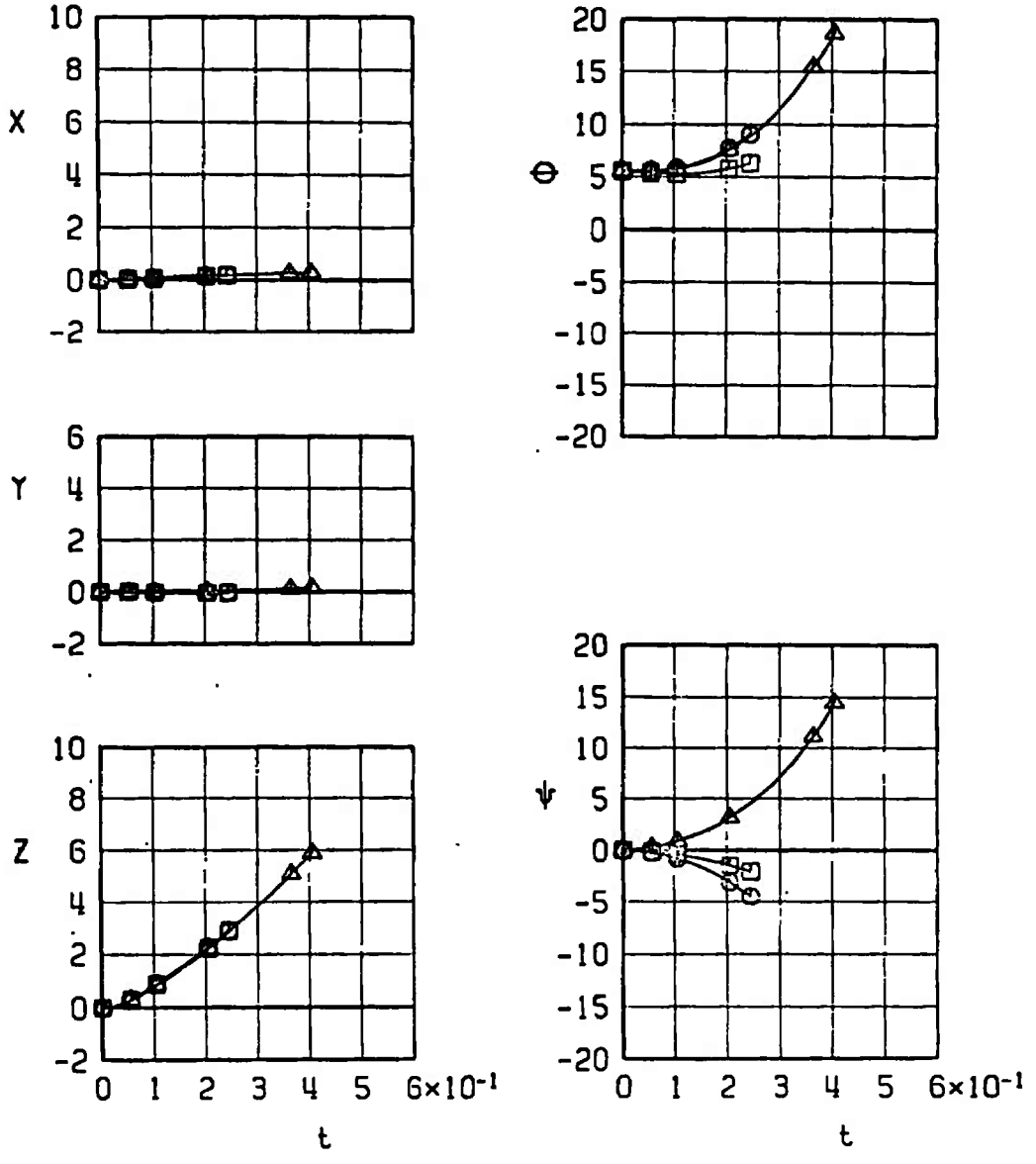

a. Configurations 8 through 10

Fig. 27 Effect of Aircraft-Loading Configuration on the Separation Trajectories of the Unfinned BLU-1C/B at Mach Number 0.42

SYMBOL	CONF.	M_∞	α	H	$\bar{\theta}$	EJECTION FORCE
□	7	0.42	8.5	5000	0	T4
△	10	0.42	8.5	5000	0	T4

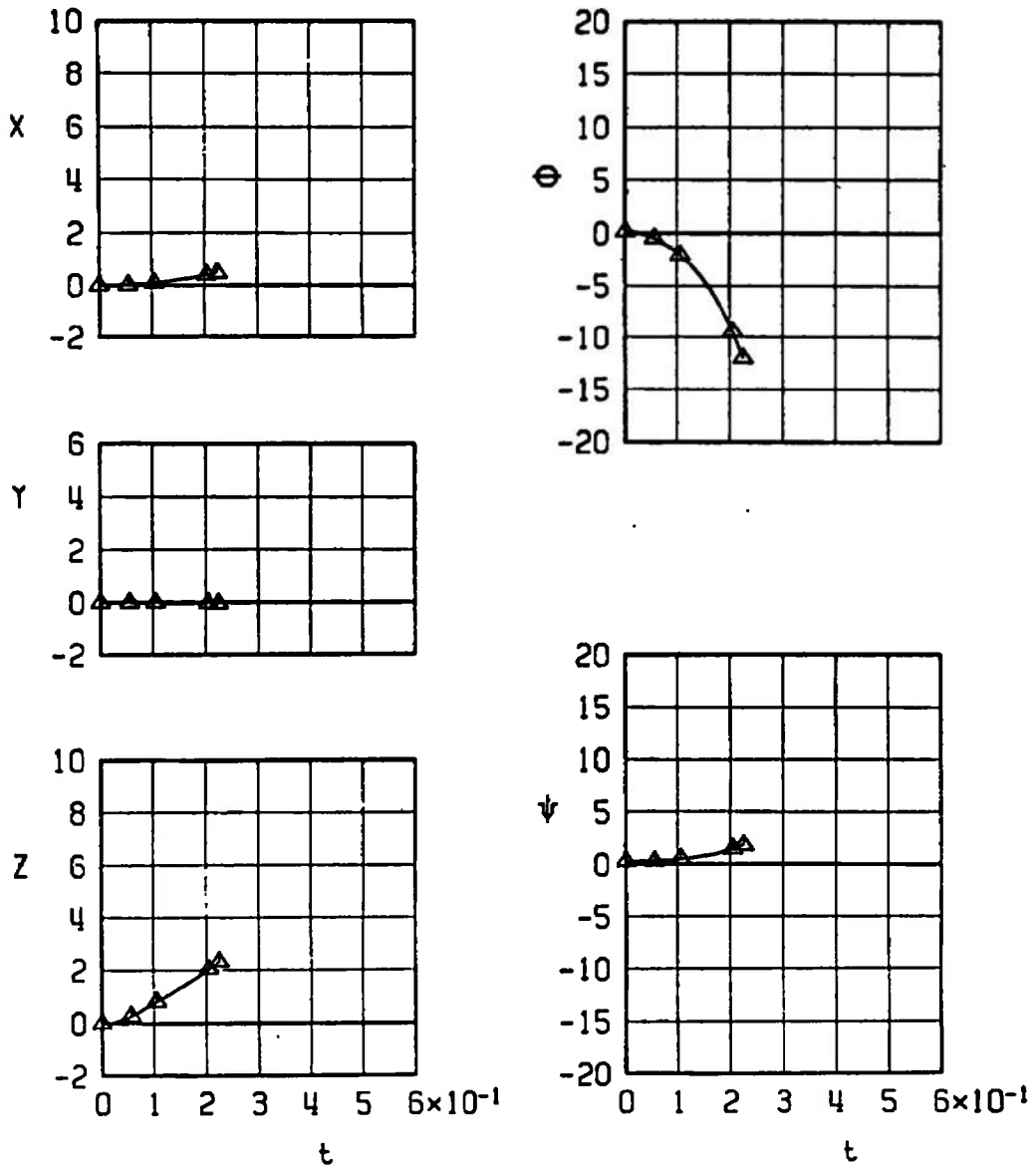

b. Configurations 7 and 10
Fig. 27 Continued

SYMBOL	CONF.	M_∞	α	H	$\bar{\theta}$	EJECTION FORCE
□	11	0.42	8.5	5000	0	T4
○	12	0.42	8.5	5000	0	T4
△	13	0.42	8.5	5000	0	T4

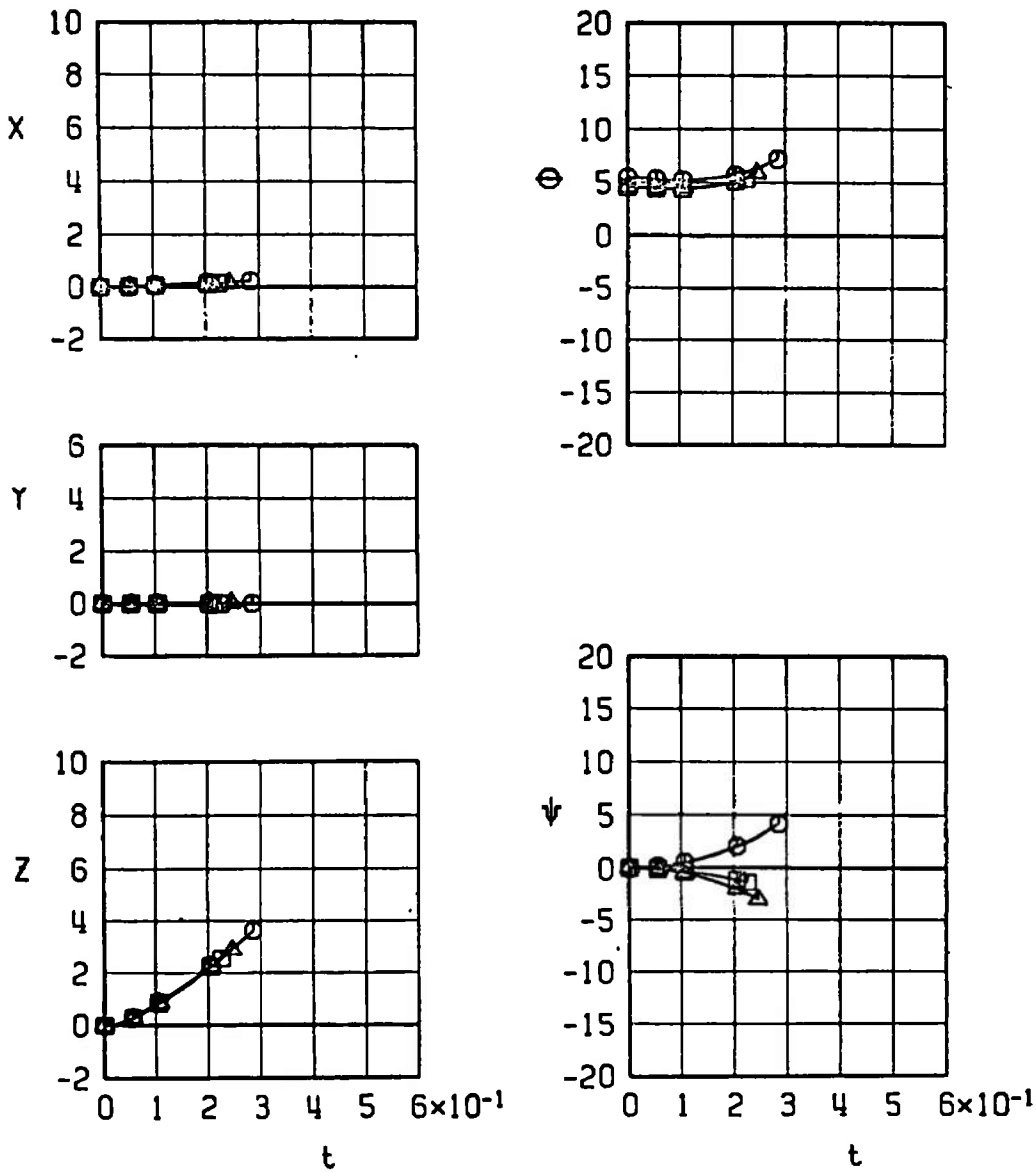

c. Configurations 11 through 13
Fig. 27 Concluded

SYMBOL	CONF.	M_∞	α	H	$\dot{\theta}$	EJECTION FORCE
□	8	0.75	3.2	5000	-35	T4
○	9	0.75	3.2	5000	-35	T4
△	10	0.75	3.2	5000	-35	T4

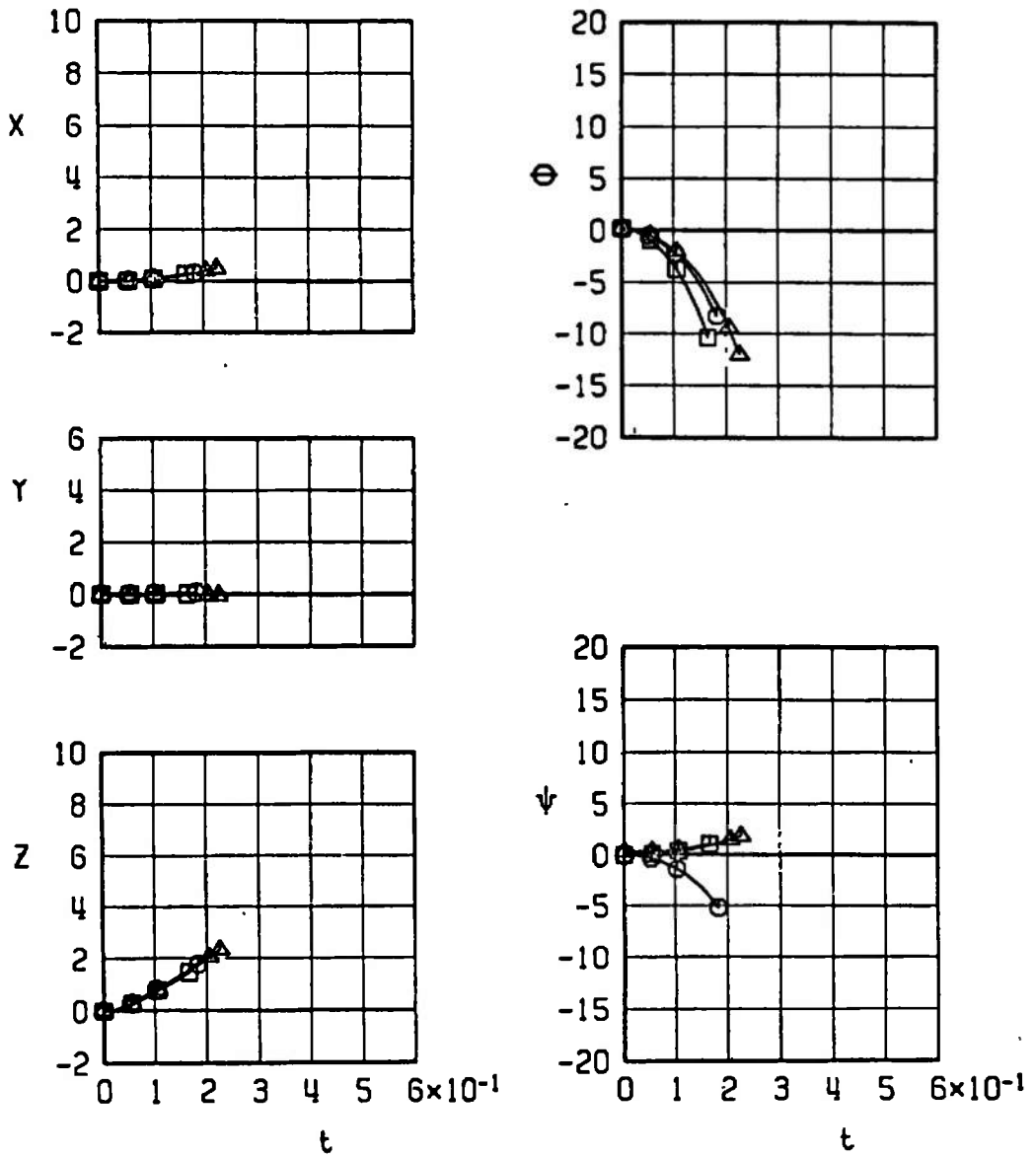

a. Configurations 8 through 10

Fig. 28 Effect of Wing-Loading Configuration on Separation Trajectories of the Unfinned BLU-1C/B at Mach Number 0.75

SYMBOL	CONF.	M_∞	α	H	$\bar{\theta}$	EJECTION FORCE
□	7	0.75	3.2	5000	-35	T4
△	10	0.75	3.2	5000	-35	T4

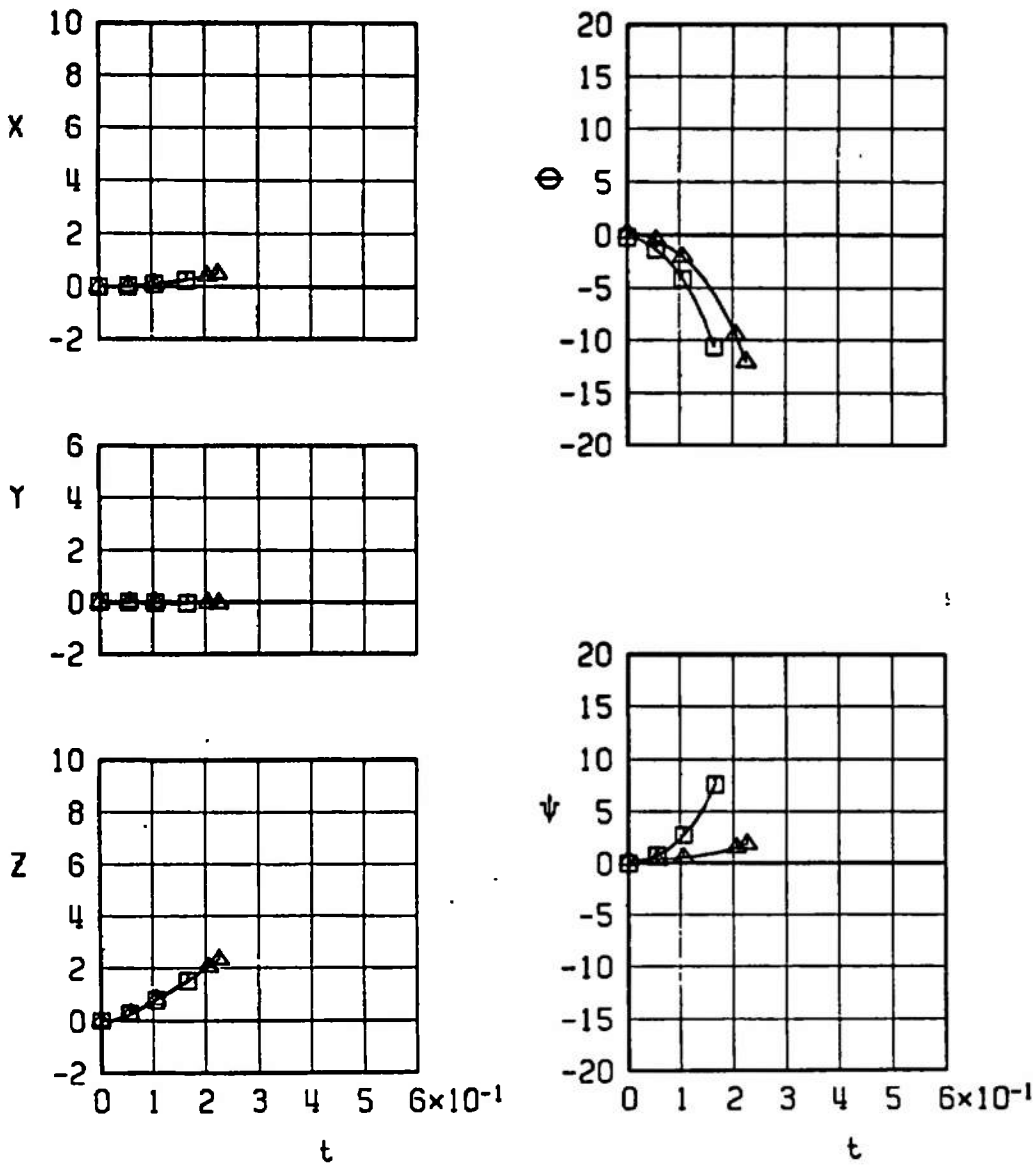

b. Configurations 7 through 10
Fig. 28 Continued

SYMBOL	CONF.	M_∞	α	H	$\bar{\theta}$	EJECTION FORCE
⊡	11	0.75	3.2	5000	-35	T4
⊙	12	0.75	3.2	5000	-35	T4
△	13	0.75	3.2	5000	-35	T4

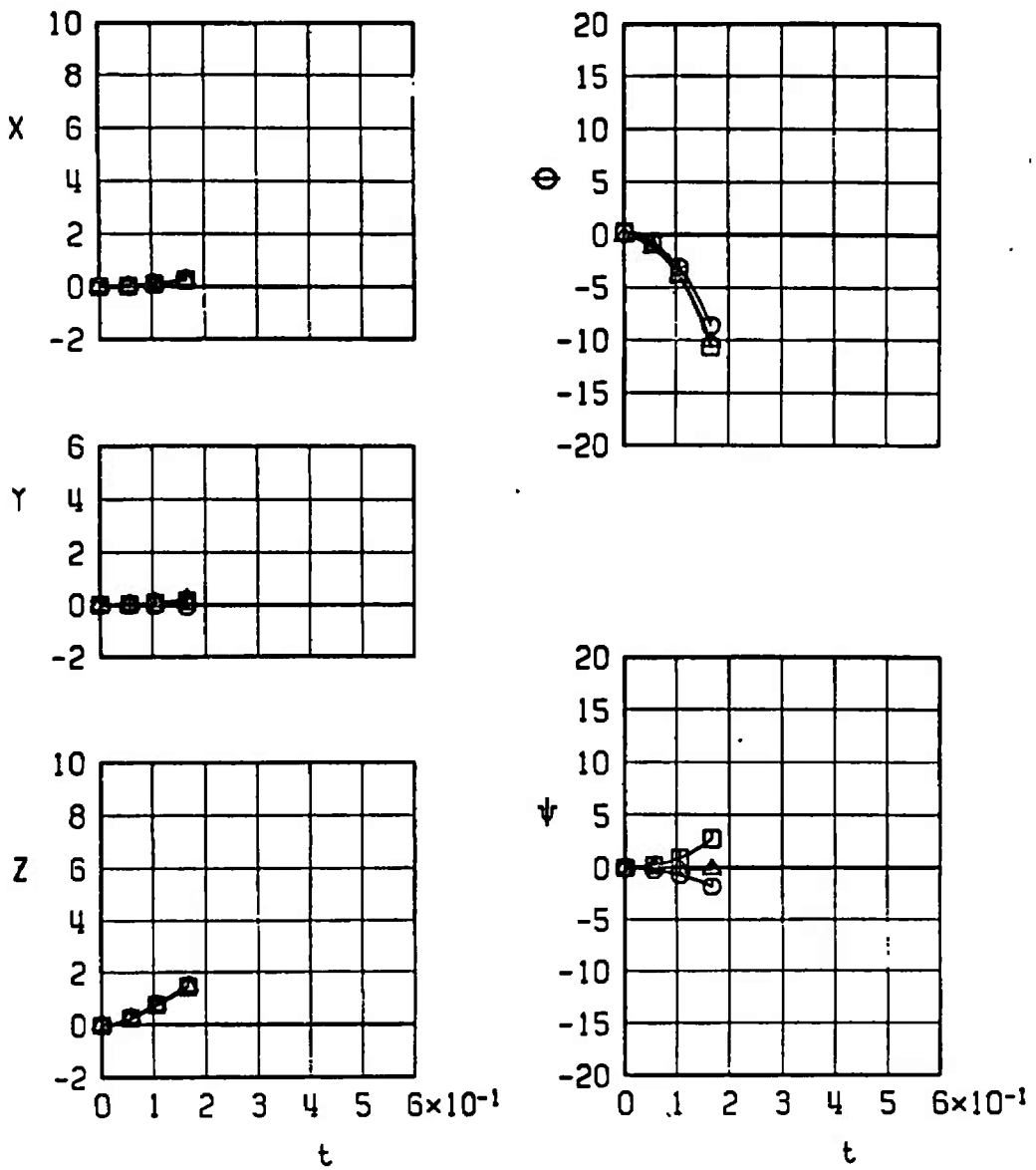

c. Configurations 11 through 13
Fig. 28 Concluded

SYMBOL	M_∞	α	H	$\bar{\theta}$	EJECTION FORCE
□	0.34	12.3	6000	0	T6
○	0.51	5.7	6000	0	T6
△	0.68	3.8	6000	0	T6
◁	0.76	3.3	6000	0	T6
▽	0.76	3.0	6000	-35	T6

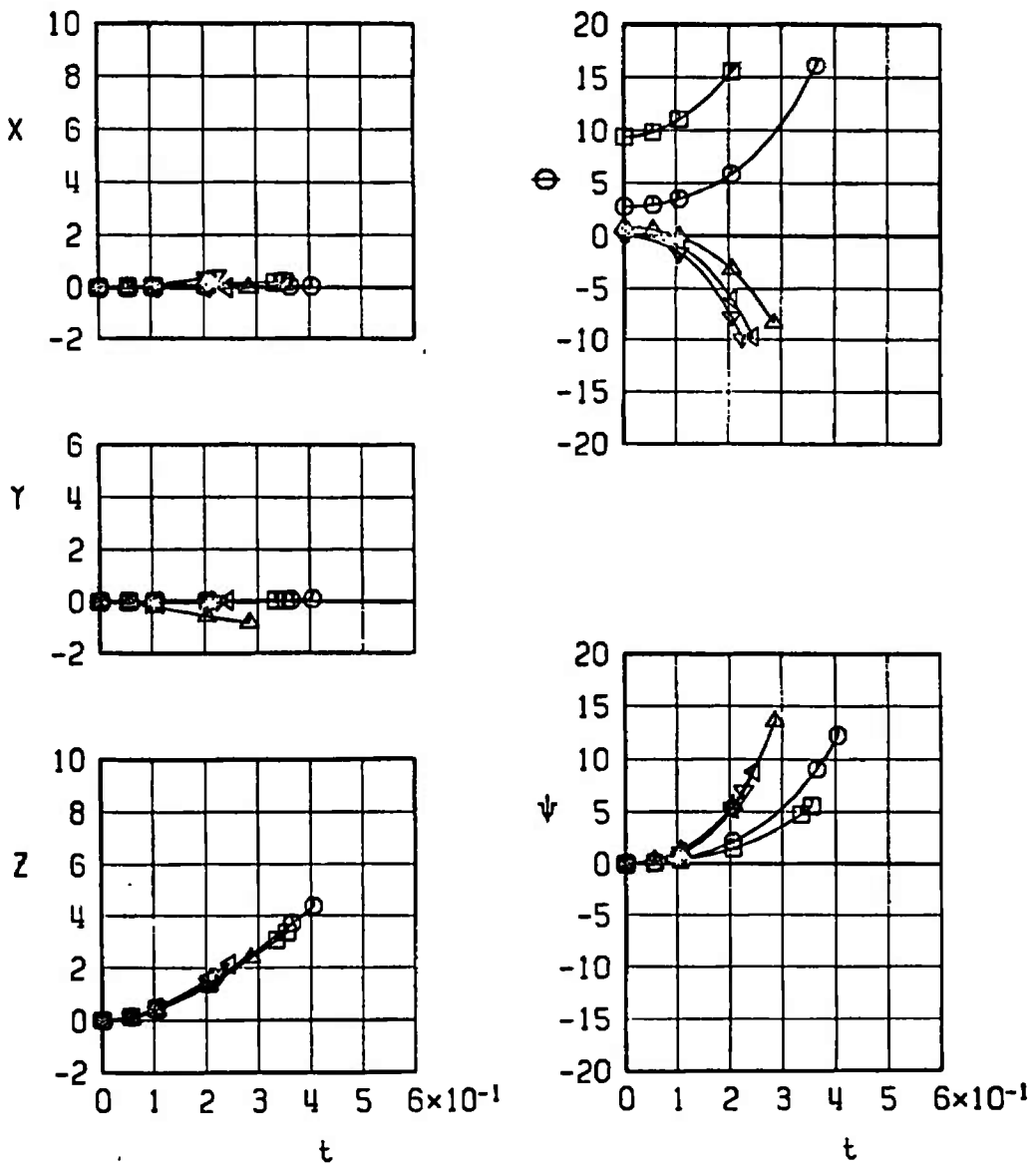

a. Configuration 14

Fig. 29 Effect of Mach Number and Climb Angle on the Separation Trajectories of the Unfinned BLU-1C/B

SYMBOL	M_∞	α	H	$\tilde{\theta}$	EJECTION FORCE
□	0.34	11.7	6000	0	T6
○	0.51	5.6	6000	0	T6
△	0.68	3.7	6000	0	T6
◁	0.76	3.2	6000	0	T6
▽	0.76	2.9	6000	-35	T6

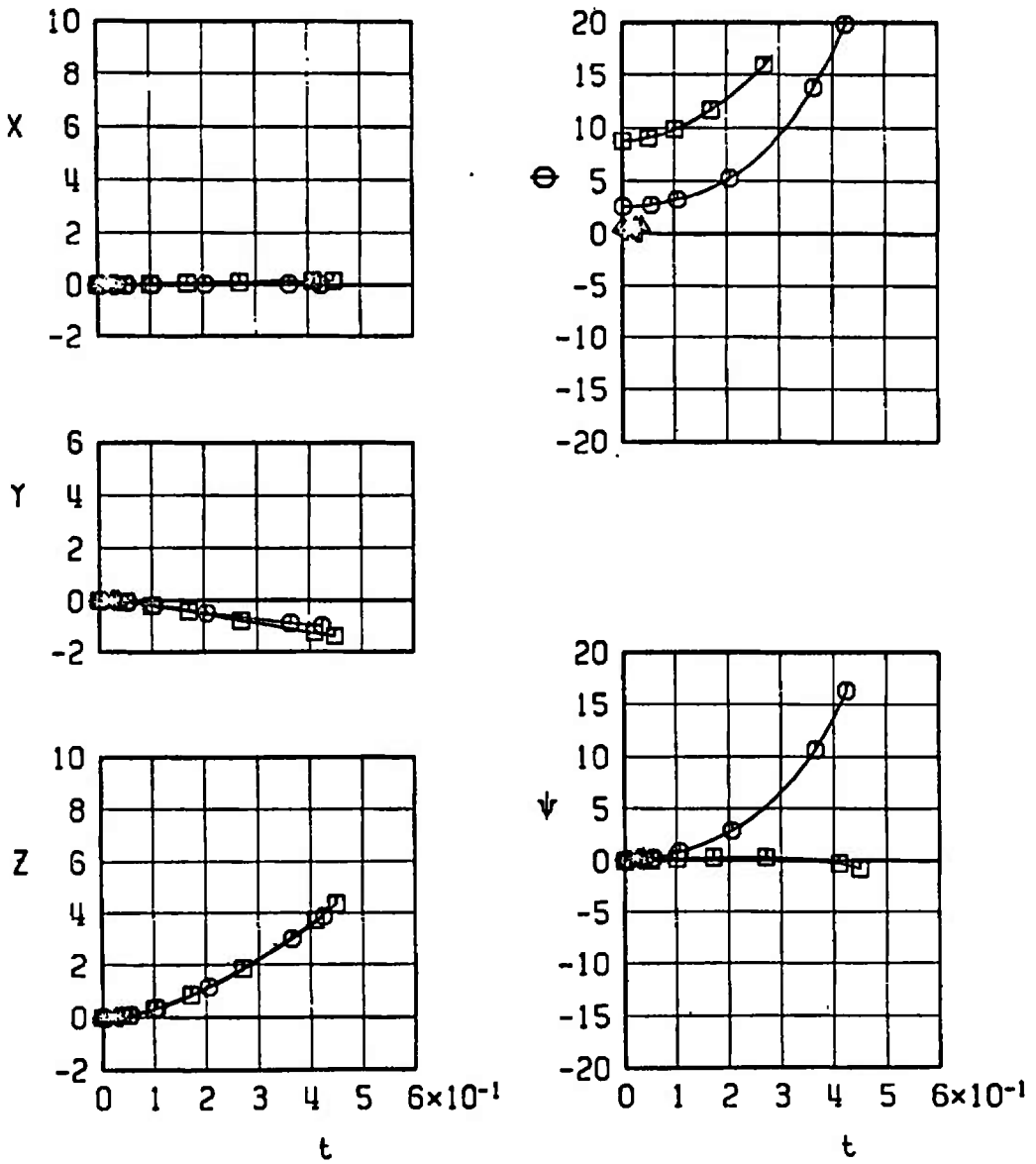

b. Configuration 15
Fig. 29 Concluded

SYMBOL	M_∞	α	H	$\bar{\theta}$	EJECTION FORCE
⊡	0.34	11.4	6000	0	T6
⊙	0.76	2.8	6000	-35	T6

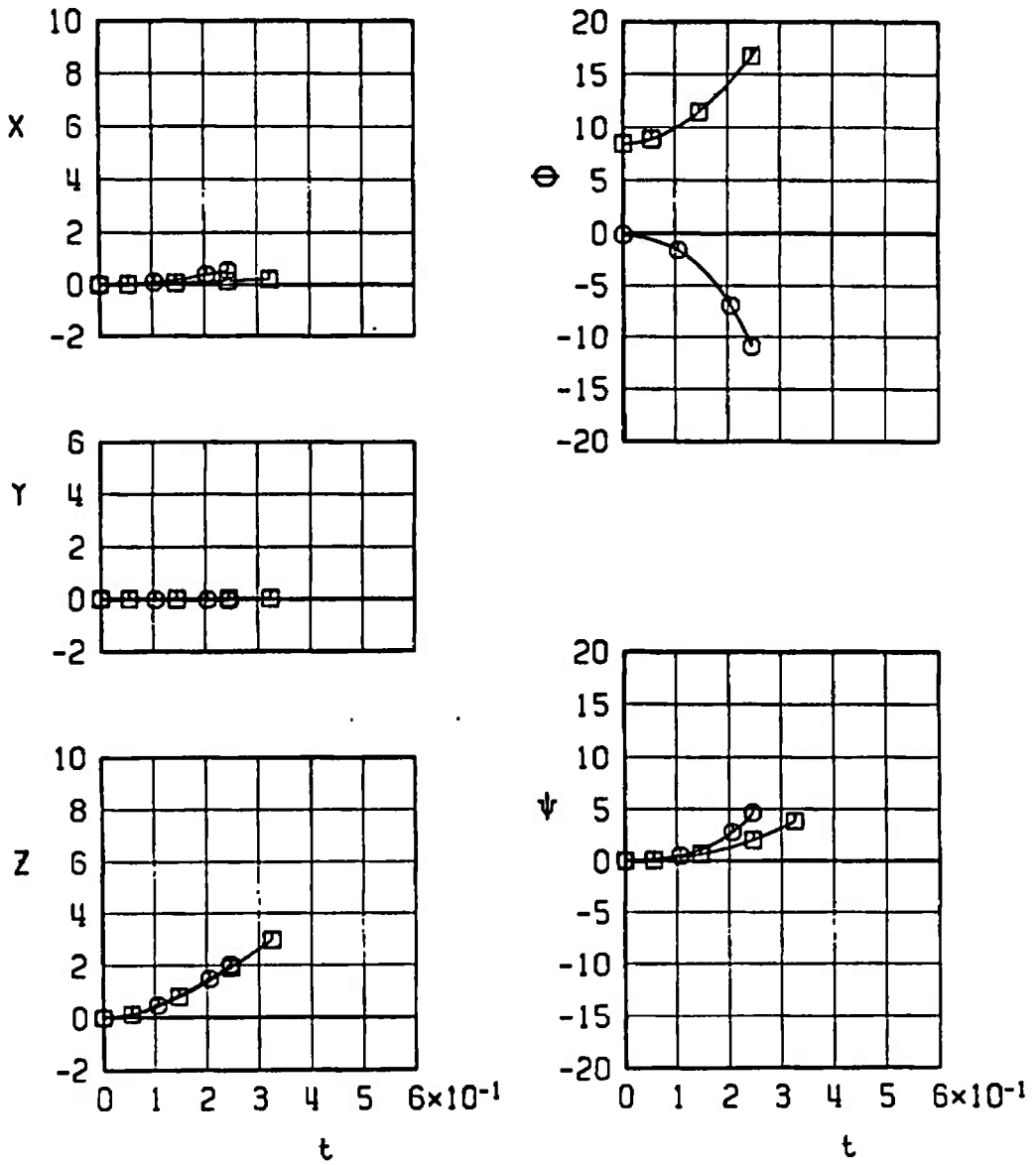

a. Configuration 16

Fig. 30 Effect of Mach Number and Climb Angle on the Separation Trajectories of the Unfinned BLU-1C/B

SYMBOL	M_∞	α	H	$\tilde{\theta}$	EJECTION FORCE
⊡	0.34	10.9	6000	0	T6
⊙	0.76	2.8	6000	-35	T6

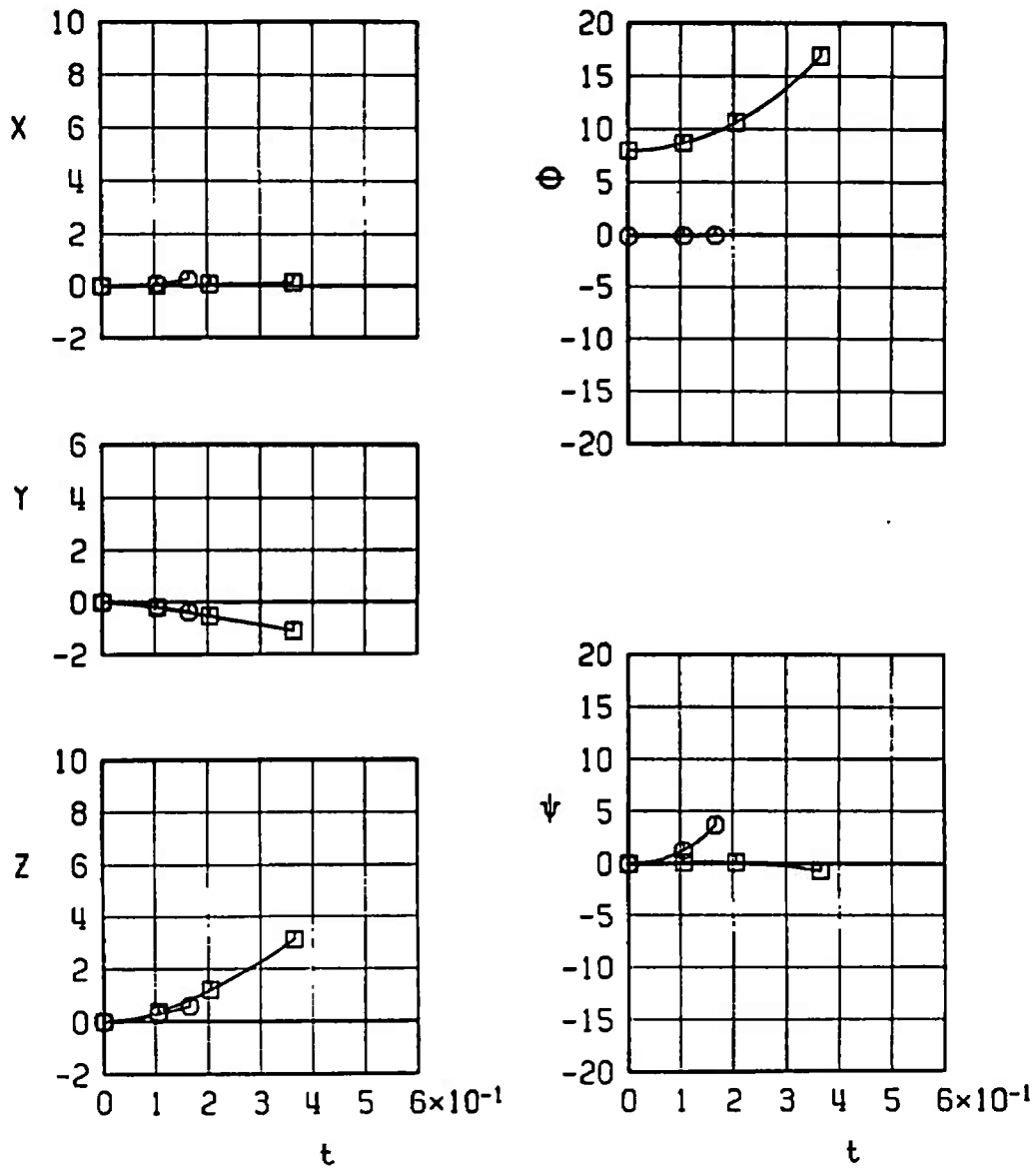

b. Configuration 17
Fig. 30 Continued

SYMBOL	M_∞	α	H	$\bar{\theta}$	EJECTION FORCE
⊡	0.34	12.5	6000	0	T6
⊙	0.76	3.0	6000	-35	T6

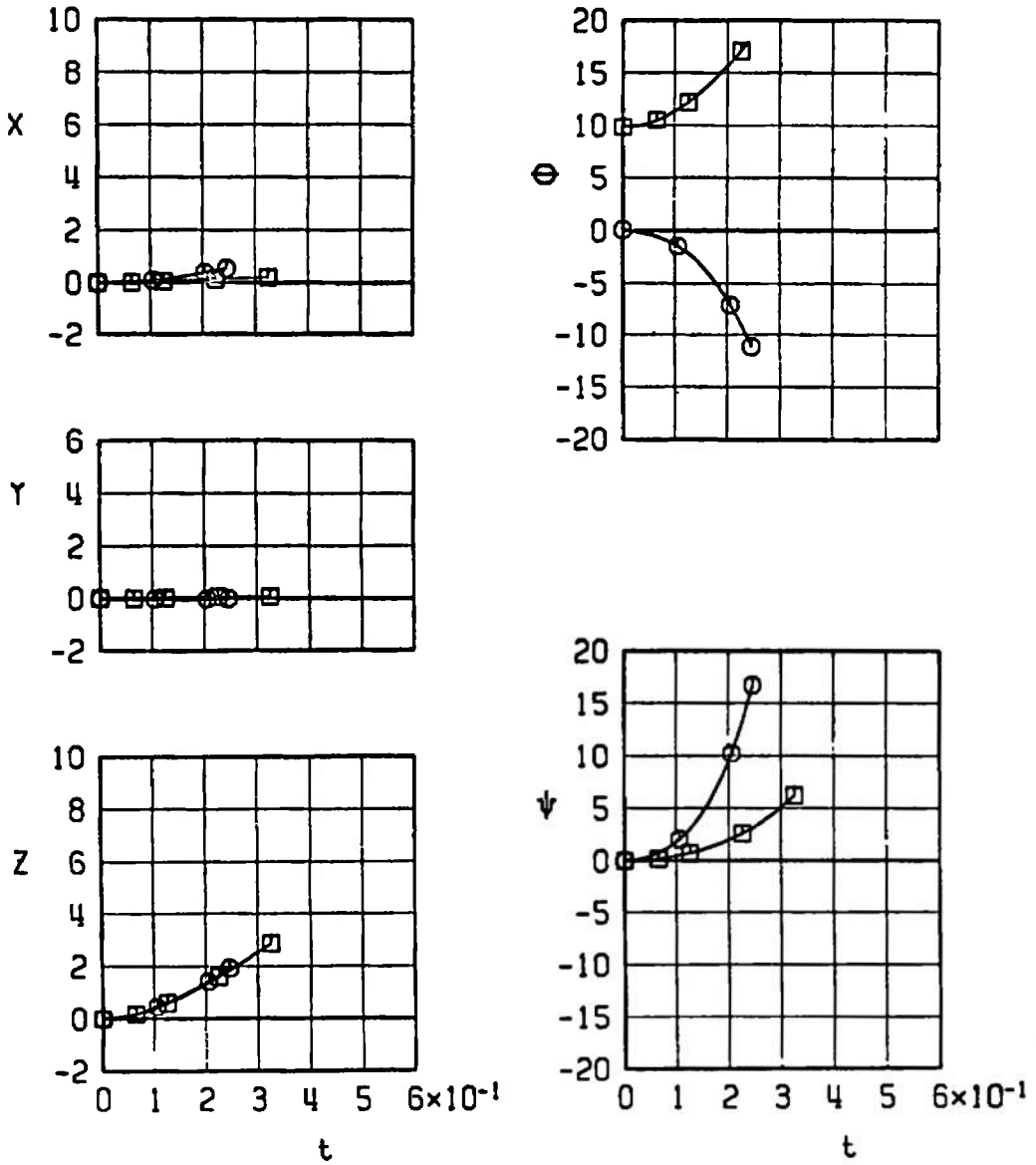

c. Configuration 19
Fig. 30 Concluded

SYMBOL	CONF.	M_∞	α	H	$\bar{\theta}$	EJECTION FORCE
□	22	0.42	8.5	5000	0	T4
○	23	0.42	8.5	5000	0	T4
△	21	0.42	8.5	5000	0	T4

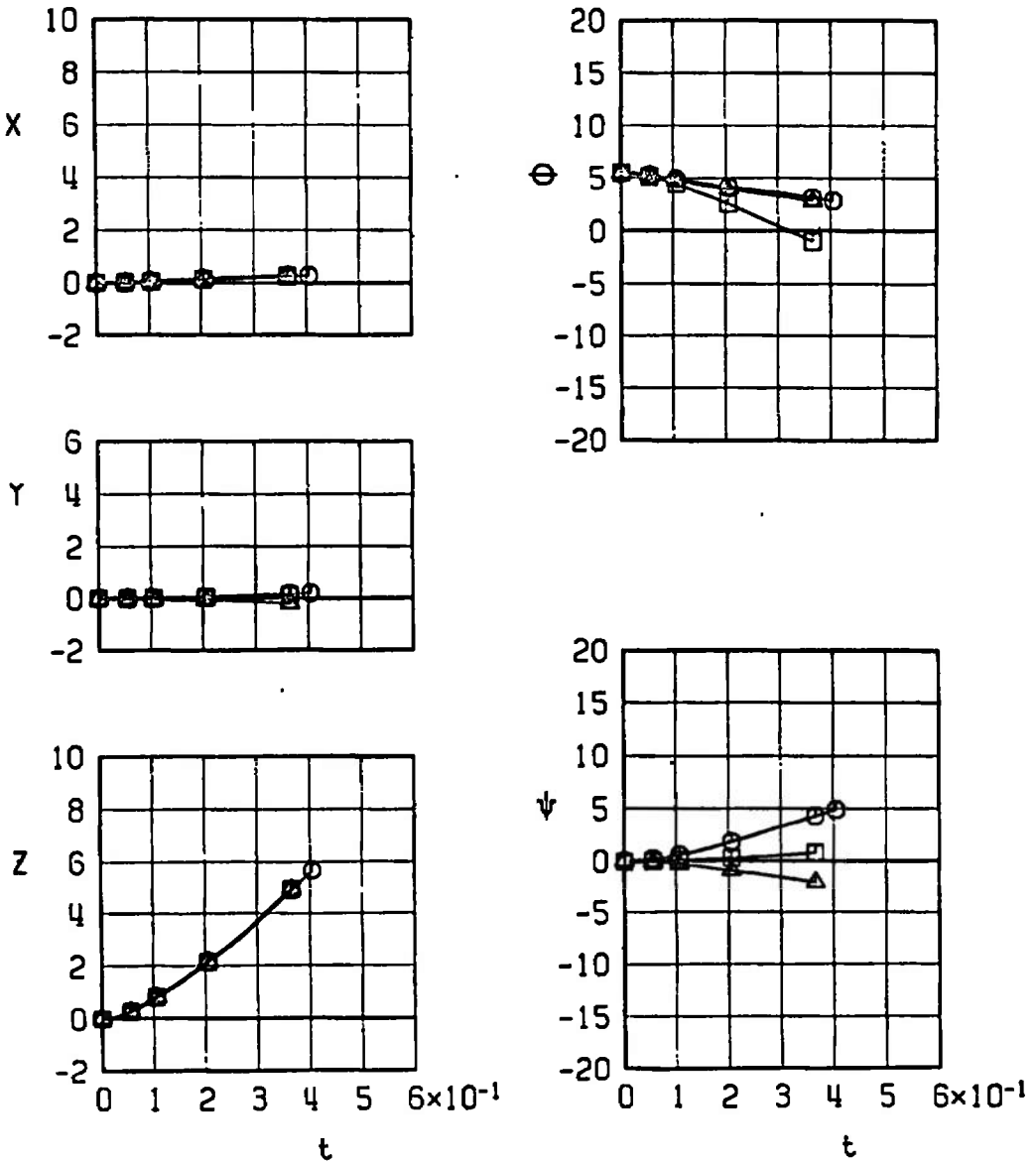

Fig. 31 Effect of Wing-Loading Configuration on Separation Trajectories of the Finned BLU-1C/B at Mach Number 0.42

SYMBOL	CONF.	M_∞	α	H	$\bar{\theta}$	EJECTION FORCE
□	22	0.76	2.7	6000	-50	T4
○	23	0.76	2.7	6000	-50	T4
△	21	0.76	2.7	6000	-50	T4

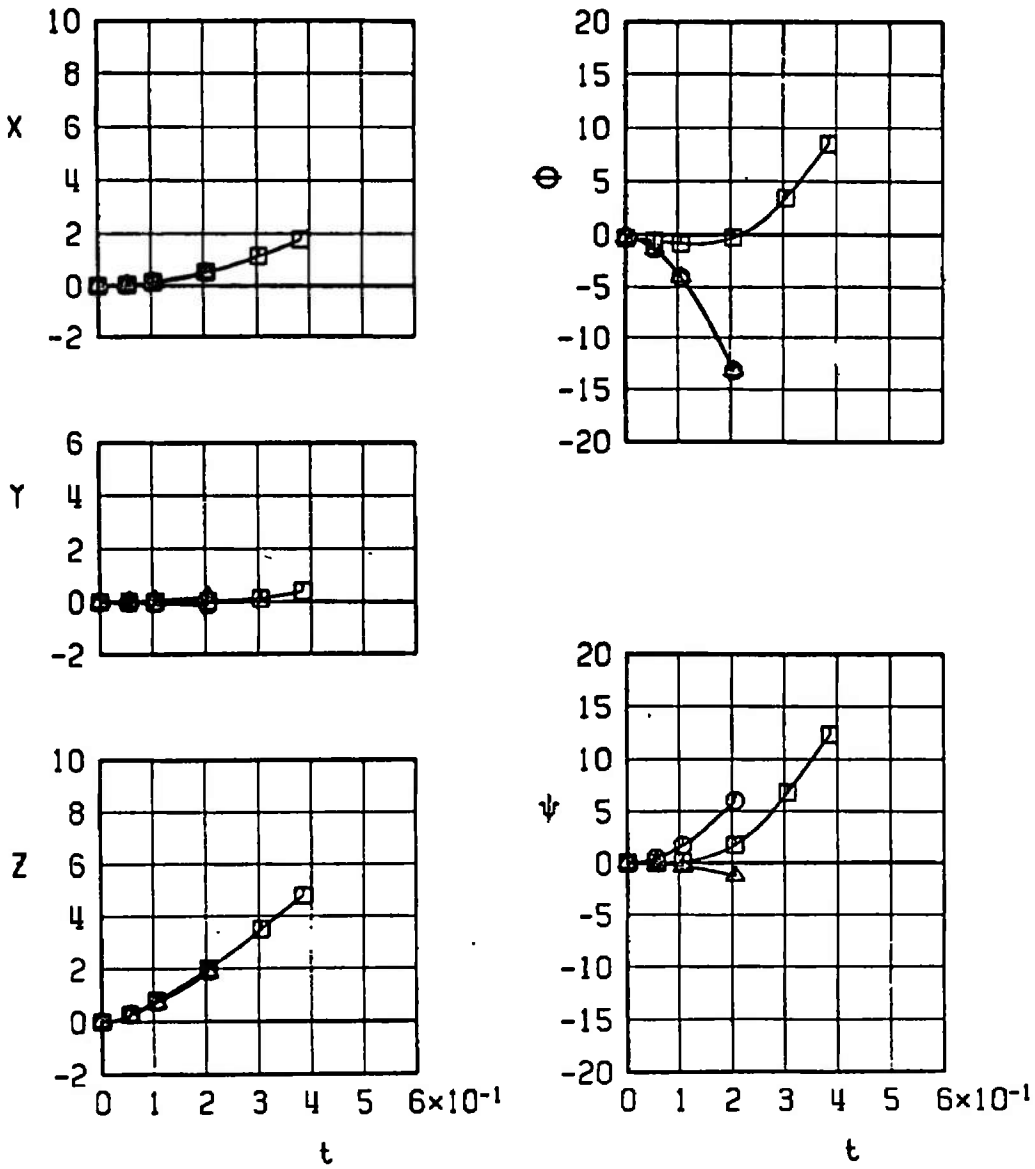

Fig. 32 Effect of Wing-Loading Configuration on Separation Trajectories of Finned BLU-1C/B at Mach Number 0.76

SYMBOL	CONF	M_∞	α	H	$\bar{\theta}$	EJECTION FORCE
□ *	24	0.86	2.0	7000	-70	T5
○ *	25	0.86	2.0	7000	-70	T5

* Indicates store-aircraft contact

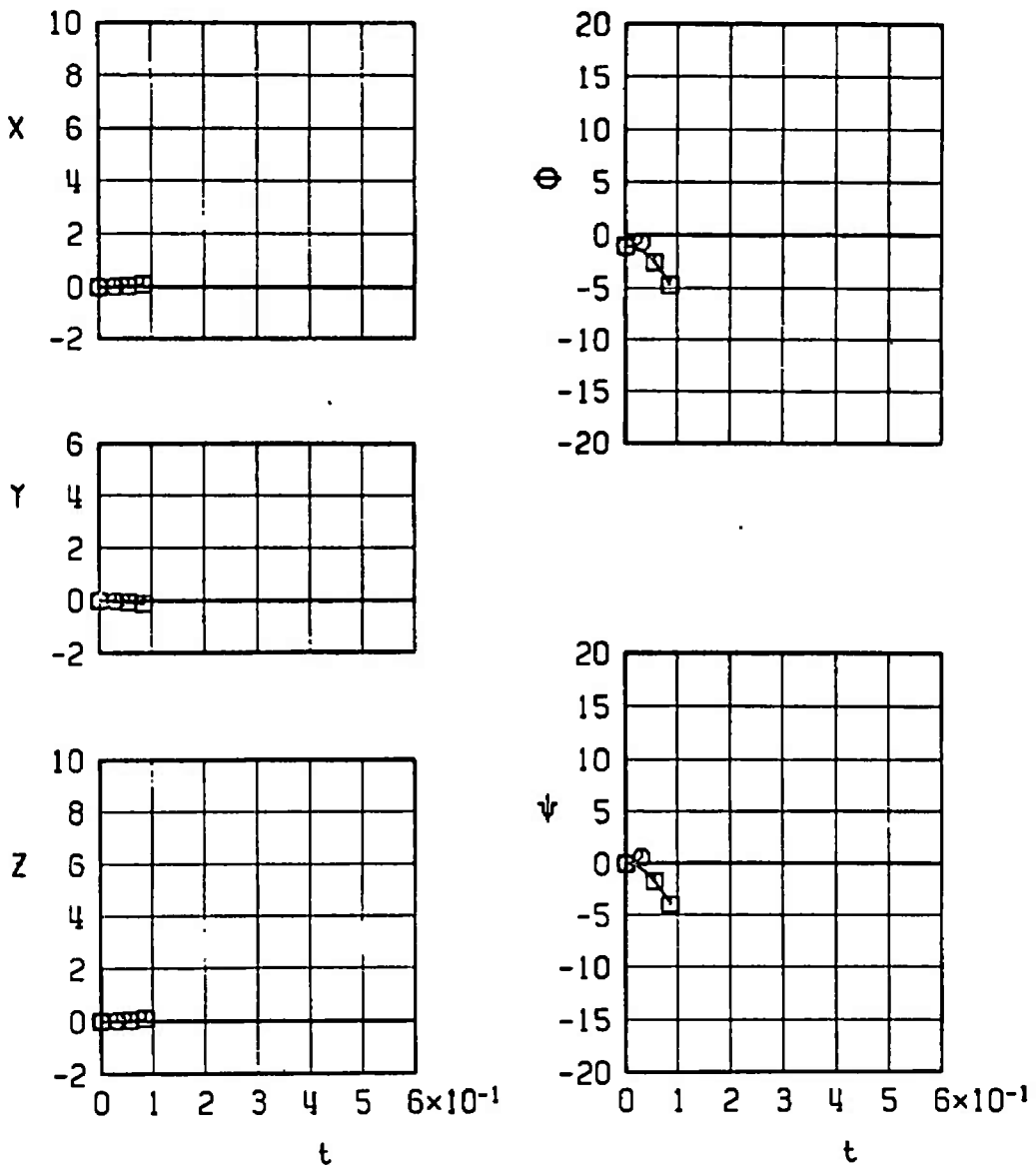

a. Configurations 24 and 25

Fig. 33 Effect of Wing-Loading Configuration on the Separation Trajectories of the M-117GP at Mach Number 0.86

SYMBOL	CONF.	M_∞	α	H	$\bar{\theta}$	EJECTION FORCE
□ *	26	0.86	2.0	7000	-70	T5
○ *	27	0.86	2.0	7000	-70	T5
△	28	0.86	2.0	7000	-70	T5
◁ *	29	0.86	2.0	7000	-70	T5

* Indicates store-aircraft contact

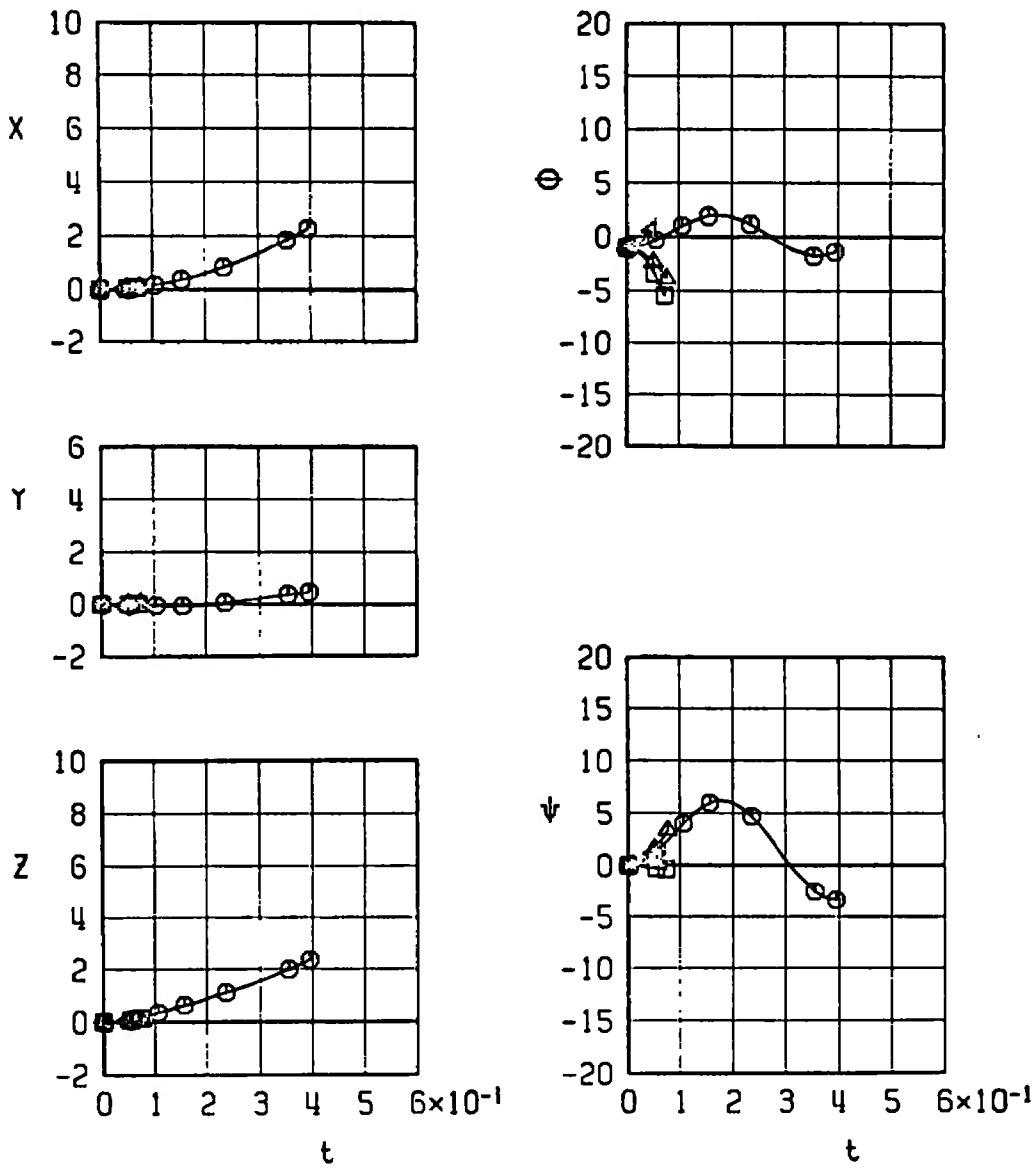

b. Configurations 26 through 29
Fig. 33 Continued

SYMBOL	CONF.	M_∞	α	H	$\bar{\theta}$	EJECTION FORCE
⊡ *	26	0.86	2.0	7000	-70	T5
⊙ *	30	0.86	2.0	7000	-70	T5

*Indicates store-aircraft contact

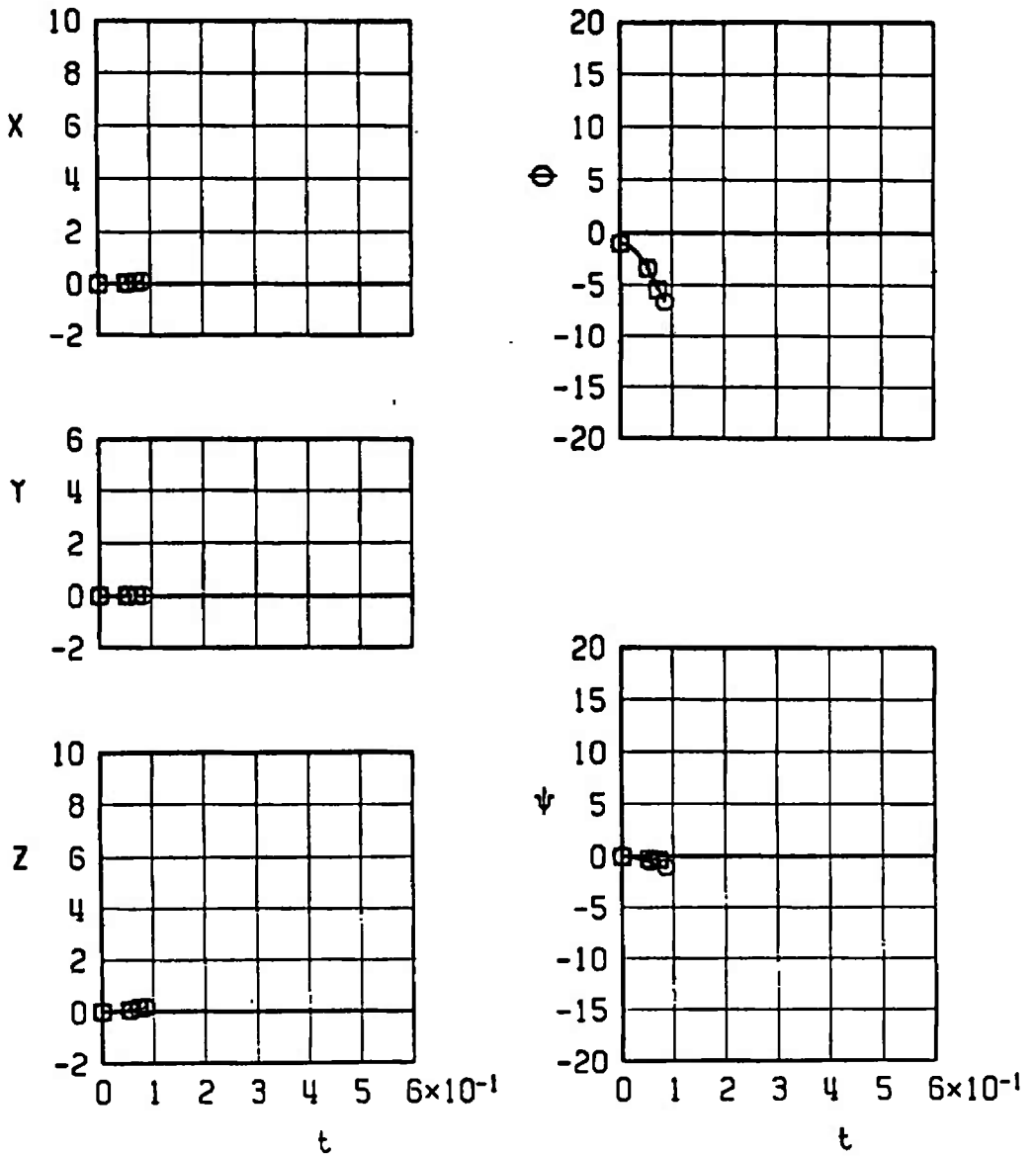

c. Configurations 26 and 30
Fig. 33 Concluded

SYMBOL	CONF.	M_∞	α	H	$\bar{\theta}$	EJECTION FORCE
□	24	0.95	1.9	7000	-70	T5
⊙ *	25	0.95	1.9	7000	-70	T5

*Indicates store-aircraft contact

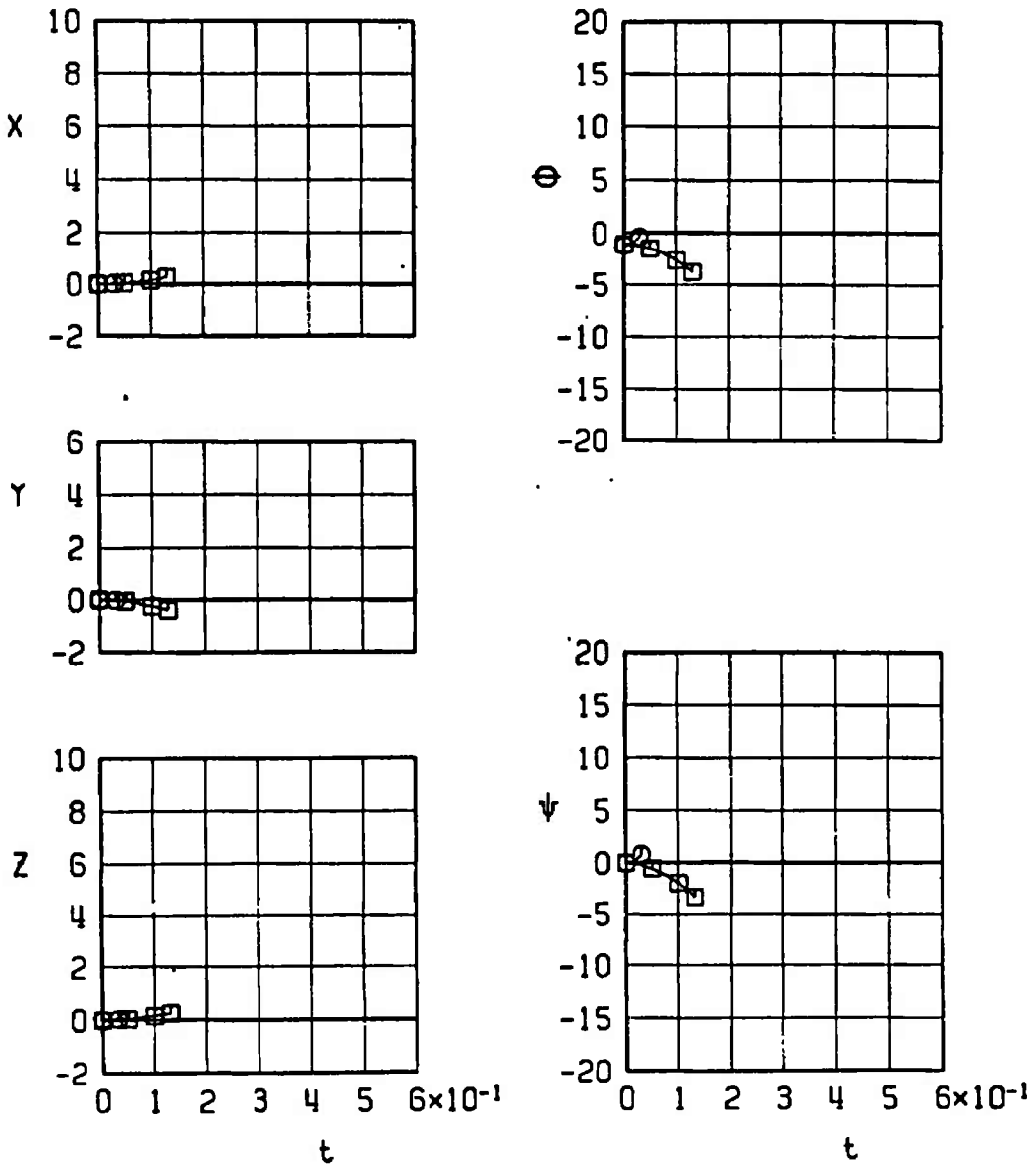

a. Configurations 24 and 25

Fig. 34 Effect of Wing-Loading Configuration on Separation Trajectories of the M-117GP at Mach Number 0.95

SYMBOL	CONF.	M_∞	α	H	$\bar{\theta}$	EJECTION FORCE
□ *	26	0.95	1.9	7000	-70	T6
○ *	27	0.95	1.9	7000	-70	T6
△	28	0.95	1.9	7000	-70	T6
◁ *	29	0.95	1.9	7000	-70	T6

*Indicates store-aircraft contact

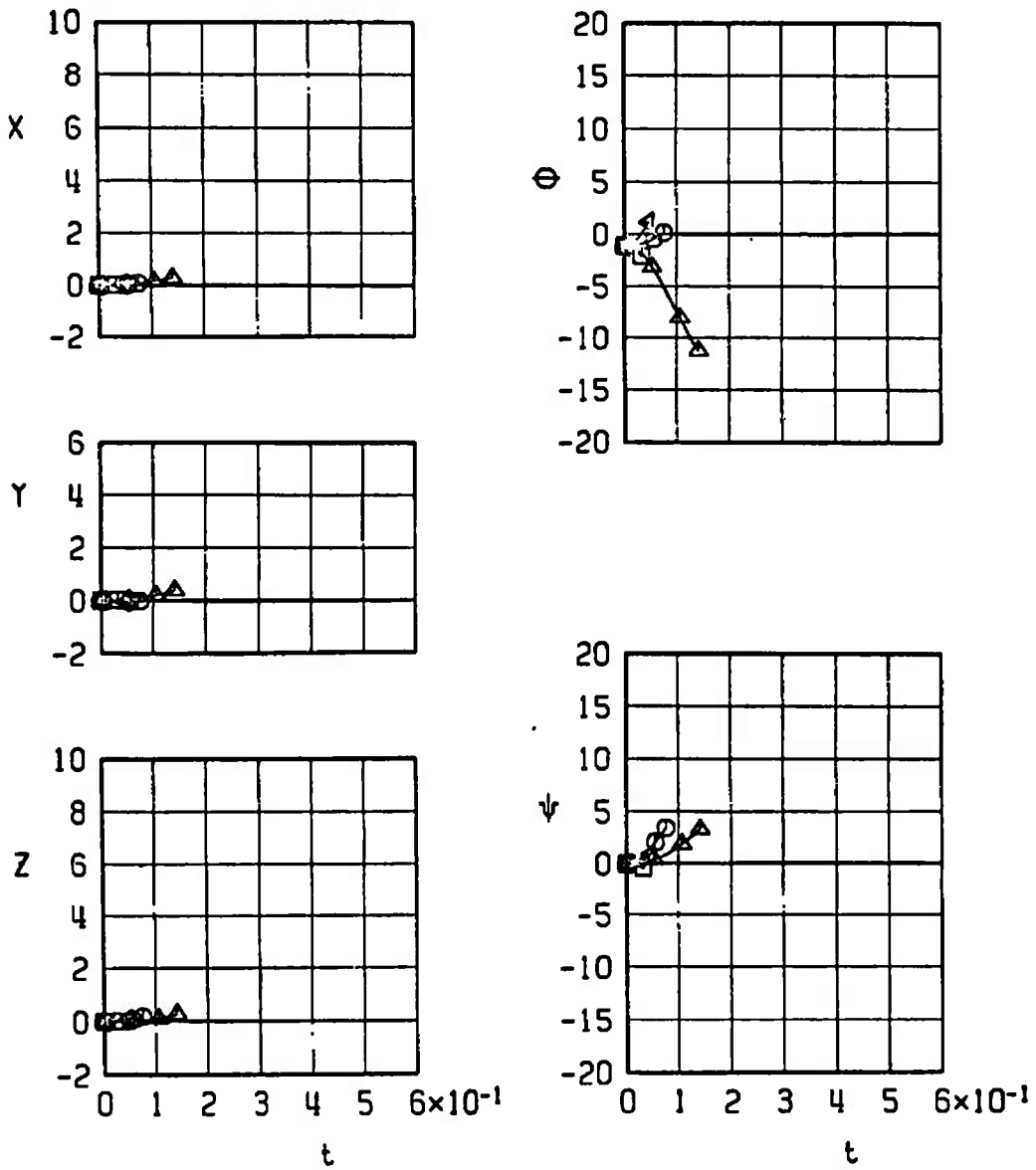

b. Configurations 26 through 29
Fig. 34 Continued

SYMBOL	CONF.	M_∞	α	H	$\bar{\theta}$	EJECTION FORCE
△ *	26	0.95	1.9	7000	-70	T5
◁ *	30	0.95	1.9	7000	-70	T5

* Indicates store - aircraft contact

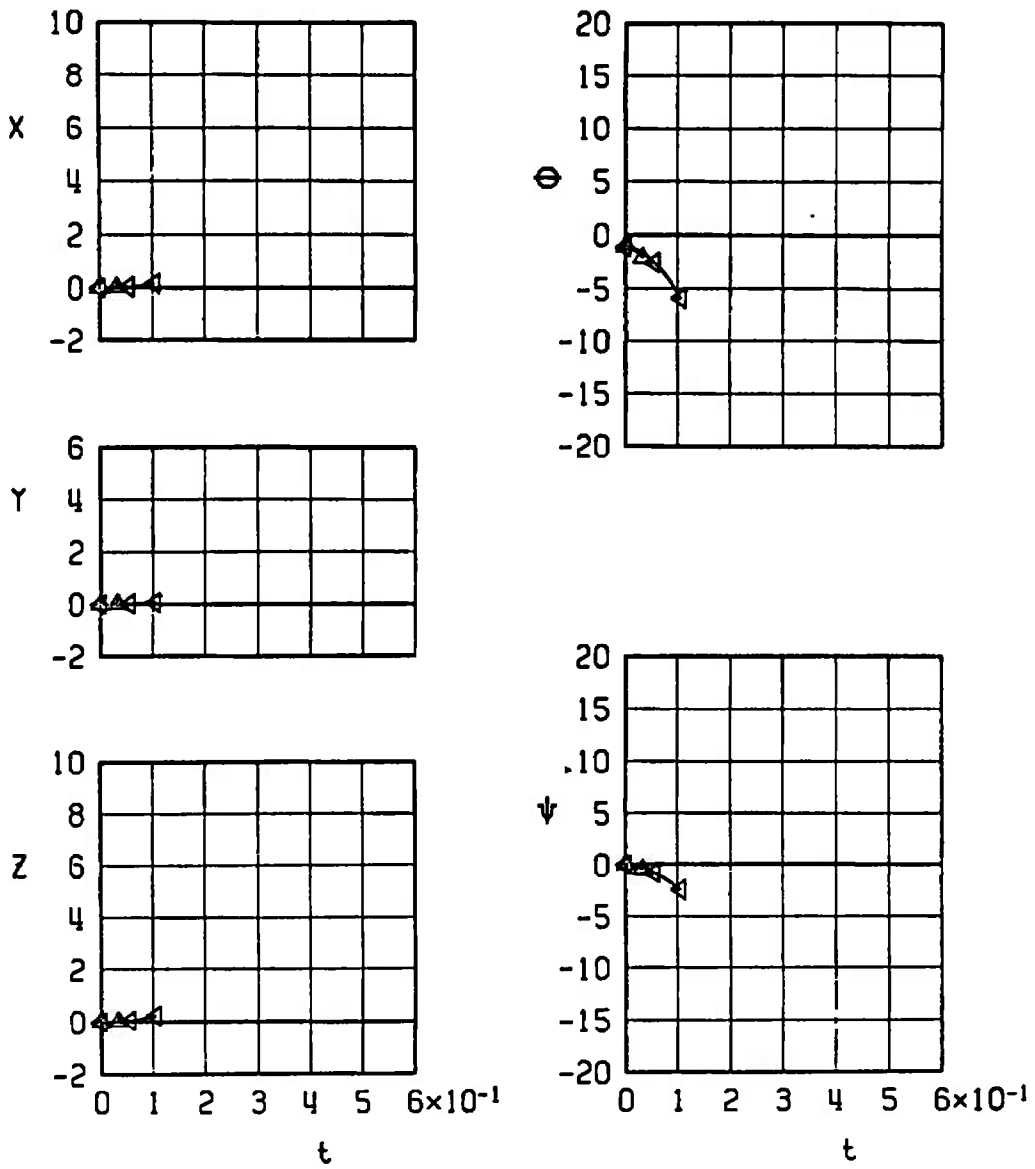

c. Configurations 26 and 30
Fig. 34 Concluded

SYMBOL	M_∞	α	H	$\bar{\theta}$	EJECTION FORCE
⊡ *	0.86	2.0	7000	-70	T5
⊙	0.95	1.9	7000	-70	T5

* Indicates store-aircraft contact

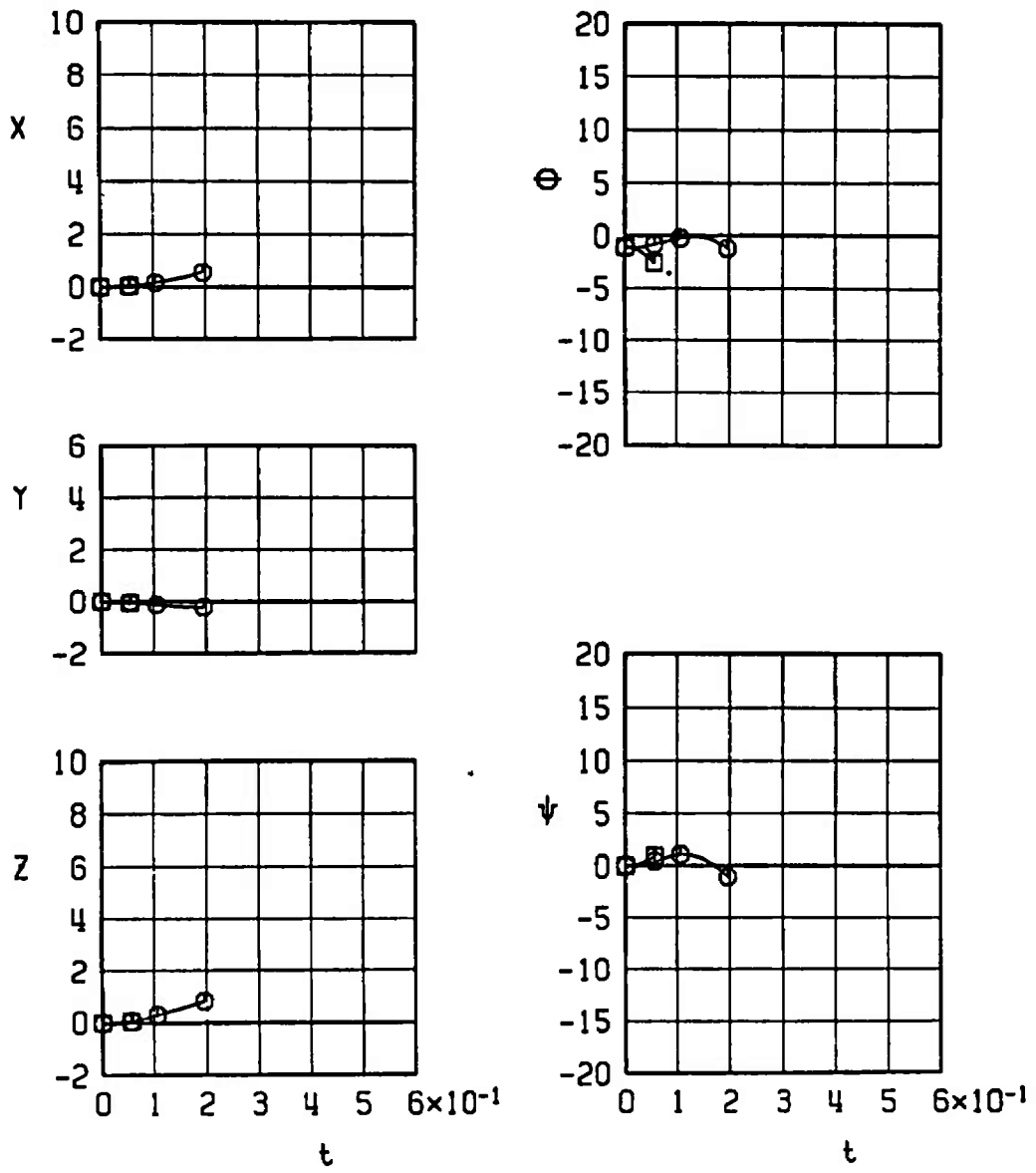

Fig. 35 Effect of Mach Number on Separation Trajectories of the MK-117GP; Configuration 31

SYMBOL	CONF	M_∞	α	H	$\bar{\theta}$	EJECTION FORCE
⊡	32	0.86	2.0	7000	-70	T6
⊙	40	0.86	2.0	7000	-70	T6

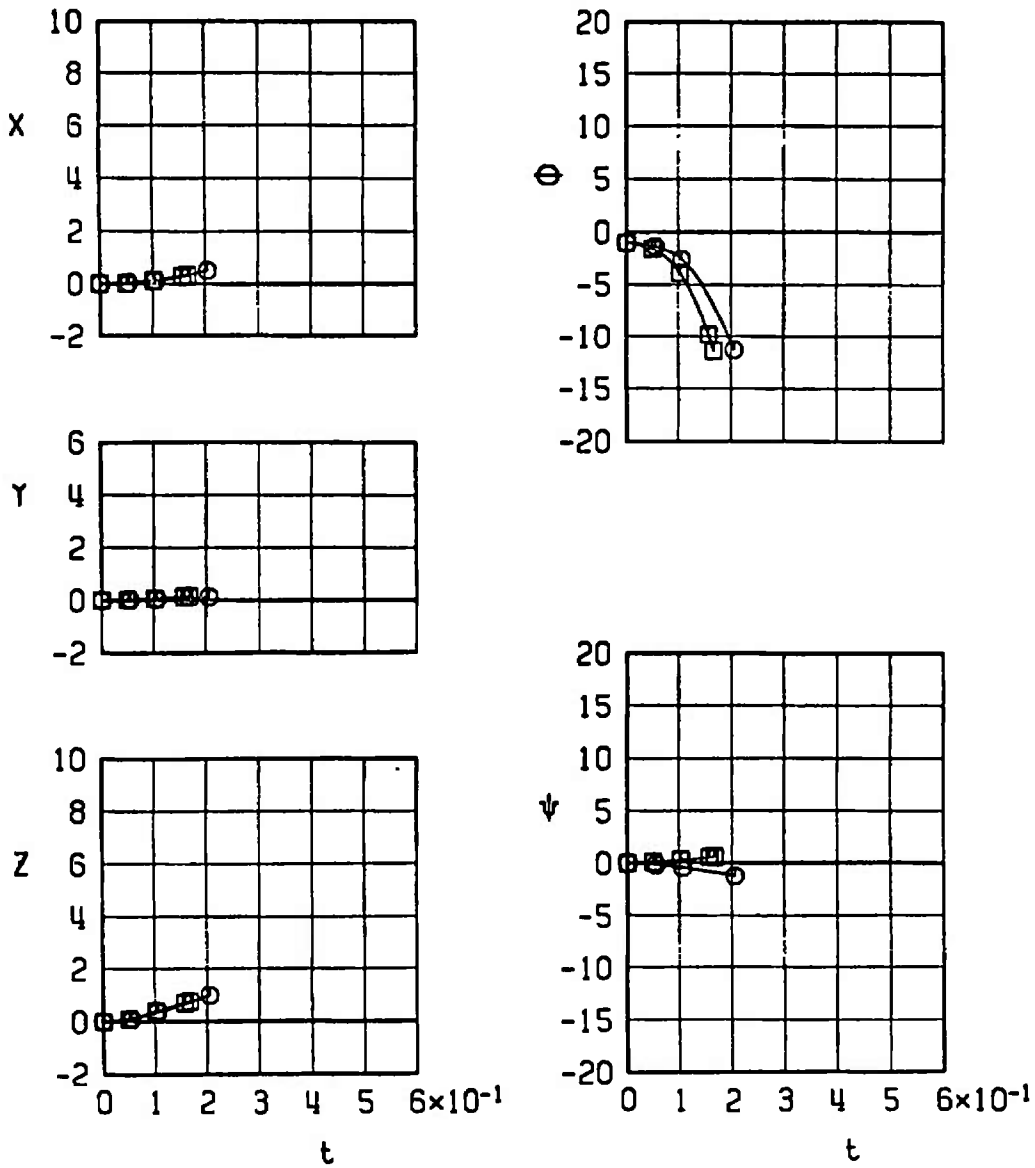

a. Configurations 32 and 40

Fig. 36 Effect of Wing-Loading Configuration on Separation Trajectories of the MK-82GP at Mach Number 0.86

SYMBOL	CONF.	M_∞	α	H	$\bar{\theta}$	EJECTION FORCE
⊡	41	0.86	2.0	7000	-70	T6
⊙	33	0.86	2.0	7000	-70	T6

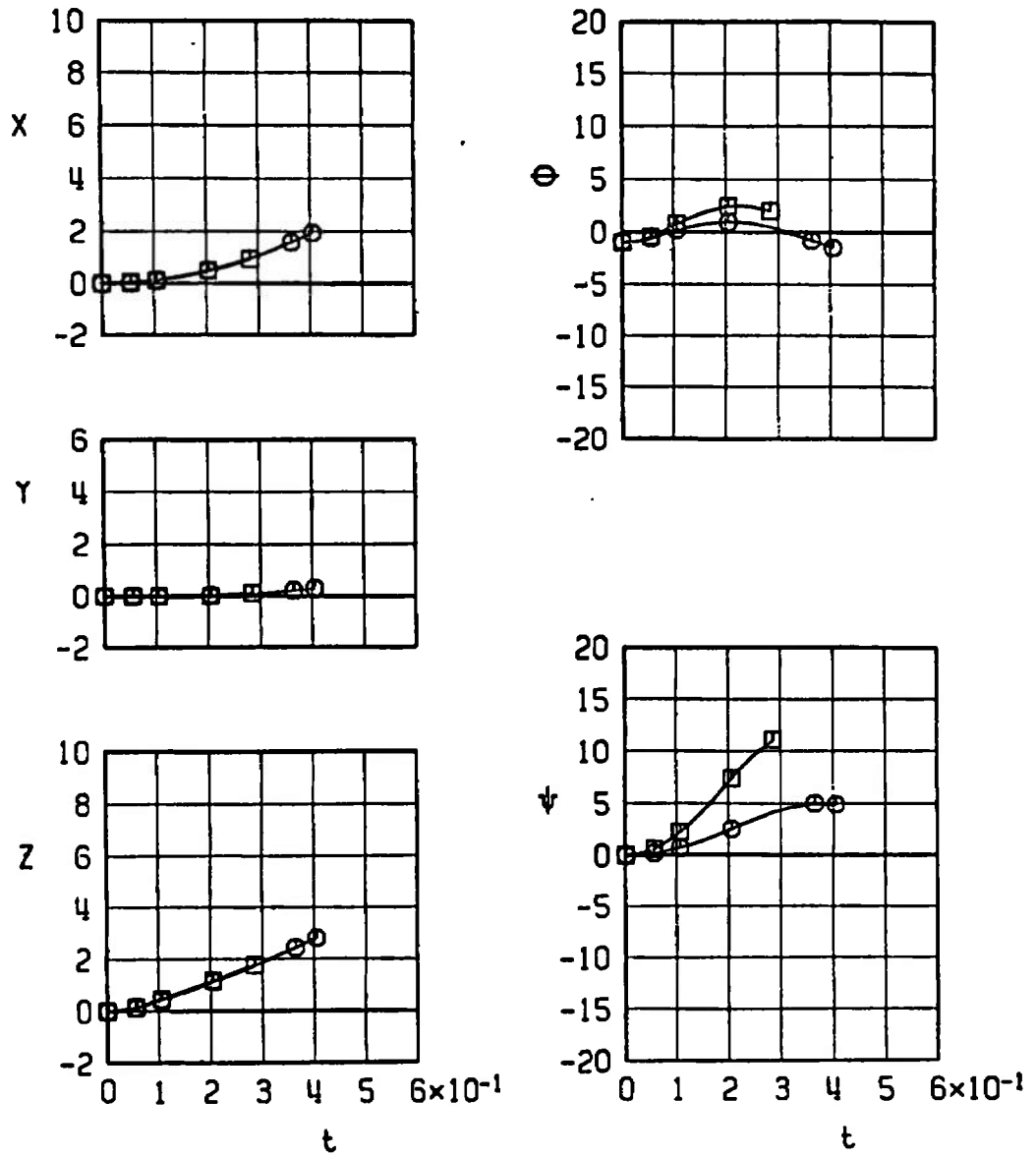

b. Configurations 41 and 33
Fig. 36 Continued

SYMBOL	CONF.	M_∞	α	H	$\bar{\theta}$	EJECTION FORCE
⊡	34	0.86	2.0	7000	-70	T6
⊙	42	0.86	2.0	7000	-70	T6

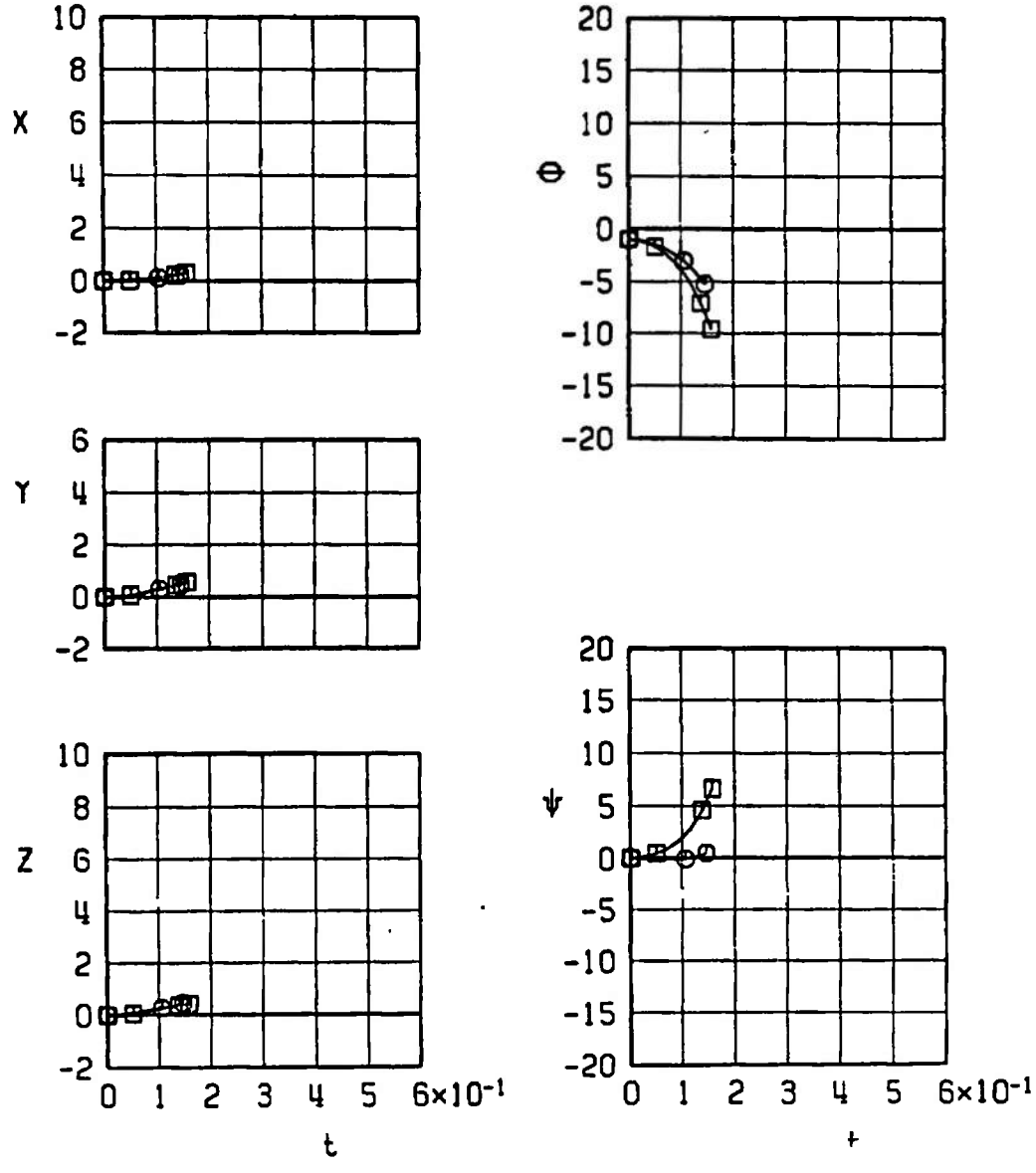

c. Configurations 34 and 42
Fig. 36 Continued

SYMBOL	CONF.	M_∞	α	H	$\bar{\theta}$	EJECTION FORCE
□	43	0.86	2.0	7000	-70	T6
○	35	0.86	2.0	7000	-70	T6

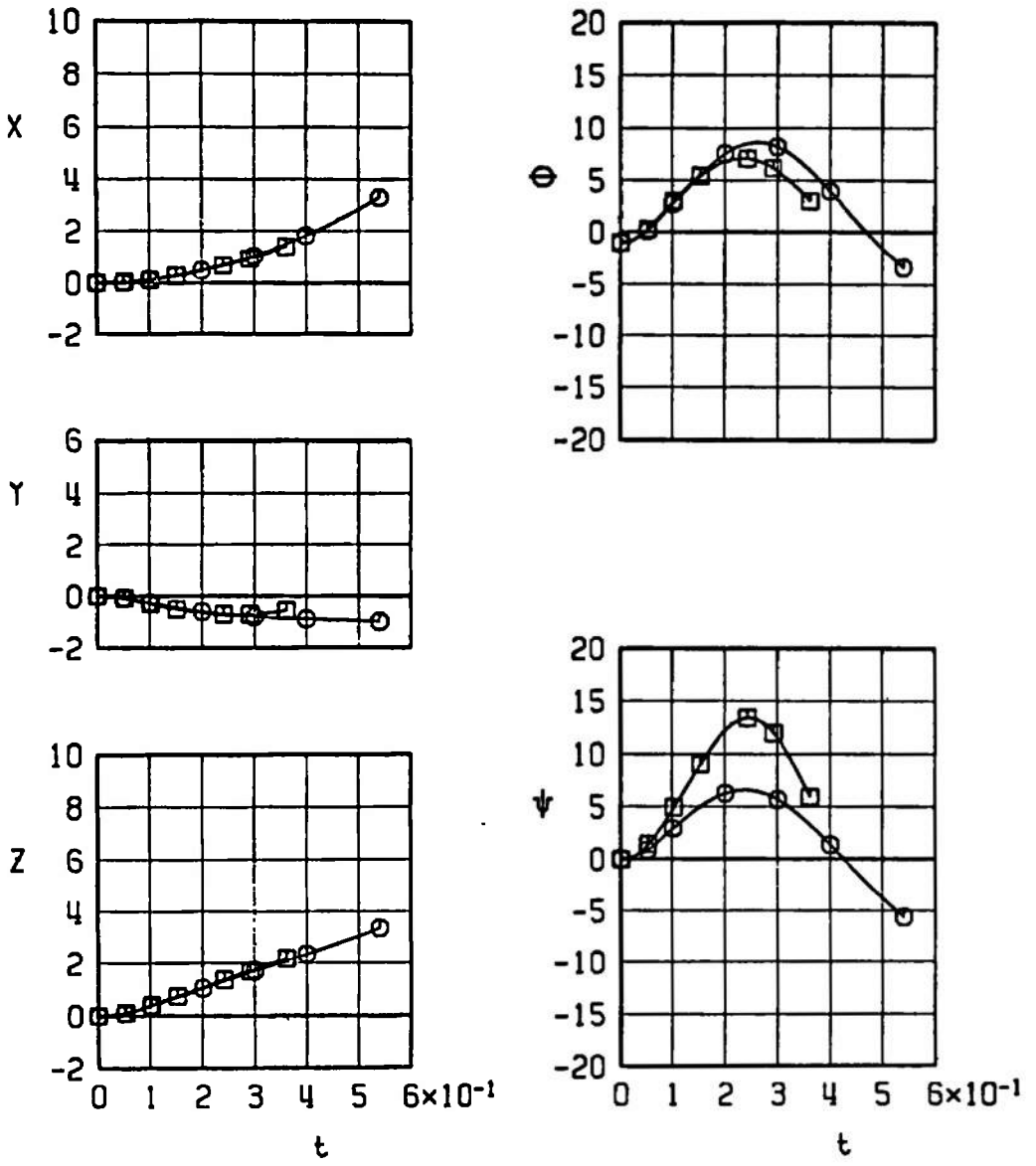

d. Configurations 43 and 35
Fig. 36 Continued

SYMBOL	CONF	M_∞	α	H	$\bar{\theta}$	EJECTION FORCE
⊡	36	0.86	2.0	7000	-70	T6
⊙	44	0.86	2.0	7000	-70	T6

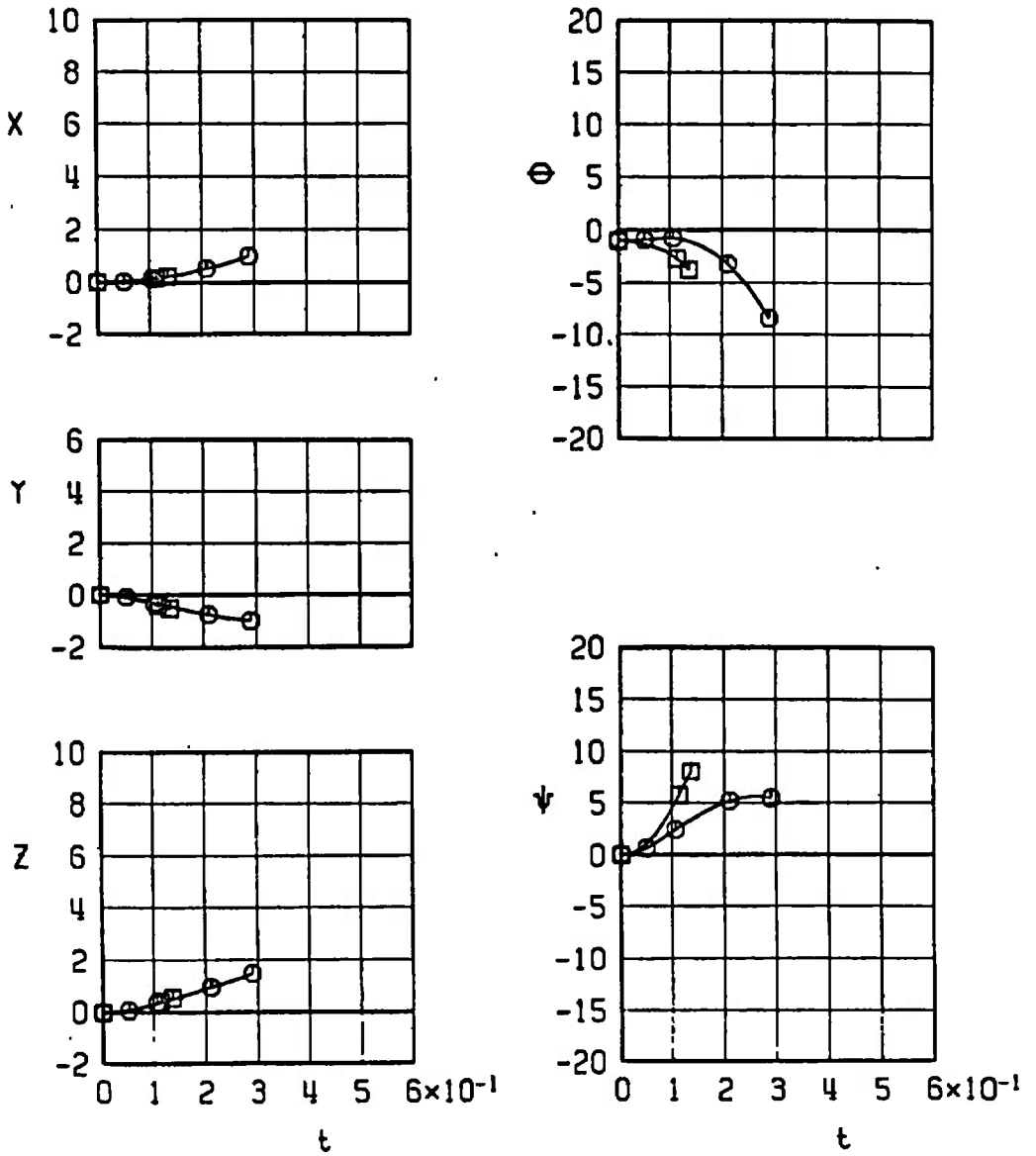

e. Configurations 36 and 44
Fig. 36 Continued

SYMBOL	CONF	M_∞	α	H	$\tilde{\theta}$	EJECTION FORCE
⊡	45	0.86	1.9	7000	-70	T6
⊙	37	0.86	1.9	7000	-70	T6

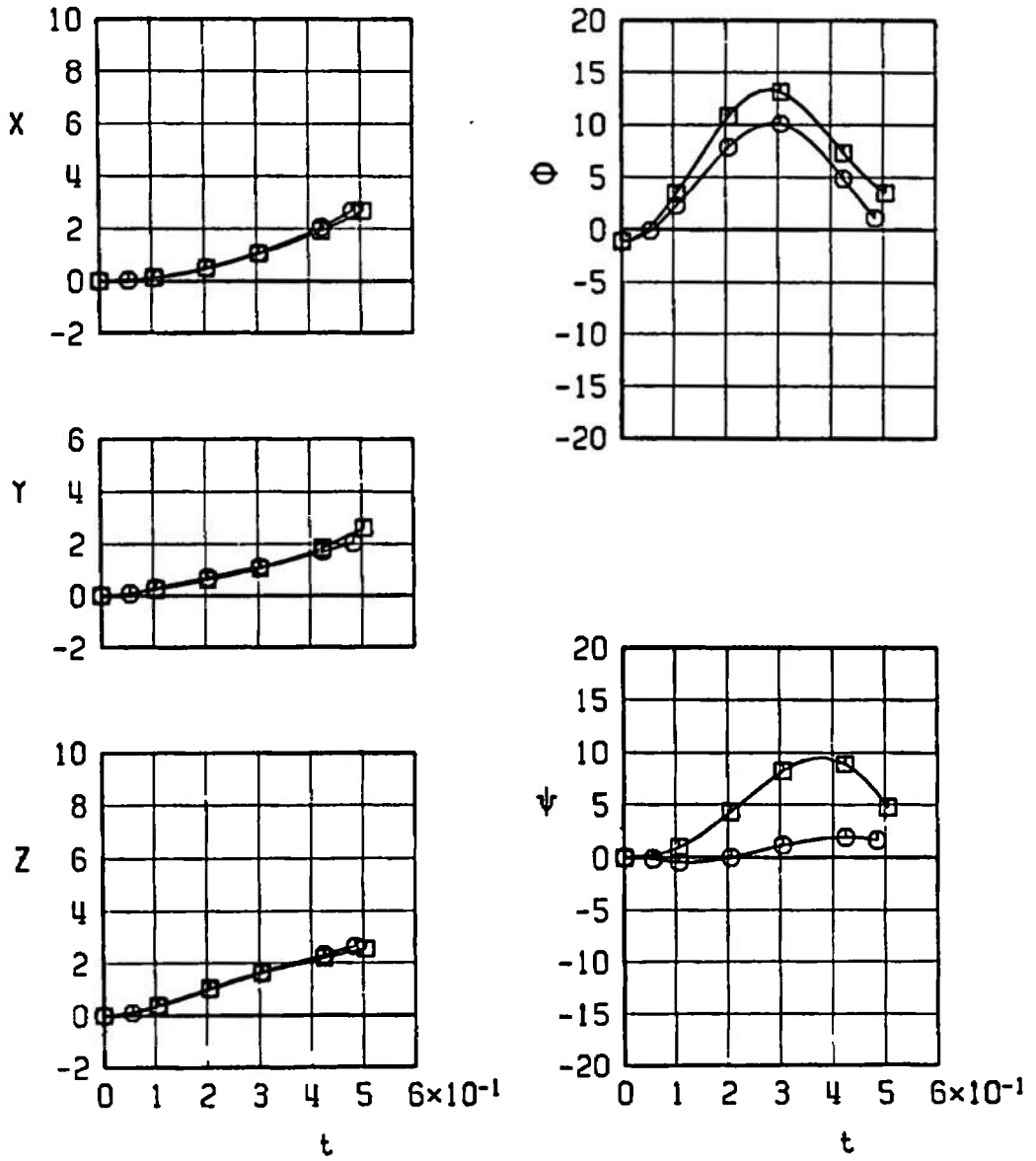

f. Configurations 45 and 37
Fig. 36 Continued

SYMBOL	CONF.	M_∞	α	H	$\bar{\theta}$	EJECTION FORCE
⊡	38	0.86	1.9	7000	-70	T6
⊙	46	0.86	1.9	7000	-70	T6

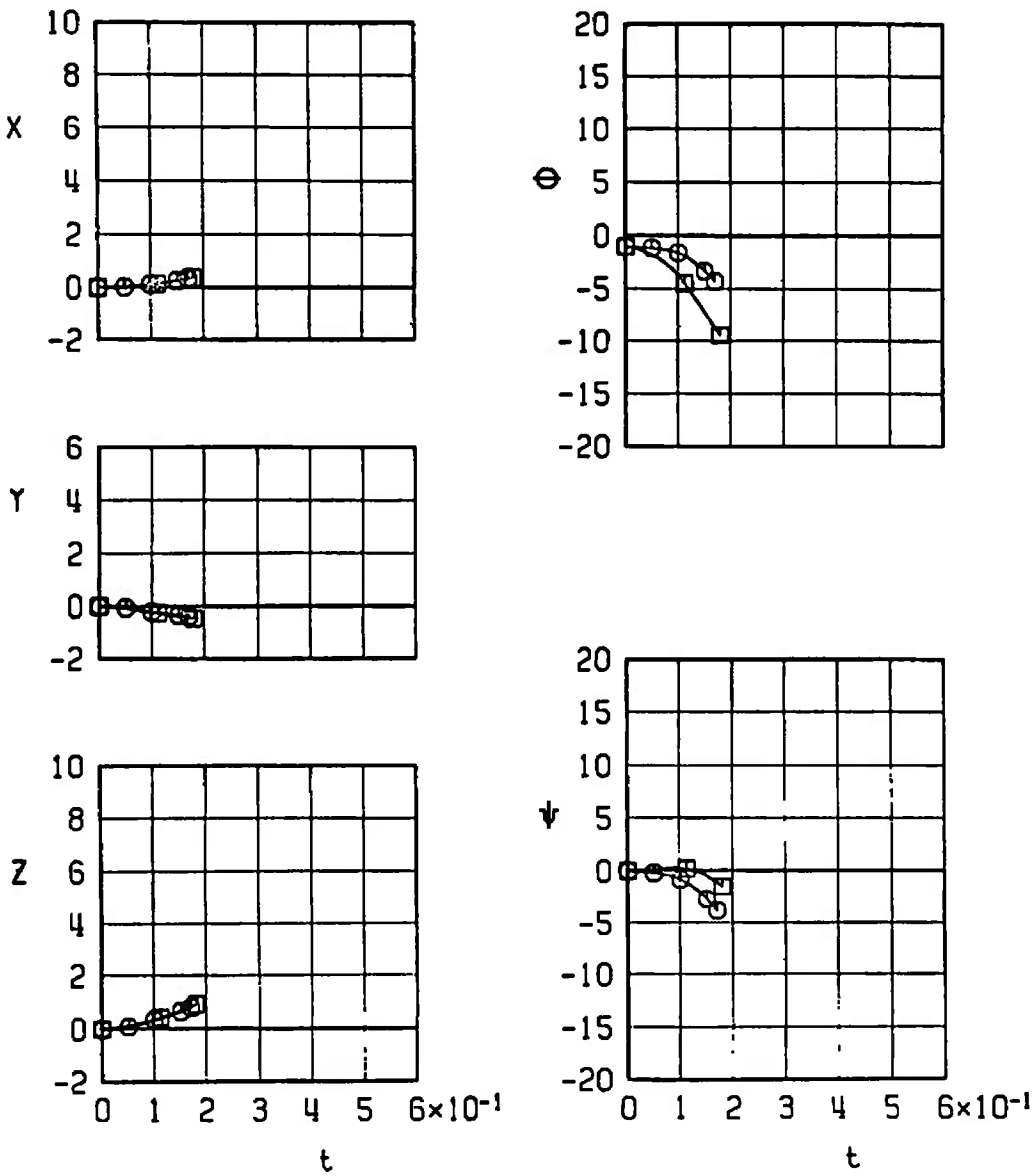

g. Configurations 38 and 46
Fig. 36 Concluded

SYMBOL	CONF.	M_∞	α	H	$\bar{\theta}$	EJECTION FORCE
⊡	32	0.95	1.9	7000	-70	T6
⊙	40	0.95	1.9	7000	-70	T6

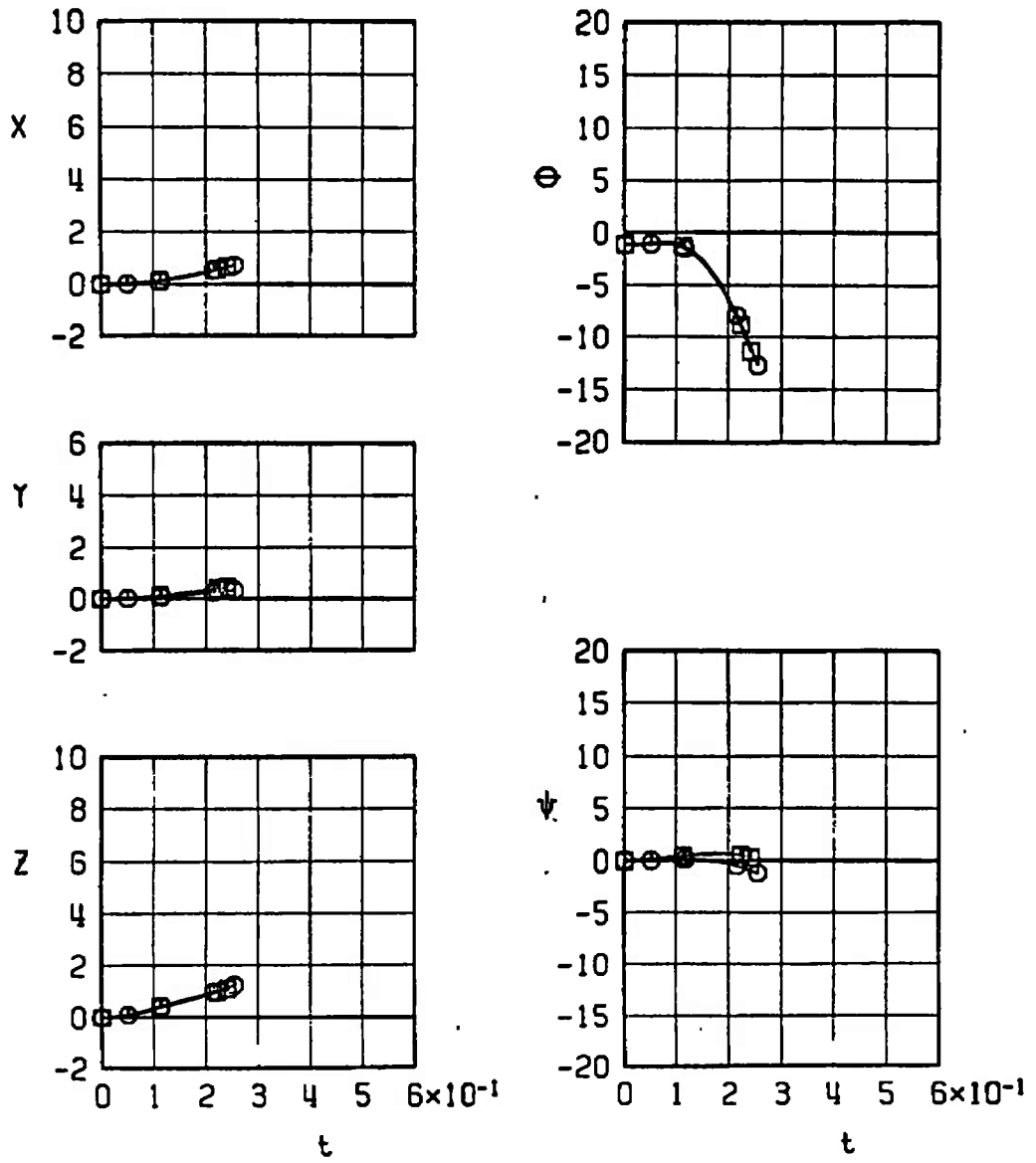

a. Configurations 32 and 40

Fig. 37 Effect on Wing-Loading Configuration on Separation Trajectories of the MK-82GP at Mach Number 0.95

SYMBOL	CONF.	M_∞	α	H	$\bar{\theta}$	EJECTION FORCE
□	41	0.95	1.9	7000	-70	T6
○	33	0.95	1.9	7000	-70	T6

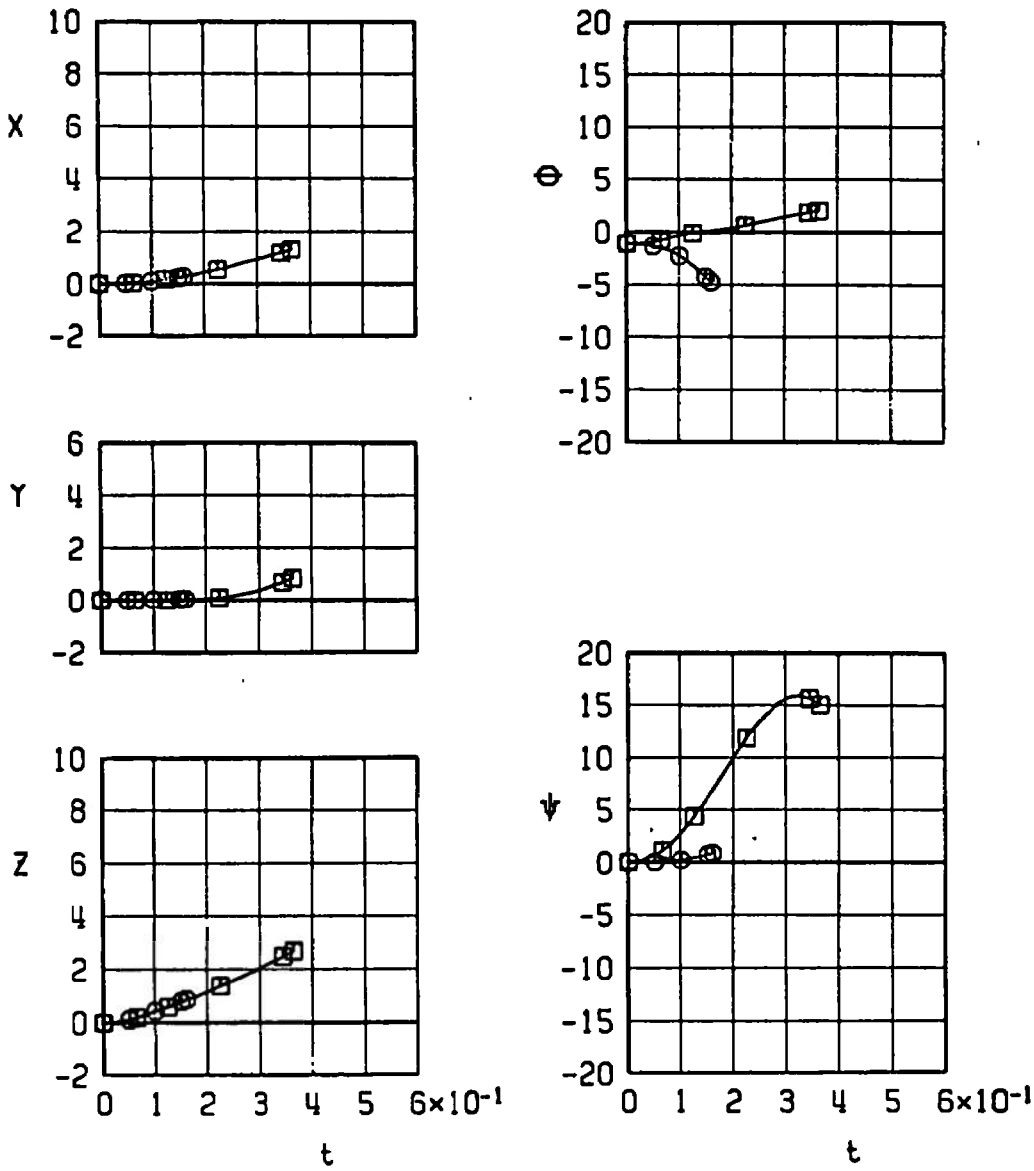

b. Configurations 41 and 33
Fig. 37 Continued

SYMBOL	CONF.	M_∞	α	H	$\bar{\theta}$	EJECTION FORCE
⊡	34	0.95	1.9	7000	-70	T6
⊙	42	0.95	1.9	7000	-70	T6

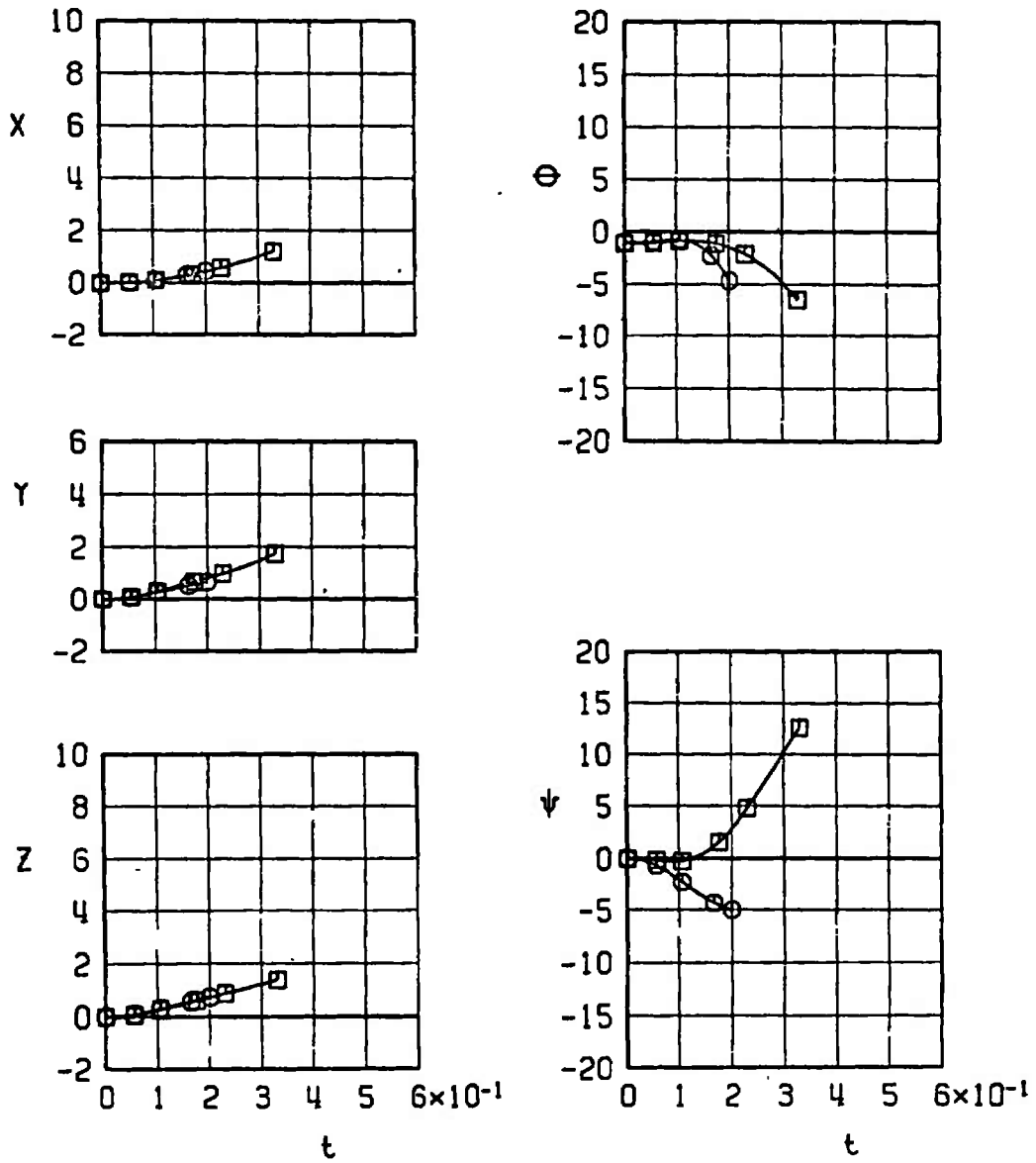

c. Configurations 34 and 42
Fig. 37 Continued

SYMBOL	CONF.	M_∞	α	H	$\bar{\theta}$	EJECTION FORCE
⊡	43	0.95	1.9	7000	-70	T6
⊙	35	0.95	1.9	7000	-70	T6

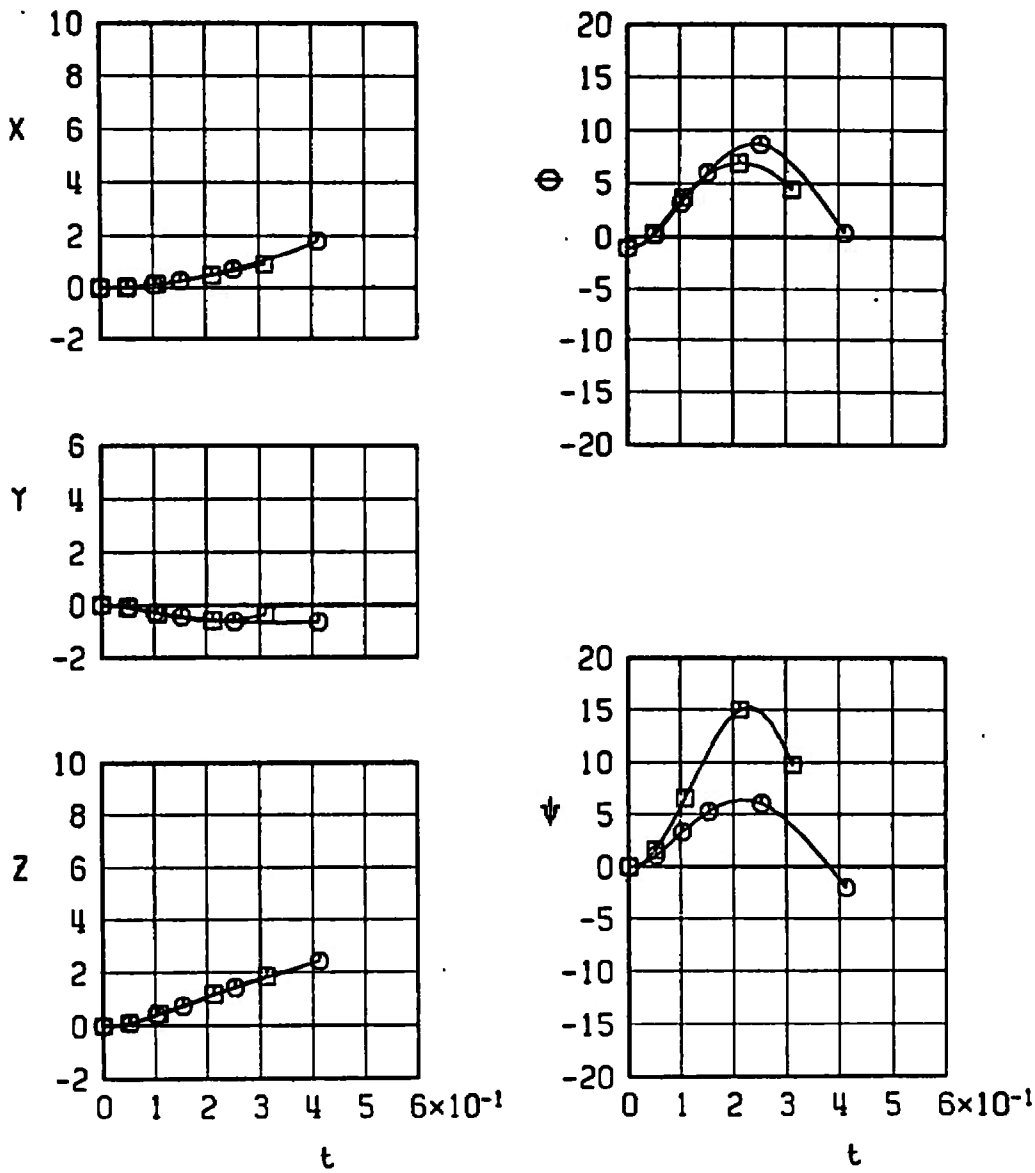

d. Configurations 43 and 35
Fig. 37 Continued

SYMBOL	CONF.	M_∞	α	H	$\bar{\theta}$	EJECTION FORCE
⊡	36	0.95	1.9	7000	-70	T6
⊙	44	0.95	1.9	7000	-70	T6

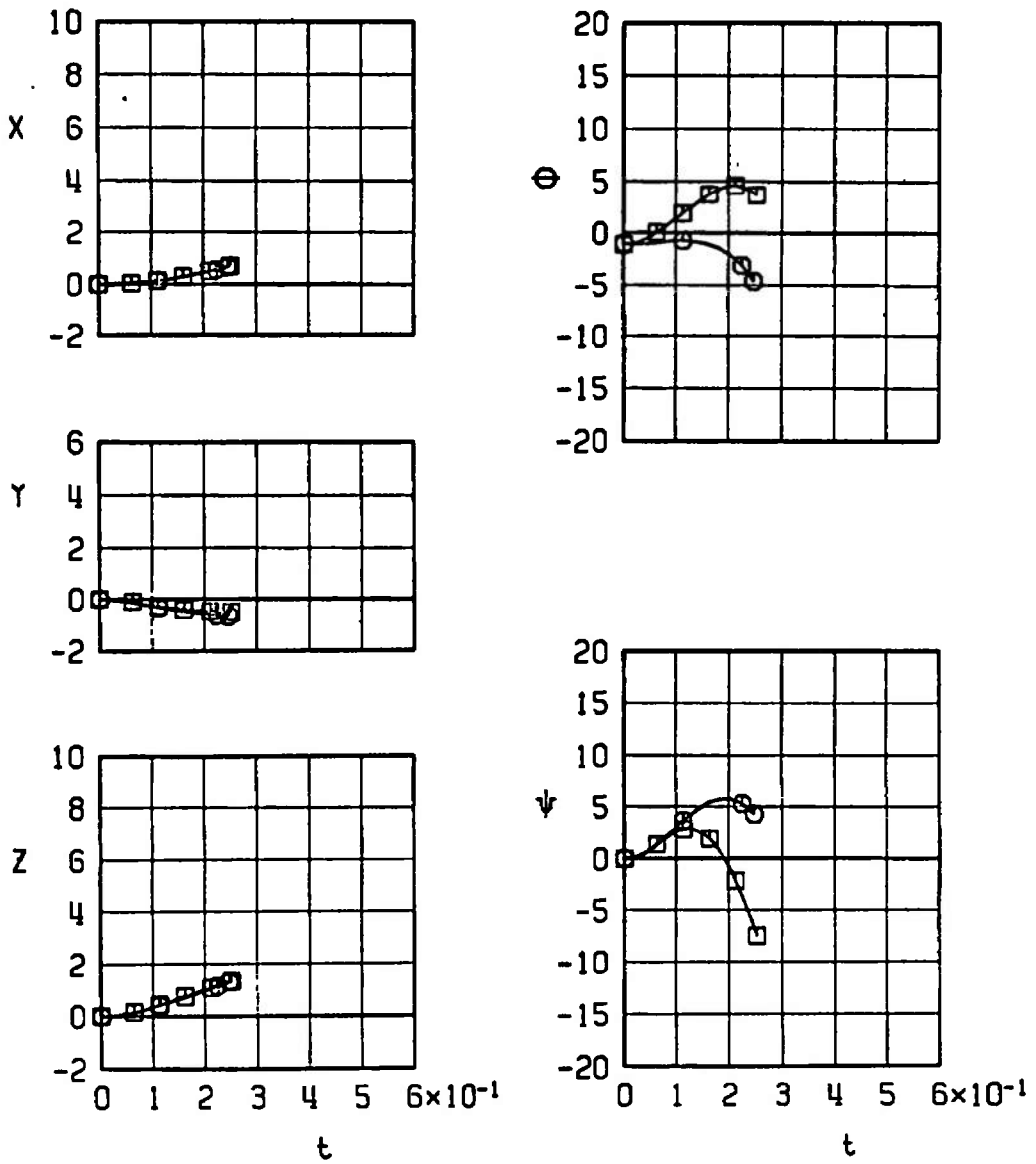

e. Configurations 36 and 44
Fig. 37 Continued

SYMBOL	CONF.	M_∞	α	H	$\bar{\theta}$	EJECTION FORCE
⊡	45	0.95	1.8	7000	-70	T6
⊙	37	0.95	1.8	7000	-70	T6

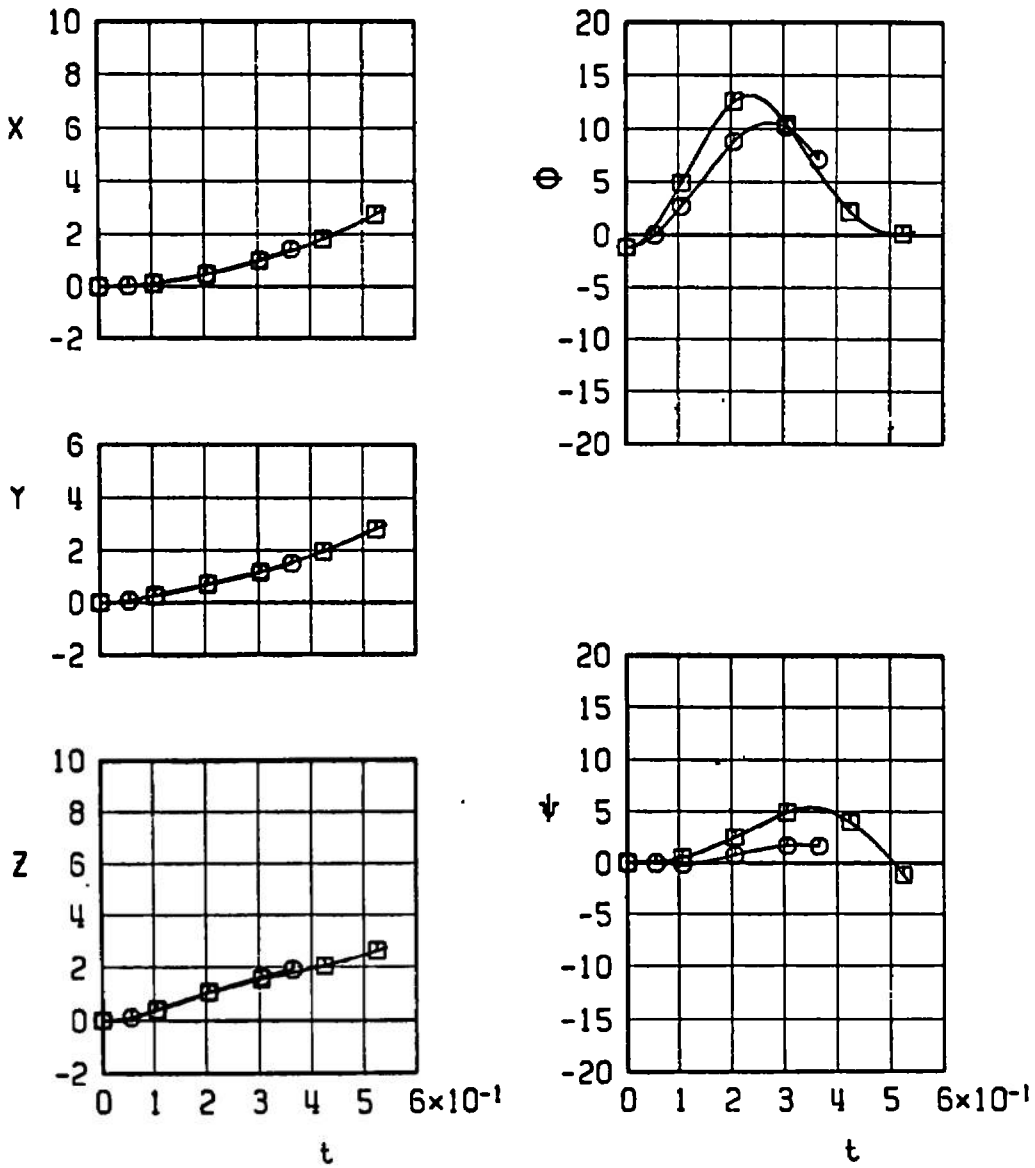

f. Configurations 45 and 37
Fig. 37 Continued

SYMBOL	CONF.	M_∞	α	H	$\bar{\theta}$	EJECTION FORCE
□	38	0.95	1.8	7000	-70	T6
⊙ *	46	0.95	1.8	7000	-70	T6

* Indicates store-aircraft contact

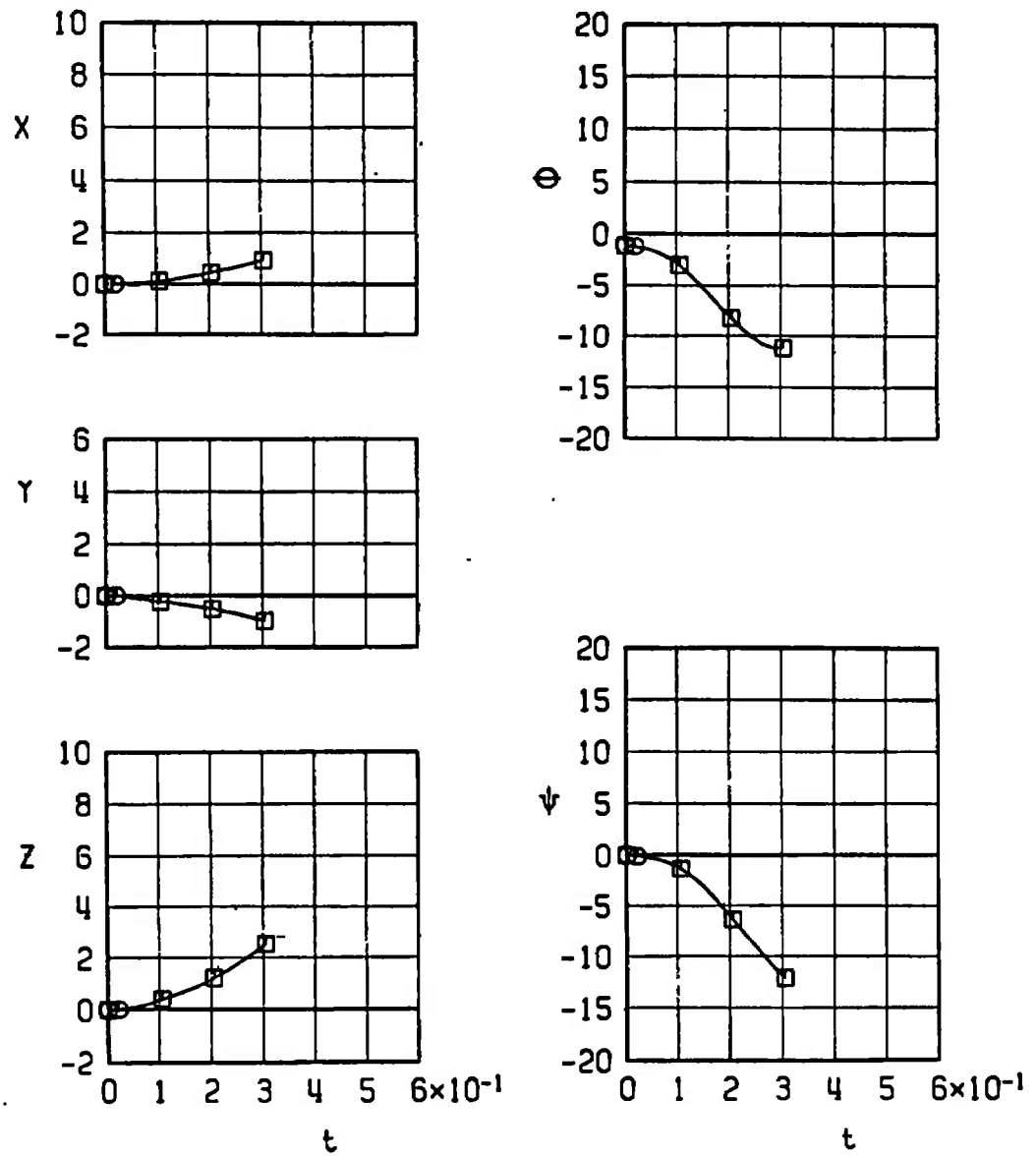

g. Configurations 38 and 46
Fig. 37 Concluded

SYMBOL	CONF.	M_∞	α	H	$\bar{\theta}$	EJECTION FORCE
□ *	39	0.86	2.0	7000	-70	T6
○ *	39	0.95	1.9	7000	-70	T6

*Indicates store-aircraft contact

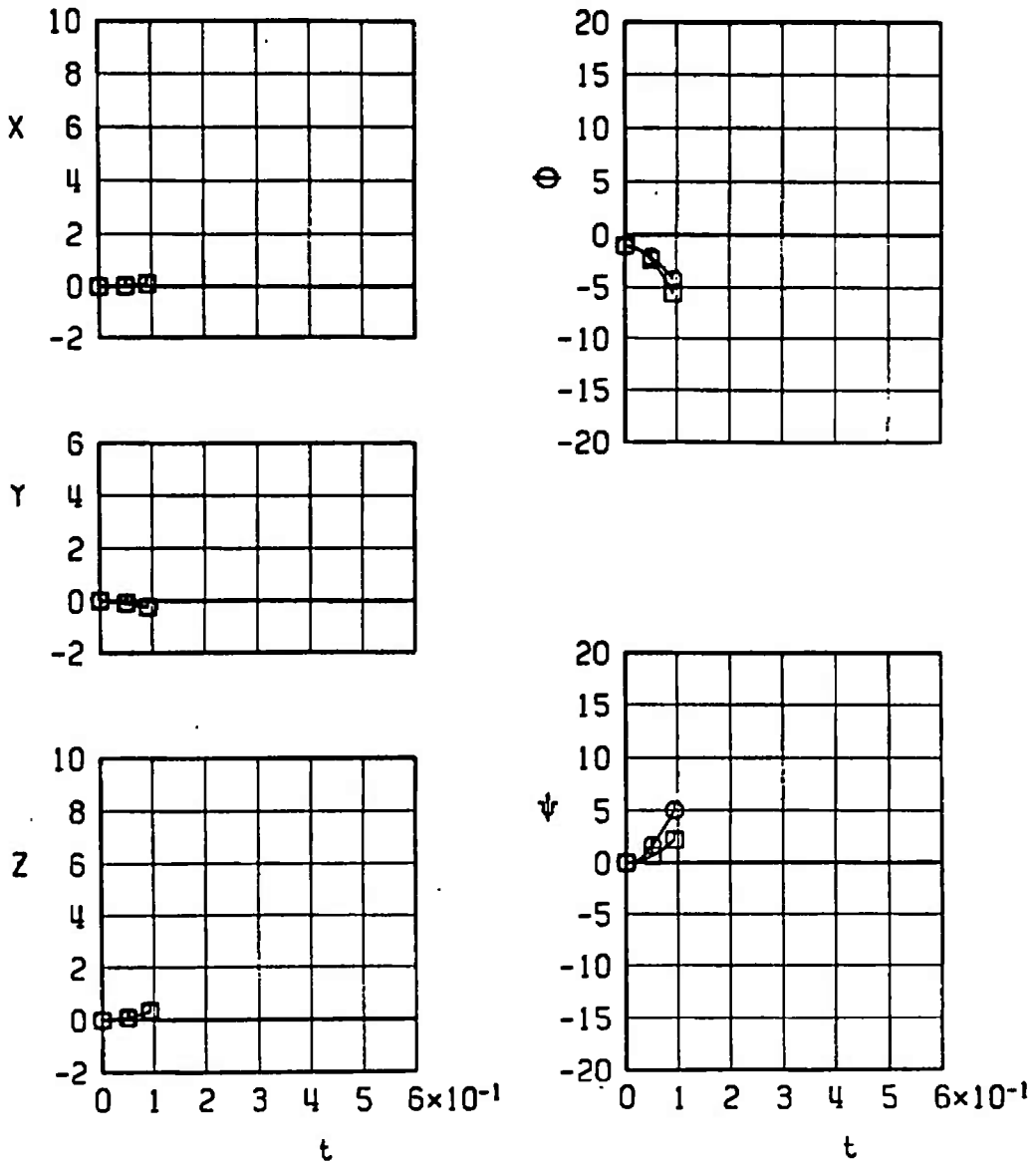

Fig. 38 Effect of Mach Number on Separation Trajectories of MK-82GP

SYMBOL	CONF.	M_∞	α	H	$\bar{\theta}$	EJECTION FORCE
□	47	0.86	1.9	7000	-70	T6
○	48	0.86	1.9	7000	-70	T6
△ *	49	0.86	1.9	7000	-70	T6

*Indicates store - aircraft contact

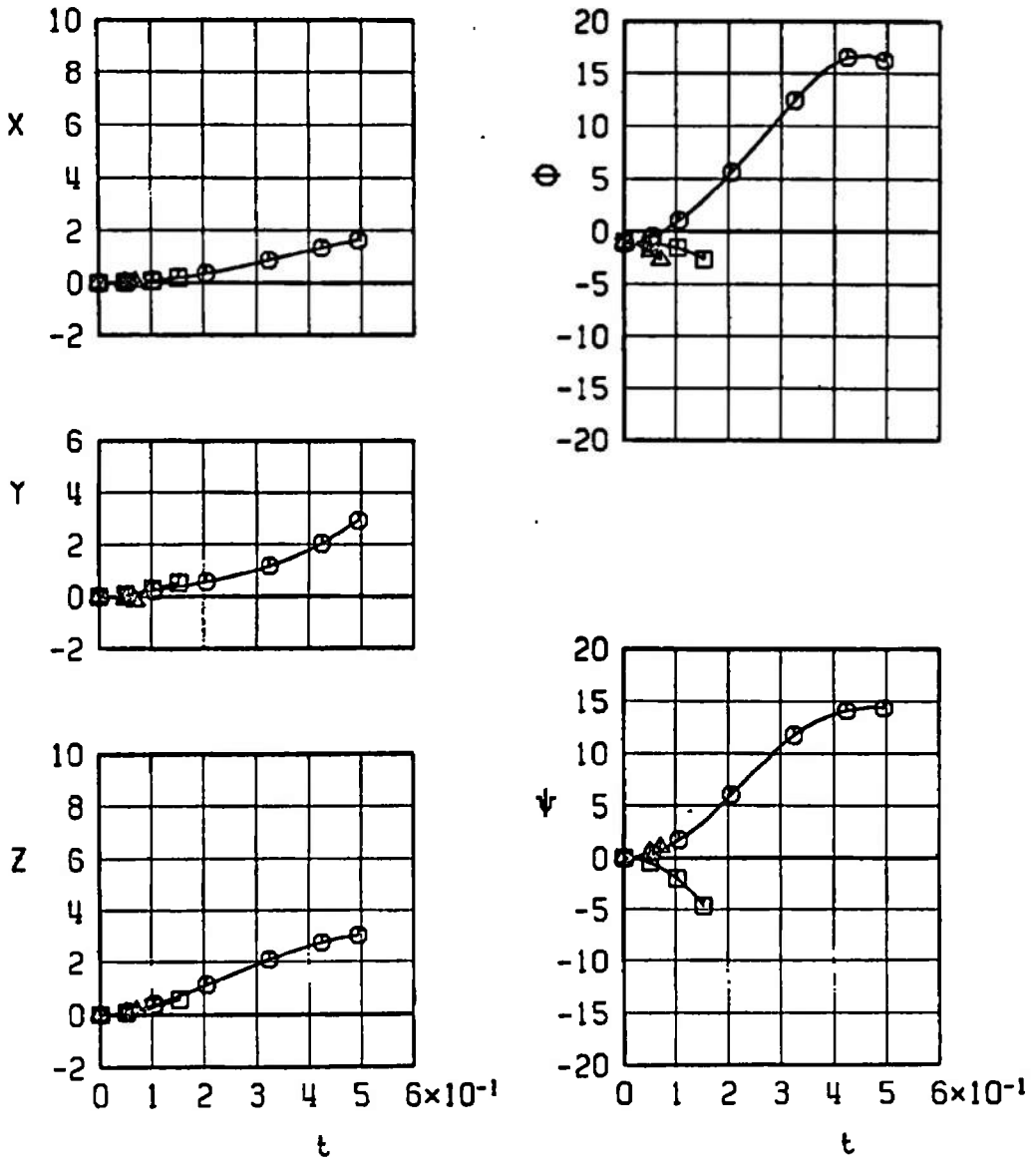

Fig. 39 Effect of Wing-Loading Configuration on Separation Trajectories of the MK-82SE at Mach Number 0.86

SYMBOL	CONF.	M_∞	α	H	$\bar{\theta}$	EJECTION FORCE
□	47	0.95	1.8	7000	-70	T6
○	48	0.95	1.8	7000	-70	T6
△ *	49	0.95	1.8	7000	-70	T6

* Indicates store-aircraft contact

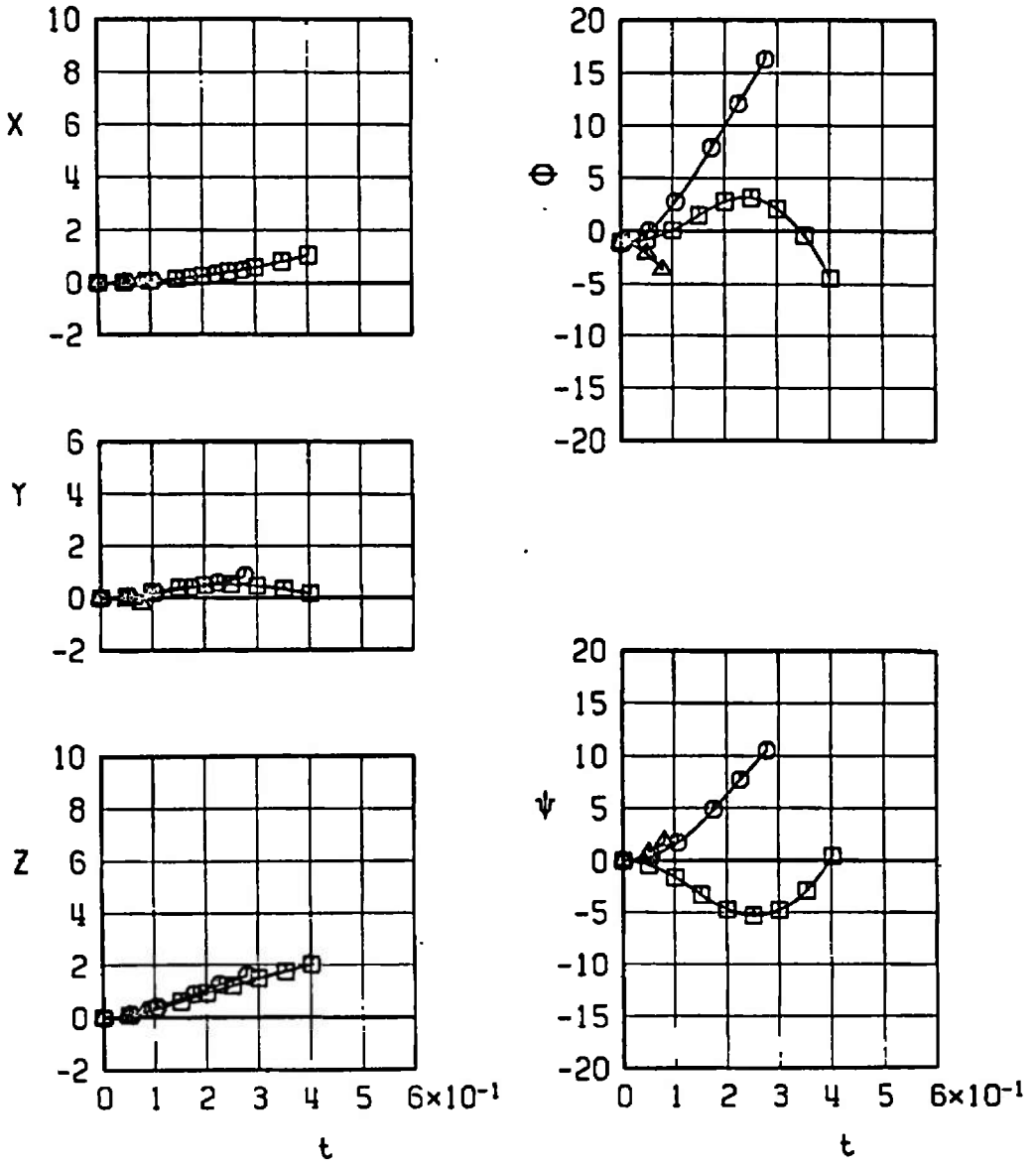

Fig. 40 Effect of Wing-Loading Configuration on Separation Trajectories of MK-82SE at Mach Number 0.95

TABLE I
FULL-SCALE PARAMETERS USED IN TRAJECTORY CALCULATIONS

Parameter	Store				
	BLU-1/B		M-117GP	MK-82GP	MK-82SE
	Finned	Unfinned			
C'_{m_q}	-0.810	-0.240	-1.34	-0.760	-0.76
C'_{n_r}	48.0	-11.80	-42.0	-53.0	-53.0
C_A	---	---	---	0.180	0.400
$\bar{m}$	23.2	22.30	24.6	15.50	16.60
X_{cg}	5.42	5.37	2.46	3.06	3.28
b	1.550	1.550	1.333	0.896	0.896
$\bar{c}$	11.808	10.815	7.325	7.467	7.613
S	1.887	1.887	1.396	0.630	0.630
Ejector piston distance forward of store cg, X_L, ft					
1. TER	---	---	-0.280	-0.300	-0.078
2. MER	---	0.183	-0.280	-0.300	-0.078
3. Pylon: Forward piston	0.875	0.833	---	---	---
4. Pylon: Aft piston	-0.791	-0.833	---	---	---
I_{yy}	147.0	131.0	48.0	36.0	48.0
I_{zz}	147.0	131.0	48.0	36.0	48.0

TABLE II
FLIGHT-TEST DATA USED IN TRAJECTORY CALCULATIONS

Store Parameters and Orientation				
Parameters	No. 1	No. 2	No. 3	No. 4
M_∞	0.68	0.80	0.68	0.68
α	3.2	2.5	3.2	3.2
H	6040	4940	5840	5840
$\bar{\theta}$	-30	-30	-30	-30
Wing-Loading Configuration	5	5	6	6
C_{m_q}	-0.2400	-0.2400	-0.2400	-0.2400
C_{n_r}	-11.800	-11.800	-11.800	-11.800
$\bar{m}$	23.000	22.100	22.900	22.900
X_{cg}	5.2300	5.5100	5.4700	5.4700
b	1.5500	1.5500	1.550	1.550
$\bar{c}$	10.820	10.8200	10.820	10.820
S	1.8900	1.8900	1.890	1.890
I_{yy}	132.90	129.00	134.80	134.80
I_{zz}	132.90	129.00	134.80	134.80
t_1	0.0690	0.0555	0.0535	0.0730
X_i	-0.0150	-0.0480	-0.0950	-0.0200
Y_i	-0.0250	0.0280	0.0900	-0.0150
Z_i	0.3440	0.3670	0.3750	0.3830
$\Delta\theta_i$	-1.9000	-2.0500	-2.8000	-3.6000
$\Delta\psi_i$	0.3000	-0.1500	0.3000	0.8000
u_i	-0.4800	0.6000	-2.4500	-0.3000
v_i	0.550	-0.8000	0.8000	-0.4000
w_i	9.400	10.500	11.0000	9.6000
q_i	-0.8600	-1.0208	-1.6927	-1.605
r_i	0.0698	0.08725	0.3665	0.2966

TABLE III
DATA UNCERTAINTIES

Store Model	ΔC_N	ΔC_Y	ΔC_A	ΔC_m	ΔC_n	ΔC_ℓ
BLU-1C/B Finned	±0.0038	±0.0042	±0.0076	±0.0043	±0.0048	±0.0018
BLU 1C/B Unfinned	±0.0076	±0.0084	±0.0152	±0.0086	±0.0096	±0.0036

TABLE IV
MAXIMUM FULL-SCALE POSITION UNCERTAINTIES CAUSED BY BALANCE INACCURACIES

Store	M_∞	t	δX	δY	δZ	$\delta\theta$	$\delta\psi$
BLU-1C/B Finned	0.42	0.2	±0.04	±0.04	±0.05	±0.5	±0.5
BLU-1C/B Unfinned	0.42	0.2	±0.01	±0.01	±0.05	±0.1	±0.1
M-117GP	0.86	0.2	±0.03	±0.03	±0.03	±0.2	±0.1
MK-82GP	0.86	0.2	---	±0.01	±0.03	±0.4	±0.3
MK-82SE	0.86	0.2	---	±0.01	±0.03	±0.4	±0.3

TABLE V
AIRCRAFT WING-LOADING CONFIGURATIONS

Loading Configuration	Wing	Launch Store Model	Inboard Pylon	Center Pylon	Outboard Pylon
1	R	Unfinned BLU-1C/B	Empty	MER: Unfinned BLU-1C/B (Sting), Sta. 1	Empty
				Unfinned BLU-1C/B (Dummy), Sta. 4, 6	
2	L	Unfinned BLU-1C/B	Empty	MER: Unfinned BLU-1C/B (Sting), Sta. 6	Empty
				Unfinned BLU-1C/B (Dummy), Sta. 4	
3	R	Finned BLU-1C/B	Empty	MER: Finned BLU-1C/B (Sting), Sta. 1	Empty
				Finned BLU-1C/B (Dummy), Sta. 4, 6	
4	L	Finned BLU-1C/B	Empty	MER: Finned BLU-1C/B (Sting), Sta. 4	Empty
				Finned BLU-1C/B (Dummy), Sta. 6	
5	R	Unfinned BLU-1C/B	Unfinned BLU-1C/B (Dummy)	Unfinned BLU-1C/B (Dummy)	Unfinned BLU-1C/B (Launch)
6	R	Unfinned BLU-1C/B	Empty	Unfinned BLU-1C/B (Launch)	Unfinned BLU-1C/B (Dummy)
7	R	Unfinned BLU-1C/B	Unfinned BLU-1C/B (Dummy)	MER: M-117 (Dummy), Sta. 1-4	Unfinned BLU-1C/B (Launch)
8	L	Unfinned BLU-1C/B	Unfinned BLU-1C/B (Launch)	MER: MK-82GP (Dummy), Sta. 1-6	Empty
9	L	Unfinned BLU-1C/B	Unfinned BLU-1C/B (Dummy)	MER: MK-82GP (Dummy), Sta. 1-6	Unfinned BLU-1C/B (Launch)
10	R	Unfinned BLU-1C/B	Unfinned BLU-1C/B (Dummy)	MER: Empty	Unfinned BLU-1C/B (Launch)

TABLE V (Continued)

Loading Configuration	Wing	Launch Store Model	Inboard Pylon	Center Pylon	Outboard Pylon
11	L	Unfinned BLU-1C/B	Unfinned BLU-1C/B (Dummy)	Unfinned BLU-1C/B (Launch)	SUU 42/A (Dummy)
12	R	Unfinned BLU-1C/B	Unfinned BLU-1C/B (Launch)	MER: Empty	Empty
13	L	Unfinned BLU-1C/B	Unfinned BLU-1C/B (Dummy)	Unfinned BLU-1C/B (Launch)	Empty
14	R	Unfinned BLU-1C/B	MER: Unfinned BLU-1C/B (Dummy), Sta. 2, 3	MER: Unfinned BLU-1C/B, Sta. 3 Unfinned BLU-1C/B (Launch), Sta. 2	MER Empty
15	L	Unfinned BLU-1C/B	MER: Unfinned BLU-1C/B (Dummy), Sta. 2, 3	MER: Unfinned BLU-1C/B (Launch), Sta. 3	MER Empty
16	R	Unfinned BLU-1C/B	MER: Unfinned BLU-1C/B (Dummy), Sta. 3	Empty	MER
			Unfinned BLU-1C/B (Launch), Sta. 2		Empty
17	L	Unfinned BLU-1C/B	MER: Unfinned BLU-1C/B (Launch), Sta. 5	Empty	Empty
18	R	Unfinned BLU-1C/B	MER: Unfinned BLU-1C/B (Dummy), Sta. 2, 3	Unfinned BLU-1C/B (Dummy)	MER: Unfinned BLU-1C/B (Dummy), Sta. 3
					MER: Unfinned BLU-1C/B (Launch), Sta. 2
19	L	Unfinned BLU-1C/B	MER: Unfinned BLU-1C/B (Dummy), Sta. 2	Unfinned BLU-1C/B (Dummy)	MER: Unfinned BLU-1C/B (Launch), Sta. 5
20	L	Finned BLU-1C/B	Finned BLU-1C/B (Dummy)	Finned BLU-1C/B (Launch)	SUU-42 (Dummy)
21	L	Finned BLU-1C/B	Finned BLU-1C/B (Dummy)	MER: Empty	Finned BLU-1C/B (Launch)
22	R	Finned BLU-1C/B	Finned BLU-1C/B (Launch)	MER: MK-82 GP (Dummy), Sta. 1-6	Empty

TABLE V (Continued)

Loading Configuration	Wing	Launch Store Model	Inboard Pylon	Center Pylon	Outboard Pylon
23	R	Finned BLU-1C/B	Finned BLU-1C/B (Dummy)	MER: MK-82GP (Dummy), Sta. 1-6	Finned BLU-1C/B (Launch)
24	R	M-117	Finned BLU-1C/B (Dummy)	MER: M-117 (Launch), Sta. 5 M-117 (Dummy), Sta. 6	Finned BLU-1C/B (Dummy)
25	R	M-117	Finned BLU-1C/B (Dummy)	MER: M-117 (Launch), Sta. 6	Finned BLU-1C/B (Dummy)
26	L	M-117	M-117 (Dummy)	MER: M 117 (Launch), Sta. 1 M-117 (Dummy), Sta. 2-4	SUU-42 (Dummy)
27	R	M-117	M-117 (Dummy)	MER: M-117 (Launch), Sta. 2 M-117 (Dummy), Sta. 5, 6	SUU-42 (Dummy)
28	L	M-117	M-117 (Dummy)	MER: M-117 (Launch), Sta. 3 M-117 (dummy), Sta. 4	SUU-42 (Dummy)
29	R	M-117	M-117 (Dummy)	MER: M-117 (Launch), Sta. 6	SUU-42 (Dummy)
30	L	M-117	Empty	MER: M-117 (Launch), Sta. 1 M-117 (Dummy), Sta. 2-4	Empty
31	L	M-117	Unfinned BLU-1C/B (Dummy)	MER: M-117 (Launch), Sta. 5 M-117 (Dummy), Sta. 6	Unfinned BLU-1C/B (Dummy)
32	L	MK-82GP	Finned BLU-1C/B (Dummy)	MER: MK-82GP (Launch), Sta. 1 MK-82GP (Dummy), Sta. 2-6	Finned BLU-1C/B (Dummy)
33	R	MK-82GP	Empty	MER: MK-82GP (Launch), Sta. 2 MK-82GP (Dummy), Sta. 3-6	Empty
34	L	MK-82GP	Finned BLU-1C/B (Dummy)	MER: MK-82GP (Launch), Sta. 3 MK-82 (Dummy), Sta. 4-6	Finned BLU-1C/B (Dummy)
35	R	MK-82GP	Empty	MER: MK-82 (Launch), Sta. 6 MK-82 (Dummy), Sta. 3, 4	Empty
36	L	MK-82GP	Finned BLU-1C/B (Dummy)	MER: MK-82GP (Launch), Sta. 5 MK-82GP (Dummy), Sta. 6	Finned BLU-1C/B (Dummy)

TABLE V (Concluded)

Loading Configuration	Wing	Launch Store Model	Inboard Pylon	Center Pylon	Outboard Pylon
37	R	MK-82GP	Empty	MER: MK-82GP (Launch), Sta. 4	Empty
38	L	MK-82GP	Finned BLU-1C/B (Dummy)	TER: MK-82GP (Launch), Sta. 3	Finned BLU-1C/B (Dummy)
39	R	MK-82GP	Finned BLU-1C/B (Dummy)	TER: MK-82GP (Launch), Sta. 3 MK-82GP (Dummy), Sta. 2	Finned BLU-1C/B (Dummy)
40	L	MK-82GP	Empty	MER: MK-82GP (Launch), Sta. 1 MK-82 (Dummy), Sta. 2-6	Empty
41	R	MK-82GP	Finned BLU-1C/B (Dummy)	MER: MK-82GP (Launch), Sta. 2 MK-82GP (Dummy), Sta. 3-6	Finned BLU-1C/B (Dummy)
42	L	MK-82GP	Empty	MER: MK-82GP (Launch), Sta. 3 MK-82GP (Dummy), Sta. 4-6	Empty
43	R	MK-82GP	Finned BLU-1C/B (Dummy)	MER: MK 82GP (Launch), Sta. 6 MK-82GP (Dummy), Sta. 3, 4	Finned BLU-1C/B (Dummy)
44	L	MK-82GP	Empty	MER: MK-82GP (Launch), Sta. 5 MK-82GP (Dummy), Sta. 6	Empty
45	R	MK-82GP	Finned BLU-1C/B (Dummy)	MER: MK 82GP (Launch), Sta. 4	Finned BLU-1C/B (Dummy)
46	L	MK-82GP	Empty	TER: MK-82GP (Launch), Sta. 3	Empty
47	L	MK-82SE	Finned BLU-1C/B (Dummy)	MER: MK-82SE (Launch), Sta. 3 MK-82SE (Dummy), Sta. 4	Finned BLU-1C/B (Dummy)
48	R	MK-82SE	Finned BLU-1C/B (Dummy)	MER: MK-82SE (Launch), Sta. 4	Finned BLU-1C/B (Dummy)
49	L	MK-82SE	Finned BLU-1C/B (Dummy)	TER: MK-82SE (Launch), Sta. 2	Finned BLU-1C/B (Dummy)

APPENDIX III
EJECTOR FORCE CALCULATION

To calculate the ejector forces required to produce the two-dimensional motion of the external store at the end of the ejector piston stroke, the two following equations of motion can be used:

$$\ddot{Z} = g\cos\bar{\theta} + \frac{F_{e_j}}{m} - \frac{F_N}{m} \tag{1}$$

and

$$\ddot{\Delta\theta} = \frac{M_m}{I_{yy}} - \frac{M_{e_j}}{I_{yy}} \tag{2}$$

where $F_{e_j} = F_{Z_1} + F_{Z_2}$ and $M_{e_j} = F_{Z_1} X_{L_1} + F_{Z_2} X_{L_2}$.

Integrating Eqs. (1) and (2) over the ejector stroke time, t_i, with the assumptions that:

1. Ejector forces and moments are constant
2. Aerodynamic forces and moments are constant

Equations (1) and (2) simplify to

$$F_{e_j} = \frac{2\bar{m}Z}{t_i} - \bar{m}\,g\cos\bar{\theta} + F_N \tag{3}$$

$$F_{Z_1} = \frac{1}{X_{L_1} - X_{L_2}} \left[M_m - \frac{2\Delta\theta\, I_{yy}}{t_i^2} - F_{e_j} X_{L_2} \right] \tag{4}$$

and

$$F_{Z_2} = F_{e_j} - F_{Z_1} \tag{5}$$

The final step is to solve for the forward ejector force, F_{Z_1}, and rear ejector force, F_{Z_2}, from flight test data of the store.

With the values listed in Table V (Appendix II) Set 1 and the additional values

$\bar{\theta}$ = -30 deg

X_{L_1} = 0.687 ft

X_{L_2} = -0.979 ft

F_N = 75 lb (scaled from wind tunnel data)

M_m = -806 ft-lb (scaled from wind tunnel data)

substituted in Eqs. (3) and (4), the following ejector forces resulted:

F_{Z_1} = 2181 lb

F_{Z_2} = 480 lb

UNCLASSIFIED

Security Classification

DOCUMENT CONTROL DATA - R & D

(Security classification of title, body of abstract and indexing annotation must be entered when the overall report is classified)

1. ORIGINATING ACTIVITY (Corporate author)
Arnold Engineering Development Center
ARO, Inc., Operating Contractor
Arnold Air Force Station, Tennessee

2a. REPORT SECURITY CLASSIFICATION
UNCLASSIFIED

2b. GROUP
N/A

3. REPORT TITLE
INVESTIGATION OF THE SEPARATION CHARACTERISTICS OF VARIOUS STORES FROM THE A-7D AIRCRAFT AT MACH NUMBERS FROM 0.34 TO 0.95

4. DESCRIPTIVE NOTES (Type of report and inclusive dates)
Final Report - April 19 to June 7, 1971

5. AUTHOR(S) (First name, middle initial, last name)
David Hill, Jr., ARO, Inc.

This document has been approved for public release and sale; its distribution is unlimited. Per TAB 7-210 dtd 10 May 74

6. REPORT DATE	7a. TOTAL NO. OF PAGES	7b. NO. OF REFS
September 1971	93	0

8a. CONTRACT OR GRANT NO.	9a. ORIGINATOR'S REPORT NUMBER(S)
F40600-72-C-0003	AEDC-TR-71-188
b. PROJECT NO.	AFATL-TR-71-116
c. Program Element 27121F	9b. OTHER REPORT NO(S) (Any other numbers that may be assigned this report)
d. System 337A	ARO-PWT-TR-71-147

10 DISTRIBUTION STATEMENT
Distribution limited to U. S. Government agencies only; this report contains information on test and evaluation of military hardware; September 1971; other requests for this document must be referred to Armament Development and Test Center (DLGC), Eglin AFB, FL 32542.

11 SUPPLEMENTARY NOTES	12. SPONSORING MILITARY ACTIVITY
Available in DDC	Armament Development and Test Center (DLGC), Eglin AFB, FL 32542

13 ABSTRACT

Tests were conducted in the Aerodynamic Wind Tunnel (4T) using 0.05-scale models to investigate the separation characteristics of the unfinned and finned BLU-1C/B, M-117GP, MK-82GP, and MK-82SE when released from various wing pylon locations on the A-7D aircraft. Captive trajectory data were obtained at Mach numbers from 0.34 to 0.95 at simulated pressure altitudes from 5000 to 7000 ft. The parent aircraft angle of attack was varied from 1.8 to 12.3, depending on Mach number, climb angle, and simulated altitude. At selected test conditions, parent climb angles of 0, -35, -50, and -70 deg were simulated. In some cases, the separation trajectories of the BLU-1C/B were initiated at the end of the ejector piston stroke using flight-test data to determine the initial store positions and velocities. In general, the separation trajectories agreed well with flight-test data for the trajectory interval of the test. For the trajectory intervals of the test, most of the stores separated from the parent aircraft without store-to-parent contact.

Distribution limited to U. S. Government agencies only; this report contains information on test and evaluation of military hardware; September 1971; other requests for this document must be referred to Armement Development and Test Center (DLGC), Eglin AFB, FL 32542.

DD FORM 1 NOV 65 1473

UNCLASSIFIED

Security Classification

14. KEY WORDS	LINK A		LINK B		LINK C	
	ROLE	WT	ROLE	WT	ROLE	WT
A-7D aircraft						
bombs (ordnance)						
separation characteristics						
transonic flow						
trajectories						
fin stabilized ammunition						
aerodynamic loads						

AFSC
Arnold AFS Tenn